DISTRIBUTED ENERGY STORAGE WITH REACTIVE AND REAL POWER CONTROLLER FOR POWER QUALITY ISSUES BY RENEWWABLE ENERGY AND ELECTRIC VEHICLES

By

LIM KHIM YAN

A dissertation submitted to the Department of Electrical and Electronic Engineering,
Lee Kong Chian Faculty of Engineering & Science,
Universiti Tunku Abdul Rahman,
in partial fulfilment of the requirements for the degree of
Master of Engineering Science
November 2016

DECLARATION

I hereby declare that the dissertation is based on my original work except for quotations and citations which have been duly acknowledged. I also declare that it has not been previously or concurrently submitted for any other degree at UTAR or other institutions.

Name : _____

Date : _____

APPROVAL SHEET

This dissertation/thesis entitled **"DISTRIBUTED ENERGY STORAGE WITH REACTIVE AND REAL POWER CONTROLLER FOR POWER QUALITY ISSUES BY RENEWWABLE ENERGY AND ELECTRIC VEHICLES"** was prepared by **LIM KHIM YAN** and submitted as partial fulfilment of the requirements for the degree of Master of Engineering Science at Universiti Tunku Abdul Rahman.

Approved by:

_____

(Prof. Dr. Lim Yun Seng)
Date:……..
Supervisor
Department of Electrical and Electronics Engineering
Faculty of Engineering and Science
Universiti Tunku Abdul Rahman

_____

(Mr. Chua Kein Huat)
Date:……..
Co-supervisor
Department of Electrical and Electronics Engineering
Faculty of Engineering and Science
Universiti Tunku Abdul Rahman

ACKNOWLEDGEMENTS

I would like to thank everyone who had contributed to the successful completion of this research. I would like to express my gratitude to my research supervisor, Dr. Lim Yun Seng for his valuable advice, guidance and his enormous patience throughout the development of the research.

In addition, I would also like to express my gratitude to my loving parents and friends who had helped and given me encouragement. Through this research, I learnt a lot and I believe this helps me in my future. And I also appreciate helps and advise from my co-supervisor Mr Chua Kein Huat, and Dr. Wong Jianhui in this long journey.

ABSTRACT

DISTRIBUTED ENERGY STORAGE WITH REACTIVE AND REAL POWER CONTROLLER FOR POWER QUALITY ISSUES BY RENEWABLE ENERGY AND ELECTRIC VEHICLES

LIM KHIM YAN

Substantial greenhouse gas emission due to the combustion of fossil fuels for electricity has caused the world to push forward the use of renewable energy sources. Photovoltaic systems and wind turbines are the two possible renewable energy sources in Malaysia because of the convincing amount of solar irradiances and wind energy throughout the year. Apart from that, electric vehicles (EV) have been used to reduce air pollution in the cities. However, the integration of renewable energy sources (RE) and electrical vehicles (EV) into the low voltage (LV) networks can create a number of power quality issues, such as voltage unbalance, low power factor and voltage rise issues when injecting power into the networks. These power quality issues cause the circulation of the neutral current around the distribution network, hence reducing the efficiency of the network. Besides, the lifespan of induction motors can be shortened due to the unbalance current around the motor windings making the motor to be overheated prematurely. Hence, these power quality issues have to be mitigated. Therefore, an energy storage system can be used to solve the power quality issues caused by the use of RE and EV on the distribution networks. This is because the energy storage system can supply or absorb the real and reactive power appropriately in order to mitigate

the power quality issues. The advantage of using the energy storage system in this aspect is that any power quality issues can be effectively corrected without wasting the harvested energy. However, the operation of the energy storage system has to be controlled appropriately in order to achieve the desired outcomes. Therefore, a novel fuzzy controller is developed and implemented into the energy storage to manipulate the flow of real and reactive power between the energy storage and the network based on the network conditions. The fuzzy controller is able to reduce any voltage excursions with the use of real and reactive power from the energy storage, hence reducing the voltage unbalance and improving the power factor. Numerous experiments have been carried out to verify the effectiveness of the fuzzy controller. The experimental results showed that the voltage unbalances and power factors are constantly maintained below the thresholds under the high penetration of PV systems and EV.

TABLE OF CONTENTS

LIST OF TABLES

LIST OF FIGURES

CHAPTER 1

INTRODUCTION

1.1 Background

Renewable energy has become a very important energy source in Malaysia to deal with the climate change and reduce the dependency on fossil fuels for energy. Photovoltaic (PV) system is the most promising renewable energy resource in Malaysia due to its abundant solar irradiance. However, most of the PV systems are single-phase and installed on the low-voltage distribution networks without proper planning. As a result, the voltage unbalance of the network may be increased, causing a large circulation of neutral currents. Consequently, the network efficiency is reduced because of the power losses from the high neutral current. In addition, Malaysia is one of the cloudiest countries in the world. The solar irradiance is often scattered due to the passing clouds. As a result, the PV power outputs tend to fluctuate substantially. The intermittent power outputs and the growth of PV systems on the LV network can cause the high voltage fluctuations and reverse power flow (Prakash K. Ray, 2013).

Promoting electric vehicles is another approach put forward by the government to create a clean environment. Therefore, electric vehicles are increasingly popular in the country. There are 19 charging stations at present and another 300 charging stations will be installed by year 2015. Therefore, power consumption can be increased with the possibility of causing a huge burden to the electrical network. Also, the use of the charging stations can increase the voltage drops and voltage unbalance on the distribution networks; hence, causing the power factor drops. When the power factor is low, significant heating effects and the premature failures of transformers and electrical machines can happen. Also, customers can be penalised by the utility companies if their power factors are lower than 0.85. Any voltage instability can damage the electrical motors or result in the disoperation of electronic equipment (Canada, 2004).

All the technical issues created by the renewable energy and electrical vehicles need to be dealt effectively in order to accommodate the rapid growth of the renewable energy and electrical vehicles in the future. There are a number of solutions available to maintain the network voltage such as static VAR compensator, static synchronous compensator and active filters (Li, Zhang, Tolbert, Kueck, & Rizy, 2008). These devices control the network voltage with the use of reactive power. Therefore, these devices are an effecitve on the transmission networks because the reactance is usually large than the resistance of the network (von Appen, Marnay, Stadler, Momber, Klapp, & Scheven, 2011). However, they may not be effective on the distribution networks where the resistance is larger than the reactance.

To solve the technical problems on the distribution networks, it is proposed to use distributed energy storage systems which can maintain the network voltage within the required tolerance with the use of both real and reactive power. A fuzzy controller has been developed to control the real and reactive power output of the energy storage system in order to solve the voltage fluctuations on the distribution network caused by the penetration of the single-phase renewable energy sources and the electrical vehicles. This fuzzy controller is the extension of the method proposed in (Wong, Lim, & Morris, 2014) which uses real power only to maintain the network voltage. This extended fuzzy controller uses both the real and reactive power to maintain the network voltage, voltage unbalance and the power factor of the network, hence improving the efficiency of the network.

The fuzzy controller developed comprises the fuzzy logic control and the Park's transformation in order to deal with fluctuating voltage rises and voltage unbalances. The Park's transformation is used to coordinate distributed energy storage systems on the three-phase network to balance the voltage effectively. The controller involves the manipulation of the reactive power from the energy storage systems in order to maintain the power factor. The performance of the fuzzy control algorithm is verified by conducting a series of experimental case studies. The experimental results showed that the fuzzy control algorithm is able to solve the voltage unbalance issue, maintain the voltage magnitude at its statutory limit, and improve the power factor of the network.

1.2 Aims and Objectives

The aims and objectives of this project are as follows:-

I. To customize a distribution network integrated with two PV systems, a wind turbine emulator and an EV charging station.

II. To develop an energy storage system integrated with the distribution networks.

III. To develop a fuzzy control algorithm for the energy storage system for mitigating power quality issues using both the real and reactive power from the energy storage system.

IV. To evaluate the performance of the fuzzy controller in mitigating the power quality issues such as voltage unbalance, low power factor, and voltage rise caused by PV and EV.

1.3 Research Methodology

In order to achieve the objectives of this project, the following research activities were carried out.

Step 1: Literature study

Literature review was carried out to understand the incentives launched by the government to promote the growth of photovoltaic systems and electrical vehicles on the distribution networks. The embedded generation system in Malaysia with PV,

wind energy, and electric vehicles was also studied. In addition, power quality issues caused by the integration of PVs, wind turbines, and EVs together with the solutions for mitigating the issues are also studied.

Step 2: Development of LV network

An experimental network emulator integrated with photovoltaic systems and electrical vehicle charging station was developed at the university campus. The network consists of PV systems, wind turbine, wind emulator, load emulator, and data acquisition equipment.

Step 3: Impact Studies

Various case studies were carried out to investigate the power quality issues caused by the single-phase PV systems and the electrical vehicle on distribution network emulator.

Step 4: Setup of energy storage system

Three-phase energy storage system was set up in the university's laboratory. 48 batteries were connected to the three bi-directional inverters which were connected to the grid.

Step 5: Simple control for the energy storage system

Communication and simple control technique was developed to control the real and reactive power output of the energy storage system manually to improve power quality issues.

Step 6: Fuzzy controlled energy storage system

Fuzzy control algorithm which uses real and reactive power of the energy storage system was developed to mitigate the power quality issues.

Step 7: Evaluation of the fuzzy control algorithm

Few case studies were carried out with different generation and loading conditions on the distribution network to assess the performance of the fuzzy controller in mitigating power quality issues caused by the PV and EV on the distribution network.

Step 8: Implementation of the fuzzy control algorithm for the three-phase energy storage system

Due to the non-uniformly installation of single-phase PV system, a fuzzy controlled three-phase energy storage system was further developed from step 6. Experiments were carried out to verify the performance of the fuzzy controlled three-phase energy storage system.

1.4 Research Outline

The layout of the thesis is structured as follow:-

Chapter 2 presents the literature review on the distributed generation. The potential grid connected renewable energies are briefly discussed, followed by the power qualities arise due to the grid connected renewable energy on distribution networks.

Electric vehicles which cause various power quality issues are also explained, followed by the literature review on solutions to mitigate power quality issues.

Chapter 3 describes how the experimental LV distribution network was constructed. The design and the development of the electrical system, emulator, renewable resources, communication and data acquisition are stated clearly. In this chapter, the design and development of the energy storage system are briefly described. It is followed by the description of the control strategy. Details of fuzzy control algorithm are elaborated.

Chapter 5 presents several case studies conducted to represent different generation and loading scenarios. Impacts caused by the penetration of renewable energy at the university premises on distribution network were investigated. Different generations and loading conditions were considered to evaluate the performance of the proposed energy storage system to mitigate power quality issues.

Chapter 6 is the conclusion for the key findings of the research work and the uniqueness of the proposed energy storage system.

CHAPTER 2

LITERATURE REVIEW

2.1 Embedded Generation

Dispersed generation or embedded generation refers to any power generation technologies integrated with the distribution systems which is close to the points of load demands. They are not centrally planned by the utility or not centrally dispatched. Generally, they are smaller than 50 - 100 MW and connected to the distribution system. Over the last few years, the popularity of embedded generation is blooming due to few reasons. Based on the survey of International Conference on Electricity Distribution (CIRED), the reasons for the growth of embedded generation are the national drivers for reducing greenhouse emissions, improving energy efficiency, improving diversification of energy resources and the security of power supply. Moreover, for commercial considerations, distributed generation is available in modular and it is smaller in space occupied. Embedded generation may reduce the transmission cost and the power losses due to the long transmission of electricity (Jenkins, 2000).

The significant penetration of embedded generation will cause reverse power flow, voltage unbalance, low power factor, voltage flickering, voltage rise, voltage sag, harmonics and etc. Embedded generation contains a wide range of technologies such as solar power, wind turbine, combined heat and power (CHP), energy storage system, biomass, hydropower, ocean renewable energy, and etc. Solar energy, wind energy, hydropower, and fuel cell are the common renewable embedded generation in Malaysia.

2.1.1 Photovoltaic System

Photovoltaic (PV) system consists of solar panels and inverters for converting the sunlight into electricity. The PV inverters are to convert the solar electricity from direct current (DC) to alternating current (AC) before the solar electricity is exported to the grid. Figure 2.1 shows the configuration of the single-phase PV system. It can be a single-phase or three-phase PV system. However, the single-phase PV system is relatively common and widely installed in household buildings. The PV systems can be ranged from small roof top mounted or the building integrated systems from few kilowatts to megawatts. The PV systems are environmental friendly as they generate little greenhouse gaseous throughout their life cycles. In addition, the operating and maintenance fees are low because the PV systems are a mature technology with the service life of 20 years or more.

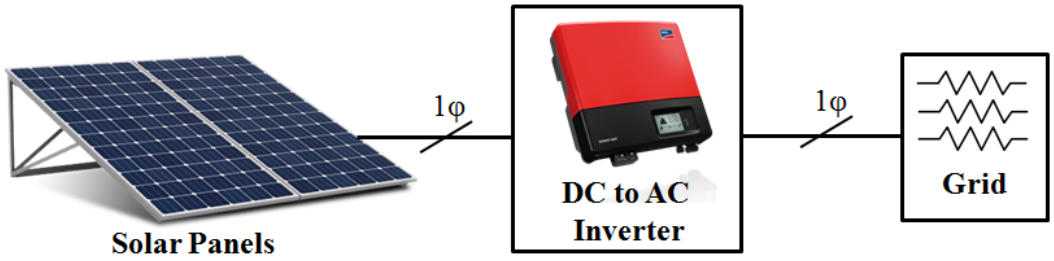

Figure 2.1: Configuration of single-phase PV system

The 8th Malaysia Plan on Energy Policy promoted several incentives to popularize clean energy. The PV system is highly encouraged as it generates clean energy from sunlight. Moreover, feed-in-tariffs and funding on renewable energy were announced in the 10th Malaysia Plan in 2010. Under the feed-in-tariff mechanism, installed PV capacities granted with feed-in approval are approximately 192.80 MW (SEDA). Table 2.1 shows the feed-in-tariff for the installed PV system. Costs are dropping due to the mass production of the technology. PV will one day be cost-effective in urban areas as well as remote ones. PV will be one of the most promising renewable energy resources in Malaysia.

Table 2.1: Feed in tariff rates of the installed PV capacity (SEDA)

Basic FiT rates having installed capacity of:	FiT Rates (RM per kWh)
(i) Up to and including 4 kW	0.9166
(ii) Above 4 kW and up to and including 24 kW	0.8942
(iii) Above 24 kW and up to and including 72 kW	0.7222
(iv) Above 72 kW and up to and including 1 MW	0.6977
(v) Above 1 MW and up to and including 10 MW	0.5472
(vi) Above 10 MW and up to and including 30 MW	0.4896

The integration of PV systems into the networks can cause power quality issues such as voltage flickers, voltage fluctuations, voltage unbalance, transient voltages, voltage rises, and harmonics due to the lack of coordination between customers and

utility companies, active power variations, and reactive power flow. In addition, the network experiences the low power factor (R. Romo, 2015). Therefore, with the penetration of PV, the machinery and motors can be damaged easily or the life span of the equipment will be shortened due to the power quality issues in the electrical networks.

Figure 2.2 is the world map showing the average amount of cloud in percentage (Ryan Eastman, Climatic Atlas of Clouds Over Land and Ocean, 2014). It shows that Malaysia has a high coverage of clouds. Hence, the cloudy sky of Malaysia is also an issue because the power output of the PV systems can be highly intermittent. It is hard to estimate the inconsistent power acquired due to the minute-to-minute variations. Besides, these cloudy sky will also create fluctuating power quality issues. Therefore, the power quality issues caused by the intermittent PV output power are unique because they are fluctuating and difficult to be solved because most of the existing technologies is to solve steady state voltage rise, voltage unbalance and power factor. (Chua, et al., 2012)

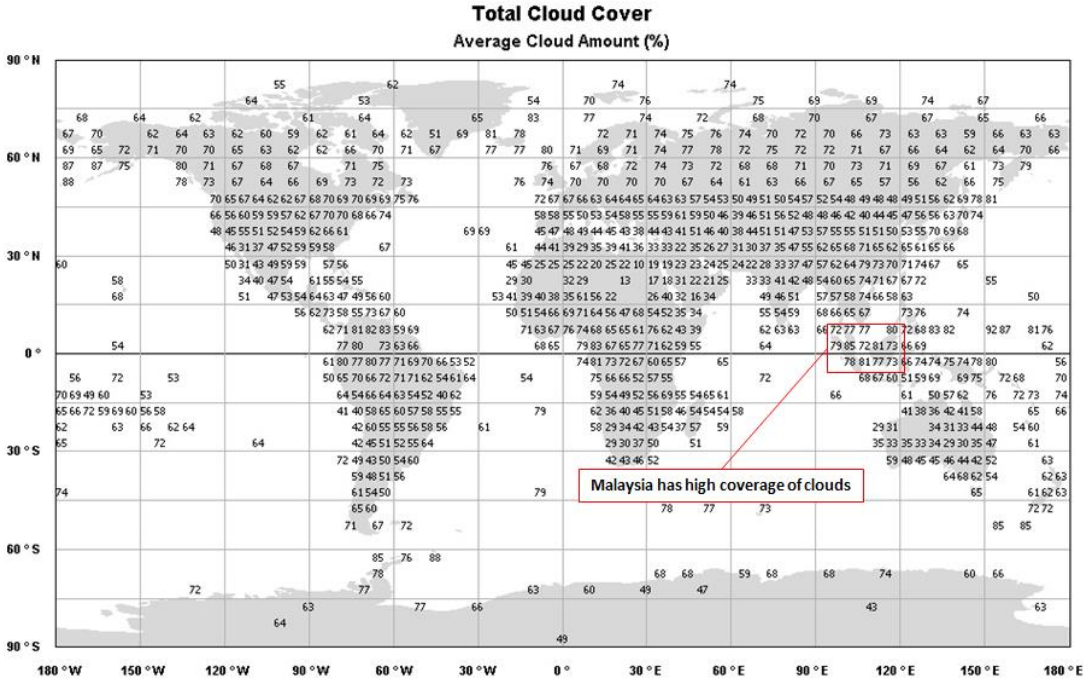

Figure 2.2: World map showing the average cloud amount in percent

Figure 2.3 shows the data collected when a single-phase PV system is integrated with the distribution network. It shows the fluctuating voltage, voltage unbalance factor and power factor due to the intermittent PV output power. Hence, it is important to mitigate the technical issues caused by PV systems in order to maintain the network stability and reliability in the future. However, the utility company needs an advanced active control in order to cater for these power quality issues.

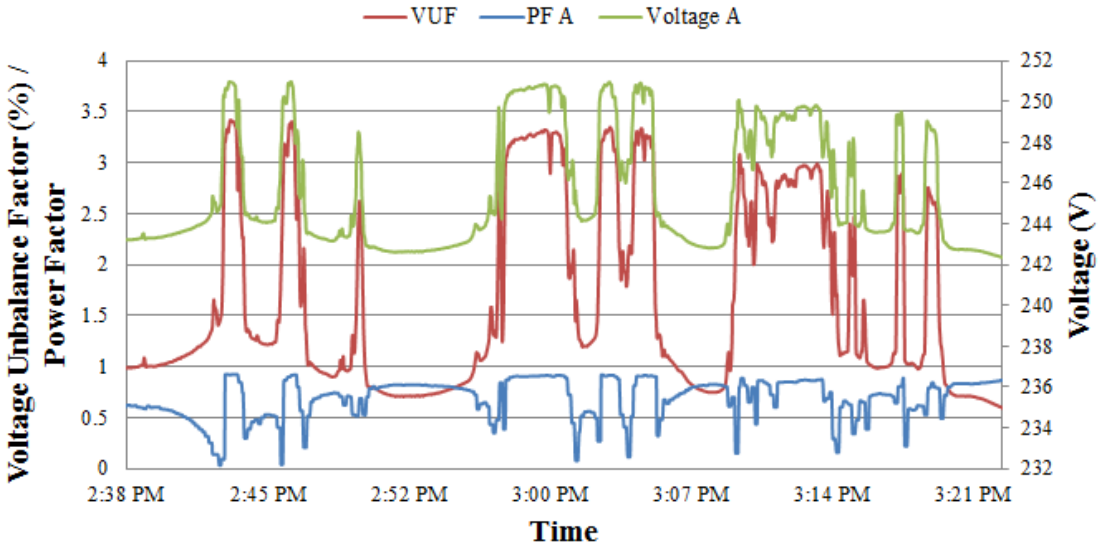

Figure 2.3: Fluctuation of voltage rise, voltage unbalance factor and power factor due to intermittent PV output power

2.1.2 Wind Energy

Wind turbines operate on a simple principle. The energy in the wind turns the blades around the rotor connected to the shaft, hence driving the generator to generate electricity. Therefore, the wind turbines convert the kinetic energy from wind into useful electricity. A wind controller and AC to DC converter are used to generate the electricity from the three-phase AC to the single-phase DC output which will be converted to single-phase AC 240 V at 50 Hz. Figure 2.4 shows the generation of wind power.

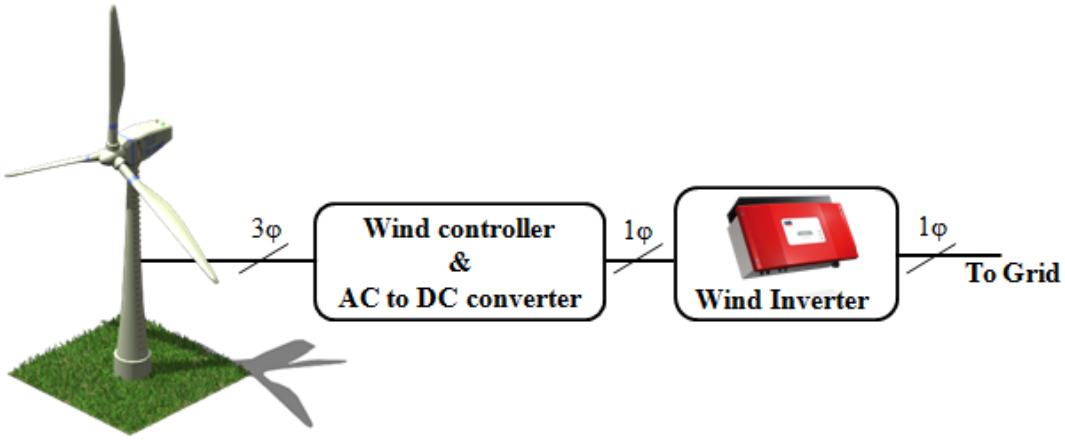

Figure 2.4: Generation of wind energy

In Malaysia, wind power is not popular compared to the solar power because the wind speed is not consistent. The wind speed is low throughout the year, 2 m/s, on average. Nevertheless, the research carried out at Serdang area showed that doubling the height of the wind turbine can increase the wind speed by 10% (Teh, 2010). Besides, harnessing wind energy in Malaysia depends on the geographical location since Malaysia is situated in the equatorial region and the wind speed relies on the monsoons. Furthermore, (S.Mekhilef, 2011) shows that the locations facing the South China Sea are the best choices for off-shore wind farms as there is Northeast monsoon season winds from November to February. Table 2.2 shows the average monthly wind speed for Magabang Telipot (Zaharim, Najid, Razali, & Sopian, 2009) and small Perhentian Island (Zuhairuse Md Darus, 2009) in 2005. It is shown that it is possible to harness wind energy in Small Perhential Island because the cut-in speed of small scaled wind turbine is 3 to 4 m/s.

Table 2.2: Average monthly wind speed for Magabang Telipot and small Perhentian Island in 2005

Month	Wind speed (m/s) for Megabang Telipot	Wind speed (m/s) for Small Perhentian Island
January	4.44	7.9
February	3.47	6.85
March	3.16	7.56
April	2.54	6.78
May	2.24	6.91
June	2.25	nil
July	2.18	6.63
August	2.13	7.16
September	1.91	6.88
October	2.4	7.12
November	2.38	7.57
December	4.58	7.88

The integration of the wind turbines with the networks can cause power quality issues such as voltage fluctuations, voltage rises, and voltage sags due to the switching operation, low power factor, and harmonic distortions (Sharad.W.Mohod, 2008). In addition, wind does not blow uniformly throughout Malaysia. Hence, power quality issues are fluctuating due to the intermittent wind power output. Fluctuating power quality issues are hard to be mitigated since the existing strategy is used to mitigate steady power quality issues. With the continued expansion of the wind power generation, the fluctuating power quality issues are concerned widely.

For the existing solutions, the static synchronous compensator (STATCOM) is used as a smooth reactive power provider to improve the power quality issues caused by the wind integrated electrical networks (Muhammad A.Saqib, 2015). However, the STATCOM is expensive and an innovative strategy should be developed to mitigate the fluctuating power quality issues caused by the integrated wind power generation.

Therefore, an energy storage system with an effective controller is proposed to solve the dynamic power quality issues caused by the wind turbines.

2.2 Electric Vehicles

Institute of Energy Research states that transportation has occupied 70% usage of petroleum, which is the highest compared to other usages. Green technology is one of the highly recommended ways to mitigate the issue while electric vehicle (EV) is the new highlight in this era to overcome this problem. Based on the analysis from GreenTech Malaysia, the migration to electric mobility from petrol vehicles will potentially help Malaysia to cut down the carbon dioxide emissions by 1.7 tonnes in the long run (Lim, Chia Ying, 2015). Electric vehicle consists of electric motor, DC/AC inverter, DC/DC converter and batteries. The architecture of electric vehicle is illustrated in Figure 2.5 (Forster, 2010). Since high voltage is required for the electrical motor to perform, DC/AC inverter plays an important role to draw power from the batteries. Batteries are controlled and monitored by the battery management system of the electric vehicle in order to avoid over discharge.

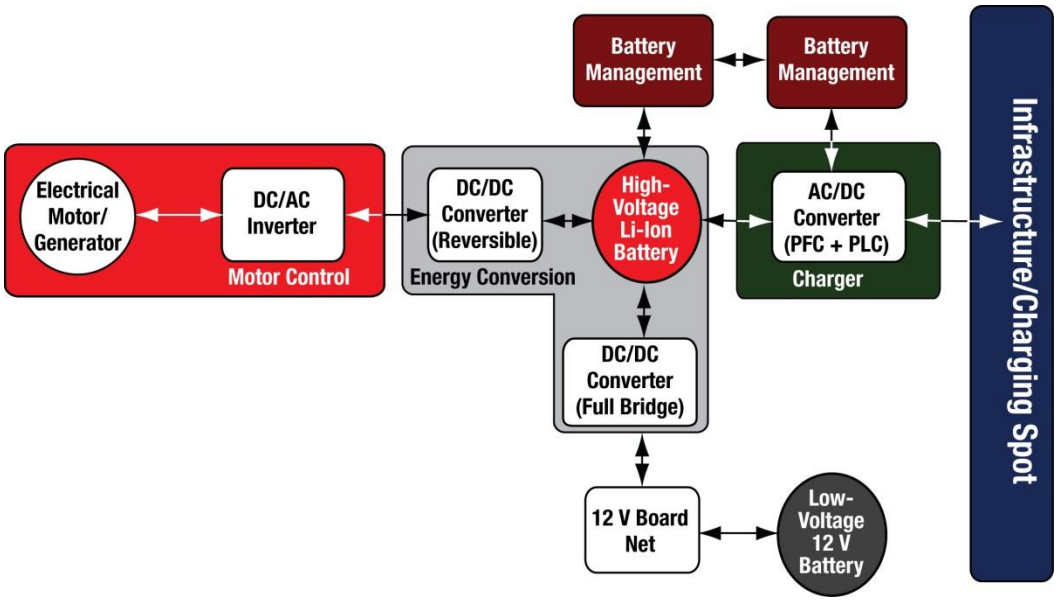

Figure 2.5: Architecture of electric vehicle (Forster, 2010)

Electric vehicles are a step closer to creating the world a greener place. Widely usage of electric vehicles indicates that charging stations will be installed everywhere. At present, electric vehicles are getting popular among the country and it is available for purchase in Malaysia. The number is expected to grow in the near future. In Malaysia, 19 charging stations have been installed and another 300 charging stations will be installed by year 2015. Figure 2.6 shows the map of the existing charging stations in Malaysia. The available charging stations are installed at Suria Kuala Lumpur City Centre (KLCC), Lot 10 Shopping Centre, Petronas Solaris Serdang, Bangsar Shopping Centre, Wisma Tan Chong, Nissan Petaling Jaya, and etc (First Energy Networks, 2015). Figure 2.7 shows the public charging stations located at P2 of Suria Kuala Lumpur City Centre (KLCC).

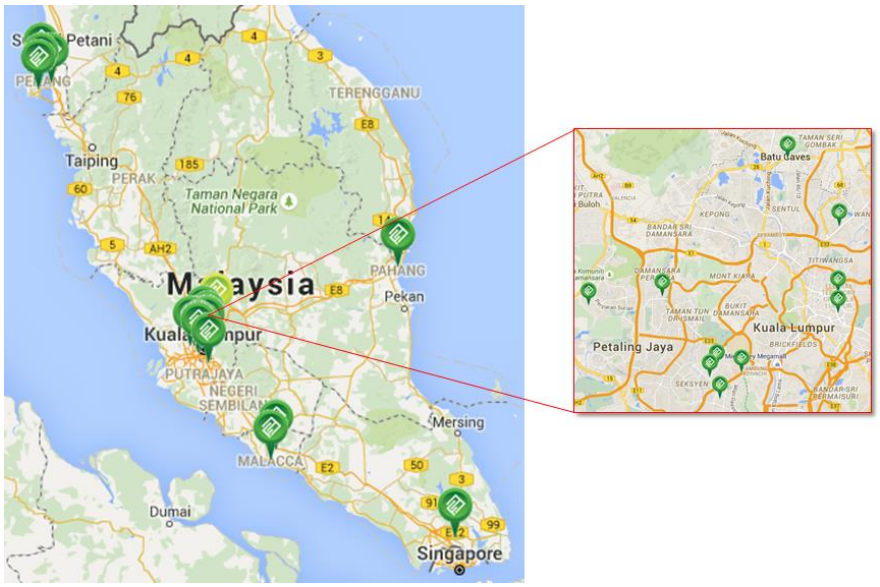

Figure 2.6: The locations of existing charging stations in Malaysia (First Energy Networks, 2015)

Figure 2.7: Public charging stations located at P2 of Suria KLCC (KeeGan Dorai, 2012)

Power quality issues caused by the penetration of EV and PV are discussed in (Masoud Farhoodnea, 2013). Simulation results showed that a severe voltage drops due to the high power consumption and unmanaged arrangement of the EV charging

stations. Due to the unplanned connection to the networks, voltage unbalance is likely to happen. Besides, charging EV with the electrical network will cause voltage variations, power factor reduction, voltage drop and harmonics distortion. In the paper, the authors also state that capacitor banks or active power conditioning devices must be used to manage the exchanged powers and control the voltage of the networks. There are some solutions proposed to mitigate these problems. In (Yong, Ramachandaramurthy, Tan, & Mithulanantha, 2015), the authors use bi-directional DC fast charging stations to solve the voltage drop issue. By controlling the switching, reactive power drawn from the DC-link capacitor can improve the power factor. Besides, vehicles-to-grid (V2G) with various charging strategies of EV as shown in (Salman Habib, 2015) can improve the technical performance of the networks in terms of stability, efficiency and reliability of the systems.

2.3 Power Quality Issues Caused By the EV, PV and Wind Turbines

The power quality has become an important issue in the distribution networks in the recent years due to the grooming of power electronics used and the distributed generation. The quality of electricity can be known as a set of values of parameters, such as voltage magnitude, deviation in transient voltages and currents, continuity of service, harmonics in the AC power and others. For IEEE Standard 1100-1999 Recommended Practice for Powering and Grounding Electronic Equipment, power quality is the ideology of powering and grounding electronic equipment which is acceptable with the functions of the equipment and compatible with the foundation wiring system and other coupled equipment (IEEE, 2005). An ordinary classification

of power quality phenomena is also provided by IEEE based on the principal spectral content, duration, and magnitude of the disturbance. Table 2.3 shows categories and characteristics of power system electromagnetic.

Table 2.3: Categories and Characteristics of Power System Electromagnetic Phenomena

No.	Categories	Typical Spectra Content	Typical Duration	Typical Voltage Magnitude
1	Transients			
1.1	Oscillatory			
1.2.1	Low Frequency	< 5 kHz	0.3 – 50ms	0 – 4 pu (per unit)
1.2.2	Medium Frequency	5-500 kHz	20μs	0 – 8 pu
2	Long Duration Variations			
2.1	Interruption, Sustained		>1 minute	0.0 pu
2.2	Undervoltages		>1 minute	0.8 – 0.9 pu
2.3	Overvoltages		>1 minute	1.1 – 1.2 pu
3	Voltage Unbalance		Steady state	0.5 – 2%
4	Waveform Distortion			
4.1	Harmonics	0 – 100th harmonic	Steady state	0 – 20%
5	Voltage fluctuations	< 25 Hz	intermittent	0.1 - 7%

Source: IEEE Std 1159-1995

Blackouts, overheating transformers, circuit breaker trips, neutral conductors overheating, and unexplained equipment downtime are the impacts of having poor power quality in the electrical power system. The power quality occurs due to many aspects. The most common technical issues can be caused by the integration of EV and RE systems are voltage fluctuation, voltage rise, voltage sags, voltage unbalance, reversed power flow, unnecessary neutral current flow, harmonics, and flickers. Furthermore, voltage rise has been recognized as the most serious power quality

issues caused by the high penetration of renewable energy sources in UK (Lyons, 2010). Therefore, power quality issues are significant issues to be concerned.

2.3.1 Voltage Unbalance Factor (VUF)

In a three-phase balance power distribution system, the three line-neutral voltages are equal in magnitude and are phase displaced from each other by 120 degree in a balanced sinusoidal supply system. Any differences that exist in the three voltage magnitudes and/or a shift in the phase separation from 120 degree is said to bring about an unbalanced supply or familiarized as voltage unbalance (Gosbell, 2002). The difference between a balanced system and unbalanced system is shown in Figure 2.8.

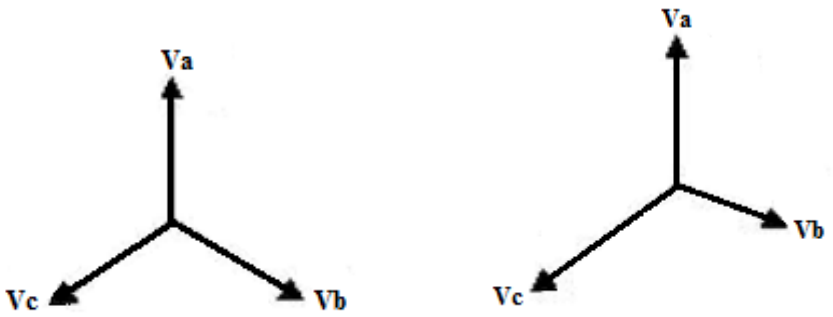

(a) (b)

Figure 2.8 (a): Phasor of the balanced three-phase voltage
(b): Phasor of the unbalanced three-phase voltage

Ideally, a three-phase power system should operate in balanced condition. However, this condition is hardly to be attained as single-phase distributed generation is increasing on the LV distribution networks. When the high penetration of small scale

embedded generation in the LV networks, voltage unbalances has become a serious issue. This is due to the fact that the distributed small-scale embedded generation is not centrally installed across the distribution networks. Moreover, the voltage unbalance in the distribution networks can be caused by continuous varying of instantaneous demand, irregular distribution of single-phase load across the three-phase network, and unbalance or unstable utility supply.

There are two definitions for voltage unbalance. National Electrical Manufacturer Association (NEMA) defines the voltage unbalance factor as the ratio of maximum deviation of the three-phase line voltages to the mean of the three-phase line voltages. According to the International Electrotechnical Commission (IEC) standards, voltage unbalance factor (VUF) is defined as the ratio of negative sequence voltage (V^-) to positive sequence voltage (V^+), as expressed below (P. Trichakis, 2006; Lee, 1999):

$$\text{VUF}\ (\%) = \frac{V^-}{V^+} \times 100$$

The negative and positive sequence of the system voltage can be calculated by the following expression:

$$\begin{bmatrix} V^0 \\ V^1 \\ V^2 \end{bmatrix} = 3 \begin{bmatrix} 1 & 1 & 1 \\ 1 & a & a^2 \\ 1 & a^2 & a \end{bmatrix} \begin{bmatrix} V_a \\ V_b \\ V_c \end{bmatrix}$$

where V_a, V_b and V_c are the three-phase line voltages while V^0, V^+ and V^- are the zero, positive and negative sequence voltages components respectively. In Malaysia, the statutory limit of the voltage unbalance is 2% (Bollen, 2002) which is much quite

similar as compared to 1.3% in the UK and 2% in EU (Trichakis, Taylor, Lyons, & Hair, 2008).

It is important to maintain the VUF below the statutory limit. This is because when voltage unbalance occurs, it will cause serious problem in distribution network where there is a returned current flow through the neutral line which causes the increase of power losses in the network and reduction in the efficiency of the distribution network. Besides that, VUF also gives impact to the induction motor. According to National Electrical Manufacturers Association (NEMA), the voltage unbalance of 1% at the terminal of fully loaded motor can create 6 -10 times the unbalance current. Consequently, this unbalance current will cause the increase in heating by 6 to 10% as shown in Figure 2.9. This can reduce the energy efficiency and lifespan of the motors. As a result, the customers may need to replace the motor more frequently. Besides generating unnecessary heat in the motor winding, voltage unbalance also producing harmonic currents to the system, this affects the efficiency of the network.

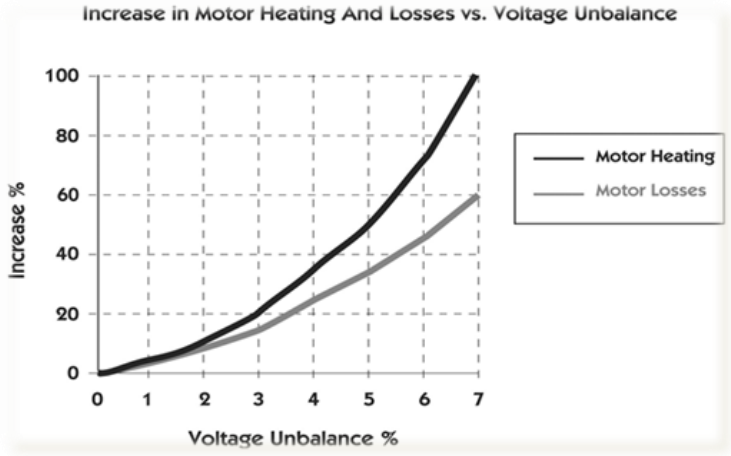

Figure 2.9: Increase in motor heating due to voltage unbalance (Bishop, 2008)

Many researches have been undertaken regards the voltage unbalance mitigation. In the paper of (Oeng & Sangwongwanich, 2016), strategy was proposed where unbalanced voltage is mitigated by the injection of negative-sequence currents. Simulation results show that 50% unbalanced voltage can be reduced using this strategy. Besides, voltage unbalance caused by single phase PV inverters in LV networks is reduced by 51% with the applied of DSTATCOM in (Shahnia, Ghosh, Ledwich, & Zare, 2010). Voltage level is maintained at the point of connection by injecting both the active and reactive power. Since single-phase PV systems worsen the voltage unbalance ratio in the network, in (Bajo, Hashemi, Kjsær, Yang, & Østergaard, 2015), three-phase PV inverters are controlled to inject and absorb the real and reactive power in each of the phases. Results show that 45% reduction in voltage unbalance can be attained. In (Chua, et al., 2012), single phase batteries were used as ESS to mitigate the voltage unbalance and a reduction of 37% can be reached. In the newer technology, electric vehicles are also used to mitigate the voltage unbalance problem. Both active and reactive power are controlled in order to compensate the uneven power flow in (Jiménez & García, 2012). The unbalance voltage with a reduction of 27% can be reached with this method.

Since EV and PV systems are highly encouraged in Malaysia and majority of the PV systems and EV are single-phase, voltage unbalance on the distribution network is likely to happen in the future. It is believed that voltage unbalance would be a serious problem when more and more EV and PV systems are integrated to the distribution network.

2.3.2 Voltage Flickers

Voltage flickers are known as luminosity variation of lights which may influence the human visual system depending on the frequency and the brightness. It is caused by rapid voltage changes due to load changes in the power system. In overall, the voltage flicker can be defined as an impression of unsteadiness of visual sensation induced by a light stimulus, whose luminance or spectral distribution fluctuates with time. Normally, the frequency is ranging from 1 Hz to 35 Hz when subject to change in the illumination intensity. There is short term index (P_{st}) and long term flicker index (P_{lt}) for the measurement of the severity of the voltage flickers. For short term index, it is computed by the fluctuating voltage over a period of 10 minutes, while long term flicker index, also called the average of short term flicker, can be calculated by the fluctuating voltage over a period of 2 hours.

Electrical furnace, welding machines, rolling mills, pumps and others are well known as flicker generators. However, variable frequency drives (VFD), switching loads, motor starting, and also variations in load current due to repetitive events such as washing machines, refrigerators, dryers, air conditioners and others also causing voltage flicker. On the other hand, the frequent switching of the PV inverters due to the dynamic change of PV output also intensifies the issue of flickering.

The quality of voltage supplied to the networks is significantly reduced due to the voltage flickers and these oscillations of voltage are kind of serious problems to the networks. Voltage flicker may affect the starting torque, slip, starting current, temperature rise, and even overloading of motors and generators. Furthermore,

domestic lighting, power electronic devices, computers and other devices also affected by the voltage flickers, and reduce the life span of those fluorescent and electronics devices.

2.3.3 Voltage Rises

Small-scale embedded generation (SSEG) such as photovoltaic modules and wind turbines are becoming common on the low voltage distribution networks. However, voltage rises are one of the issues that limit the penetration of SSEG. Simulation studies using Power World simulation software demonstrate that the integration of PV system is likely to increase the voltage level (Lewis, 2011). Voltage rises can happen due to the reversed power flow with the severity depending on the system impedance, generation location, generation characteristics and system load.

In Malaysia, the voltage tolerance boundary is set at a range of +10% and -6% for the primary distribution networks with the voltage level of 240V. Any equipment will perform satisfactorily if the voltage is always maintained within the statutory limits by the network operators. There are different methods that can be used to mitigate the voltage rise such as the generator active power curtailment, the wide area voltage control, the reactive power management, and the energy storage system. The main limitation for these approaches is the significant cost needed for the installation of equipment, sensors, control systems, communication and other infrastructure changes. In this project, the energy storage system is used to cater for the voltage rise issues to

ensure the voltage is within the voltage tolerance. It can store the excess power during minimum load connected and discharge when it is peak load times.

2.3.4 Low Power Factor

Power factor is an index used to calculate the efficiency of electricity consumption, which is a measure of how effectively the power is being converted into useful output. The connection between the real and reactive power is expressed by the right triangle shown in Figure 2.10 where real power is the horizontal axis and reactive power is in vertical axis. The overall burden deposited on the grid by the load from both its real and reactive parts is known as the apparent power.

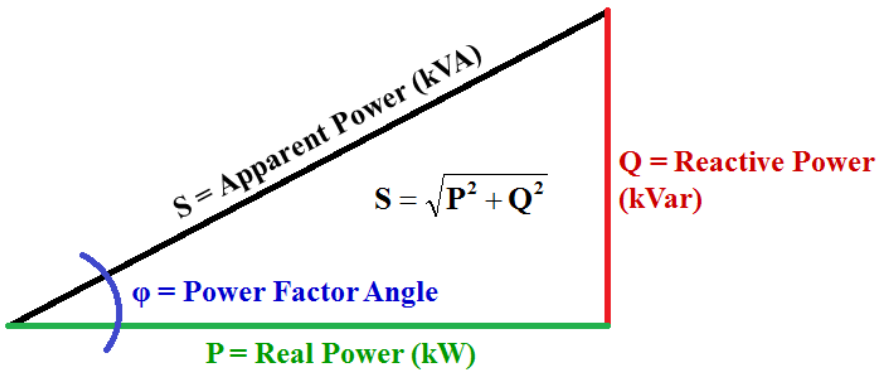

Figure 2.10: Relationship between real, reactive and apparent power

Power factor is the cosine of the angle, PF = cos φ. The load is resistive when φ is zero degrees and power factor is unity. If the load also includes reactive elements, the reactive power will be non-zero and the apparent power will go beyond the real power as shown in Figure 2.10. Hence, when two loads are given, each consuming the same amount of real power, the one with the higher power factor will be draw

less circulating current and more efficient than the other with the lower power factor. A poor power factor can be the result of inductive loads such as an induction motor, lighting ballasts, power transformer, welder or induction furnace, or it can be due to high harmonic content or distorted or discontinuous current waveform. This composes a loss to both the consumer as well as the utility company. The losses in the cable conductors at a power factor of 0.8 are 1.57 times the losses at unity power factor, and the losses at a power factor of 0.4 will be 6.25 times that at unity power factor (REEEP, 2006).

PV systems that supply power to the utility can actually deteriorate the power factor after the system is connected to the grid (R. Romo, 2015). An example will be used to show how PV system can affect the network power factor. In Figure 2.11, it shows a network with a load connected to the power grid. The load draws 1000 kW of real power and 450 kVar of reactive power which results in 1096 kVA of apparent power. By using $P = S \cos \varphi$ or $Q = S \sin \varphi$, φ can be calculated as 24.2^{o} and hence, the power factor is 0.912 as shown in figure 2.11. In Figure 2.12, a PV system is placed to displace 50% of the real power from the power grid. Therefore, each of the power grid and the PV system feeds 500 kW to the load. In fact, the PV inverter is designed to operate with a unity power factor. The PV system with the unity power factor only supplies real power to the grid. Hence, the power factor angle is increased to 42^{o} after the PV system is connected to the system. Therefore, the power factor drops to 0.743. This example shows clearly that the power factor drops after the PV system is connected.

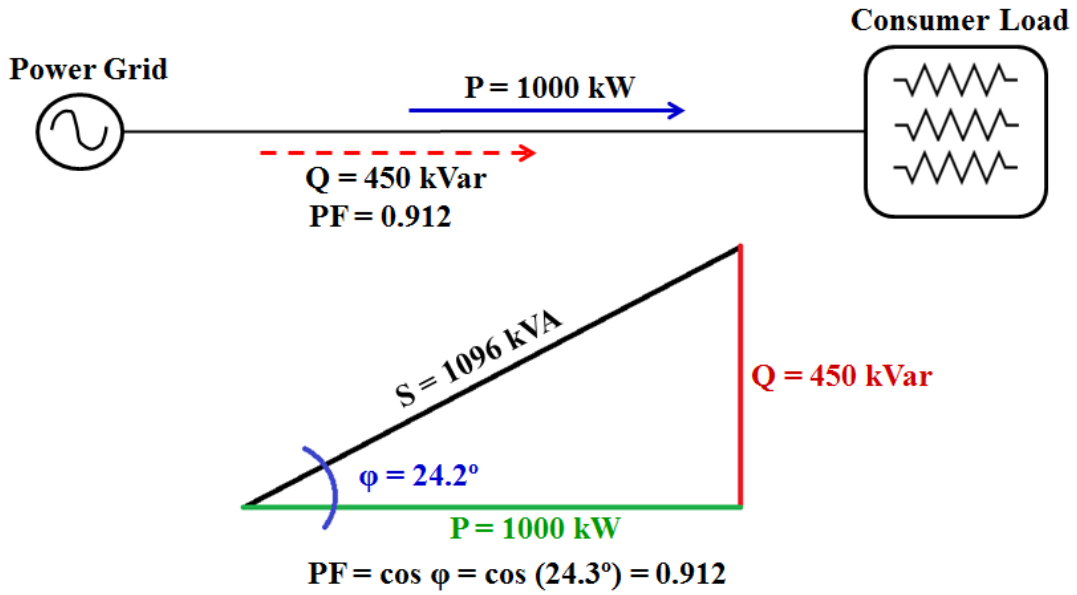

Figure 2.11: Normal power factor in the network

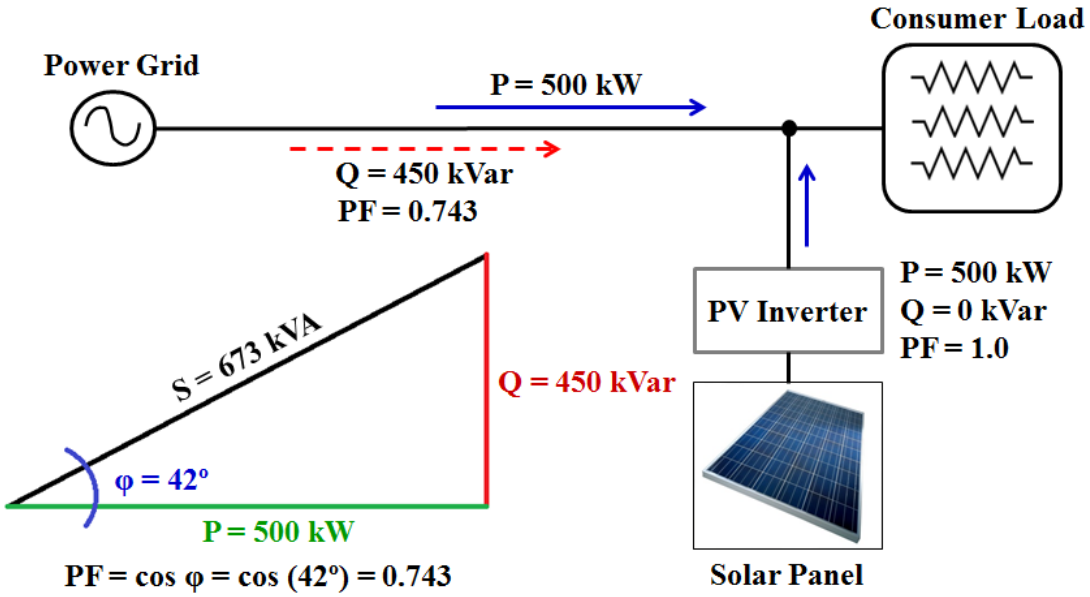

Figure 2.12: Power factor being reduced when the PV system is integrated

The inefficiencies associated with the low power factor means that the current along the distribution lines are high. As a result, the utility company will impose power factor penalty on the customers. The utility company must set minimum power factor standards in accordance with applicable tariffs. In Malaysia, any customers with low

power factor will be penalised by Tenaga National Berhad (TNB). The power factor penalty is calculated as follows:

(a) For every 0.01 less than 0.85 power factor, 1.5 % surcharge of the current bill is imposed.

(b) For every 0.01 less than 0.75 power factor, 3 % surcharge of the current bill is imposed.

For example, if the total unit used by a company is 5000 kWh per month at the rate of RM 0.323/ kWh and the power factor is 0.5, the total electricity bill is calculated as 5000 x RM 0.323 or RM 1615. The monthly surcharge on the low power factor is (0.85 – 0.75) x 1.5 + (0.75 – 0.5) x 3 = 0.9 due to the rate stated above. Hence, low power factor penalty is calculated as 0.9 x RM 1615 or RM 1453.5. Therefore, the total amount of the electricity bill for the month is RM 1615 + RM 1453.5 = RM 3068.5. In this example, the low power factor causes 90% increase of its original bill.

In reality, PV power output is not constant and fluctuating throughout the day depending on the clouds and position of the sun. Fluctuating power factor will have a high risk to get the power factor penalty as the low power factor surcharge is charged based on the amount of monthly reactive energy consumption. This is because the average power factor over the month is calculated by $\frac{P}{\sqrt{P^2+Q^2}}$, where P is the active energy consumption and Q is the reactive energy consumption. If the average power factor drops below the standards, power factor needs to be increased to improve the network efficiency. The supply of the reactive power from the grid has to be reduced in order to attain the unity power factor. Therefore, customers are advised to install KVAR generators such as, capacitor, corrector, synchronous

generators, and synchronous motors. There are a number of solutions available to maintain the network reactive power such as static VAR compensator, static synchronous compensator and active filters (Li, Zhang, 2008; Wu & Liu, 2011; Muhammad A. Saqib, 2015).

2.4 Solutions for Mitigating the Power Quality Issues

The increasing amount of renewable energy penetration to the electrical networks will raise the power quality issues. Besides, electric vehicles are also one of the significant elements to affect the power quality of the conventional electrical systems. Voltage rise, voltage unbalance, voltage sags, voltage regulation, power factor are the common technical issues caused by the integration of renewable energy and electric vehicles. Demand side management, renewable energy curtailment, Flexible AC Transmission System (FACTS), energy storage, and on-load-tap-changer control are the existing strategies used to improve the power quality on the distribution networks.

2.4.1 Demand Side Management

Demand side management (DSM) refers to actions taken on the consumer's sides to change the amount of the electricity usage. One of the main functions of DSM is to manage the load in order to change the power demand profile of customers (CHUANG & GELLINGS, 2008). DSM programs consists of planning, scheduling,

monitoring and executing activities of power demand for the objectives of minimizing the electricity prices, reducing the energy infrastructure investments, enhancing the energy security and others ancillary advantages. There are four basic schemes of DSM as follow (Johnson, 2007):

1. Peak Demand Clipping: Decrease the peak demand
2. Energy Efficiency and Conservation: reduce overall energy usage
3. Load Building: Maximize demand to off-peak hours
4. Load Shifting: Relocate demand to off-peak hours

The DSM strategies have the objectives of increasing end-use effectiveness to prevent or delay the construction of new generation plants (Lim Yun Seng, 2006). Besides, the DSM is also a series of interconnected and flexible programs whereby customers play a great role to decide their own demand for electricity during peak time and cut down their energy consumption in overall (Dabur, Singh, & Yadav, 2012). In (Tande, 2000), the DSM can be used as an effective method to mitigate the power quality issues due to the wind energy integration. The load controller is used to control the loads in order to match with the wind power generation to mitigate the voltage quality issues with the minimum constraints on the renewable energy sources.

Besides, the authors of (Lim, WHITE, NICHOLSON, & TAYLOR, 2005) states that DSM provides a robust solution to mitigate voltage rise issues on a LV distribution network with a large amount of renewable energy sources. However, DSM is not popular in Malaysia. There is insufficient of controlled loads for demand side management to function effectively. In addition, the DSM is highly relies on costly and proprietary technology solutions. Hence, the impact of various DSM programs

should be investigated. Besides, the downside of the DSM is that the customers' acceptance is still very low. Therefore, it is difficult to implement DSM efficiency.

In the paper of (Ning, Luis, & Daniel, 2011), EV is ideal appliances for DSM scheme. This is because the interruption of the charging of an electric vehicle for a few minutes is not a major inconvenience. Hence, electric vehicles will be the first loads to be inhibited during peak time to reduce the peak load and hence, reduce the voltage rise of the networks.

2.4.2 Static Synchronous Compensator (STATCOM)

STATCOM is one of the flexible AC transmission system (FACTS) devices. It is a shunt compensator to control the real and reactive power flows by injecting the current with a controllable angle. It is widely used to control the power factor, regulate the voltage, stabilize the power flow, and improve the performance of the power systems. Under balanced condition, STATCOM works well, whereas a large amount of negative sequence current will be induced when it goes through the STATCOM under unbalanced condition. Therefore, in the paper of (Li, Liu, Wang, & Wei, 2007), novel strategies are proposed to compensate the utility voltage unbalance using the STATCOM. In (Hendri Masdi, 2004), the designed D-STATCOM which is the distribution static compensator can mitigate the voltage sags caused by the three-phase balanced fault. It is the matter of the amount of reactive current needed to be compensated by the D-STATCOM.

The traditional STATCOM are limited to improve the system stability as it has no significant active power capability. Nevertheless, in the paper of (Aarathi A.R, 2014), the usage of STATCOM integrated with super capacitor energy storage system able to enhance the system stability with the grid connected photovoltaic system. In another similar paper, (Xi, Parkhideh, & Bhattacharya, 2008) also states that the D-STATCOM integrated with ultracapacitor, which is kind of energy storage, is suited to mitigate the voltage regulation and voltage sags in the distribution systems. In (E. Ghahremani, 2014), the authors also state that the combination of ESS and STATCOM would add the benefits as individual such as reduced power flows, increased system loadability, lower the transmission line losses, and improve the power system stability. However, the STATCOM is always an expensive option for reactive power control (T. Aziz, 2013).

2.4.3 Energy Storage System

At the moment, there are different mechanisms available for the storage technologies. They can be classified into two categories: short term discharge energy storage devices and long term discharge energy storage devices. For the short term discharge, it responses fast to the power system needs. These kinds of energy storage devices are normally applied in improving the power quality issues, to cover the load during start up, synchronization of the backup generators and to compensate the dynamic response of renewable power sources (Tande, 2003). For long term discharge, it is able to supply power from few seconds to few hours. Their response is usually slower than the short term discharge. It is usually applied on energy management,

renewable energy sources integration and power grid congestion management (Price, Bartley, Male, & Cooley, 1999). Batteries that used commonly are considered as long term discharge devices.

The energy storage system is an expensive option as batteries in this stage of development is expensive, especially those using lithium ion batteries. Currently, lead acid batteries are cheaper than lithium ion batteries. However, the lead acid batteries have relatively short lifespan and its life is reduced when depth of charge and discharge are too high. Nevertheless, it can avoid the renewable power curtailment and reversed power flow (Zito, 2010). In addition, research has been carried out to determine the feasibility of the energy storage system to improve the power quality and provide ancillary services to the electrical networks (Nguyen and Flueck, 2012).

Energy storage systems can be used for many other applications, such as load levelling, load shifting, peak clipping and others. On the other hand, the energy storage system can offer additional benefits in utility settings because it can decouple demand from supply, hence mitigating the frequency deviations and allowing increased asset utilization, facilitating the penetration of renewable sources, and improving the reliability, flexibility, and efficiency of the electrical network (Schoenung, 1996).

The ability to store the energy for later use is important in many circumstances such as the variable and uncontrollable power generation of renewable energy. In the paper (Andreas Poulikkas, 2014), the storage system is introduced to mitigate the

problem of overvoltage due to the PV integration to the LV distribution feeder of Cyprus. Apart from that, the energy storage can provide power whenever the grid reaches its peak demand due to large amounts of plugged-in EV or due to the low penetration of RE to reduce the voltage sags occurred in the networks. The authors of (T. Shigematsu, 2002) states that voltage sags can be mitigated and fluctuating wind power output can be stabilized by using the energy storage system. Hence, the energy storage has smoothing function when the power is not constant. Besides, voltage rise and voltage unbalance caused by intermittent PV can be mitigated using novel fuzzy controlled energy storage on LV distribution networks stated in (Wong, Lim, & Morris, 2014).

An appropriate control strategy of the ESS is important in mitigating the power quality issues. Without any control algorithm used, ESS was controlled manually to obtain the optimum result in the paper of (Chua, et al., 2012). VUF was reduced from 1.6% to 0.8%. It is a 50% reduction in VUF. However, in the paper of (Chua, et al., 2012), the VUF mitigation in low voltage distribution networks with photovoltaic is done with the energy storage system using the PI controller. The results showed that the VUF was reduced from 1.4% to 0.9%, which is a 35.7% drop in VUF. With the fuzzy control strategy in (Wong, Lim, & Morris, 2014), VUF was reduced from 1.9% to 0.9%, which is a VUF mitigation of 52.6% in 5 minutes. Hence, different control strategy of ESS can vary the efficiency in the mitigation of VUF. In this project, fuzzy control algorithm is used as it has the higher percentage in the VUF mitigation.

In conclusion, the integration of energy storage appears as a very positive solution for the power unbalance mitigation. It can act as a frequency control at the transmission level, voltage control and capacity support at the distribution level. Besides, it can be installed to provide peak shaving at the consumer level. Also, the energy storage system can be used to mitigate the power quality issues caused by renewable energy and electric vehicles provided it is equipped with an appropriate control strategy.

2.5 Summary

The government has launched variety of incentives and programmes to promote the penetration of renewable energy and electric vehicles to reduce the greenhouse gas emissions. However, power quality issues such as voltage rise, voltage unbalance, power factor and voltage sags influence the performance of the electrical network due to the large integration of distributed renewable energy sources and plugged-in electric vehicles. The existing methods on mitigating power quality issues might not be economically attractive because the super-capacitor, STATCOM and SVC are too expensive. In addition, they are generally used in transmission system rather than LV distribution networks to cater the problems. The active management is also one of the solutions to overcome the technical issues as it can respond based on the network conditions. Since the energy storage system is also considered as an active management system, the energy storage system can be an appropriate solution for mitigating these power quality issues due to the penetration of renewable energies and electric vehicles.

CHAPTER 3

ARCHITECTURE OF THE EXPERIMENTAL LV NETWORK

3.1 Introduction

The Malaysian LV distribution network is a radial three-phase four-wire system with voltages of 33 kV, 11 kV, and 415 V. A laboratory scale experimental LV distribution network is designed to emulate the real LV distribution network in Malaysia. This is to investigate the effects of the penetration of RE and EV on the distribution networks. In this chapter, the design and each of the elements of the experimental LV distribution network are explained. The physical architecture of the proposed energy storage system is also presented in this chapter

3.2 Experimental LV Distribution Network

An experimental LV distribution network is developed to investigate the effectiveness of the fuzzy controller as shown in Figure 3.1. This network is a Terra-Terra (T-T) earthing three-phase four-wire system. It consists of a network emulator, two single-phase 3.6 kW_p PV systems, a 2.0 kW single-phase wind turbine emulator, a 9 kW three-phase load emulator, an electric vehicle and the fuzzy controlled energy

storage system. Each of the devices will be further elaborated in the following subsection.

Bb

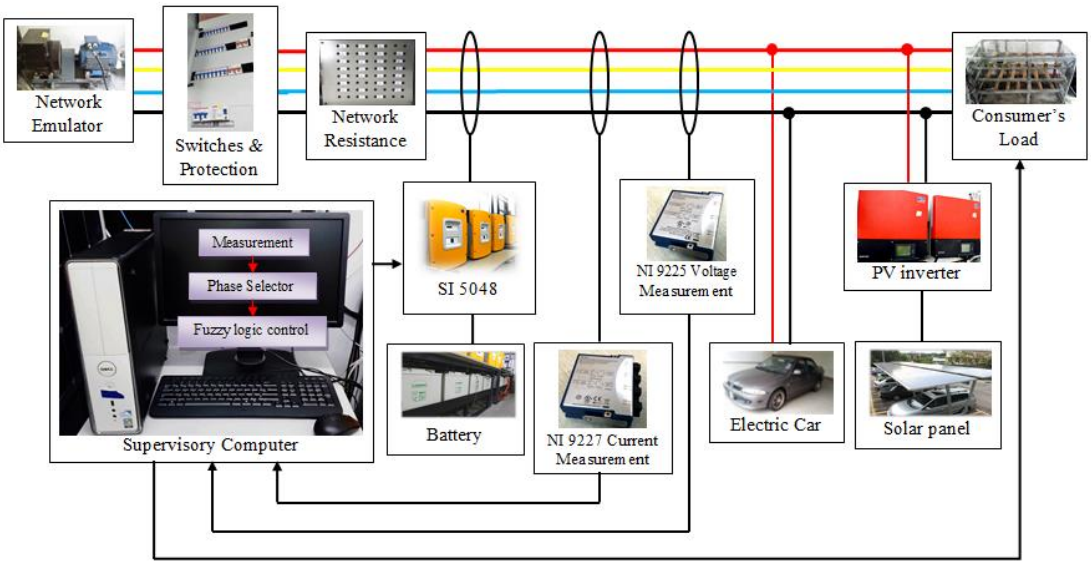

Figure 3.1: Experimental network diagram

Figure 3.2 shows the flexible LV panel. All the loads, electric vehicle, energy storage system, wind turbine emulator and PV are connected to the LV network through this LV panel via 5-pin plug. There are phase selector switches installed for PV systems, wind emulator systems, and electric vehicles. Therefore, these single-phase devices can be switched to other phases according to the condition. All the power meters are mounted on this LV panel for monitoring purposes. The main circuit breaker is used to protect the load bank from overcurrent and short circuit. Moreover, overcurrent protection and residual current circuit breaker are installed in the panel for safety and protection purpose and to protect the equipment. There is also an emergency stop to disconnect the incoming power from the grid to avoid any hazard accident to happen. Figure 3.3 shows the experimental setup in the laboratory.

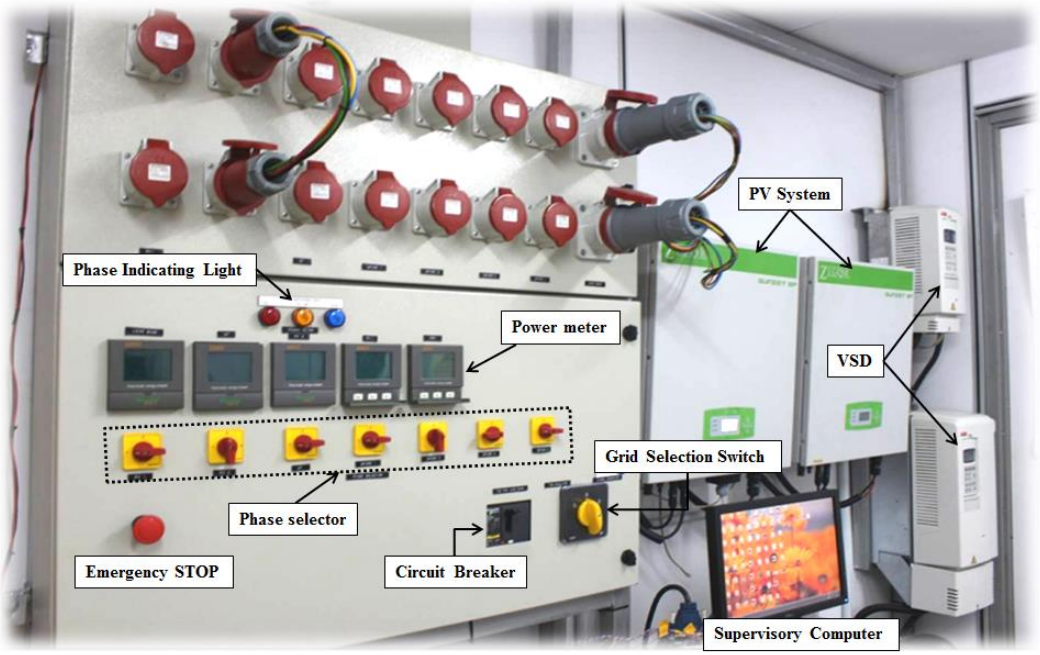

Figure 3.2: Flexible LV panel

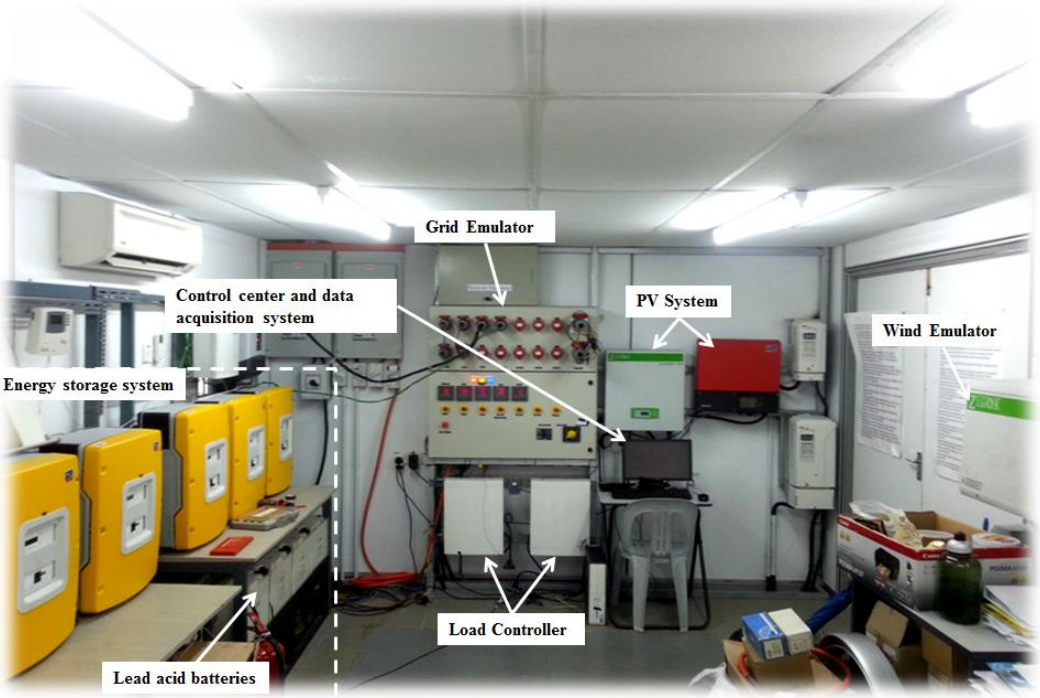

Figure 3.3: Experimental setup

3.2.1 Network Emulator

A network emulator is used to represent the LV distribution network in Malaysia. The network emulator is a 15 kVA synchronous generator coupled to an induction machine controlled by a variable speed drive (VSD) as shown in Figure 3.4. Figure 3.5 shows the VSD of ABB with model number of ACS800-01-0025-3+E200+K458. Figure 3.6 is the synchronous generator coupled to an induction motor. The specification of the VSD is also shown in Table 3.1. The system frequency can be varied by changing the reference speed of the VSD. The VSD drives the induction motor at 1500 rpm. Hence, the system frequency is regulated at 50 Hz, 240 V for the experiments. The network emulator can provide power balance over the three-phase system. With this design, it can decouple the experimental network emulator from the utility grid. This network emulator is a three-phase four wire configuration with T-T earthing system which is a common configuration in Malaysia.

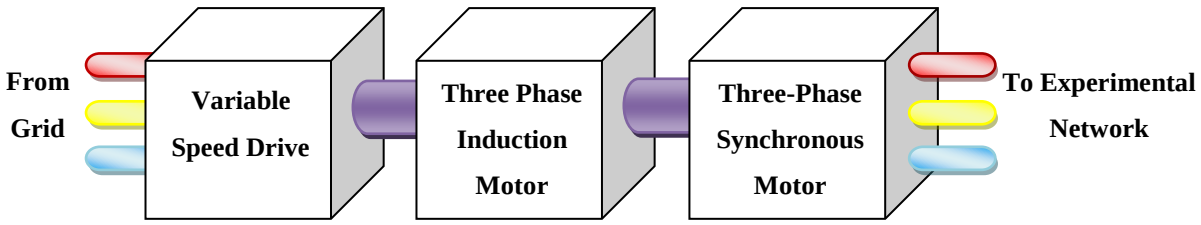

Figure 3.4: Grid emulator

Figure 3.5: Variable speed drive used to drive the induction motor

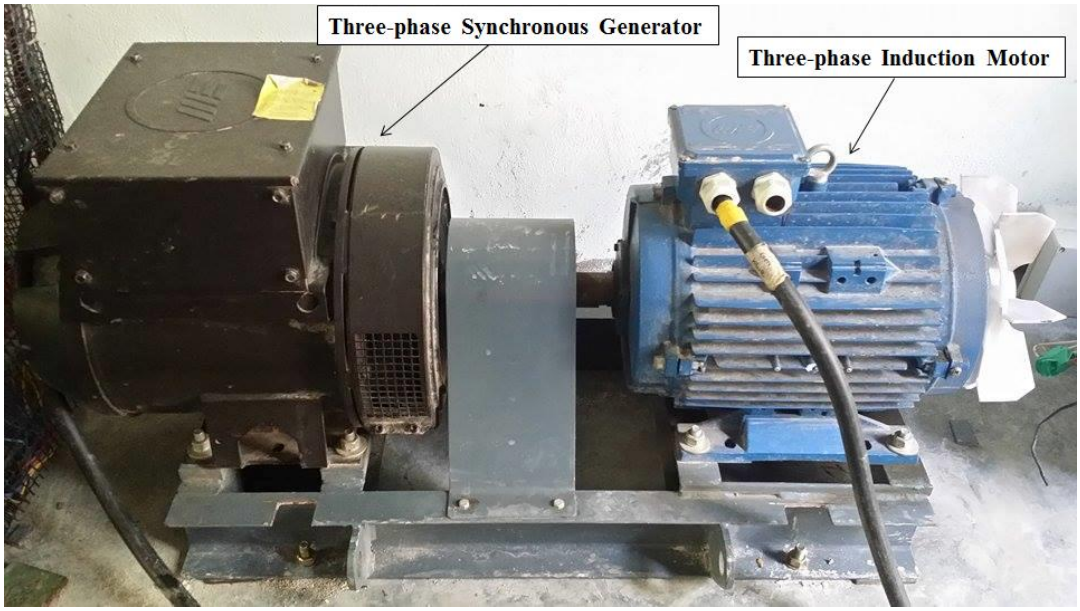

Figure 3.6: Synchronous generator coupled to an induction motor

Table 3.1: Specifications of VSD for network emulator

Characteristics	**Specifications**
Input Voltage	3~ 380…415 V
Input Current	42 A
Input Frequency	48…63 Hz
Output Voltage	3~ 0…U_{Input} V
Output Current	44 A
Output Frequency	0…300 Hz

3.2.2 Photovoltaic Systems

Solar panels that used in this experiment are built by 32 panels of polycrystalline PV modules, a product of Panasonic with model number VBMS230AE01. These panels are categorized to 4 strings, 8 panels in a string. From the specifications of the PV modules in Table 3.2, each module can contribute a maximum power of 230 W. Therefore, each string will have the capacity of 1.84 kWp and the total capacity of the PV system is 7.36 kWp. The PV modules are oriented 5º tilt to face north. This allow the dust on the PV modules be washed by the rain water and allow sunlight to penetrate on the PV modules throughout the day. Figure 3.7 shows the line diagram which PV modules are connected to the 3.88 kWp PV inverter named Sunny Boy Transformerless Inverter, SB 3600TL-21. Figure 3.8 is the solar panel mounted on the 3.3 m height metal structure in the real experimental setup.

Table 3.2: Specification of PV modules

No	Characteristics	Specifications
1	Maximum power (P_{max})	230 W
2	Short circuit current (I_{sc})	8.42 A
3	Open circuit voltage (V_{ac})	37 V
4	Maximum power current (I_{pmax})	7.83 A
5	Maximum power voltage (V_{pmax})	29.4 V
6	Maximum system open circuit voltage	1000 V

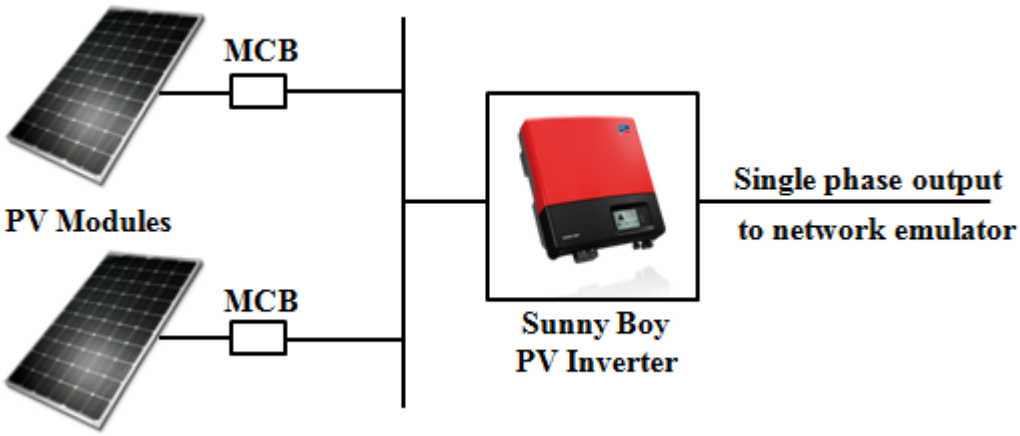

Figure 3.7: PV system

Figure 3.8: Photovoltaic panel mounted on a metal structure

3.2.3 Wind Turbine Emulator

The wind turbine emulator is consisted of a three-phase induction motor coupled with a three-phase synchronous machine, a variable speed drive, a rectifier and a single-phase inverter known as SMA Windy Boy 2500. This wind turbine emulation system is illustrated in Figure 3.9. The variable speed drive (VSD) is used to control the speed and torque of the induction machine in order to emulate the actual speed and torque characteristics of the wind turbine. The VSD from ABB with model

number of ACS800-01-0005-3+E200+K458 is used in this project as shown in Figure 3.10 (b). Figure 3.10 (a) is the induction motor coupled with the synchronous machine which is used as the emulator. The specification of the VSD is also shown in Table 3.3. The three-phase output is then rectified using a rectifier to supply DC voltage to the Windy Boy. Due to the specification of Windy Boy in Table 3.4, it will provide 50 Hz, single phase AC voltage with nominal voltage of 230 V_{ac} to one of the phases of the experimental LV distribution network. Figure 3.11 (a) and (b) show the rectifier and SMA Windy Boy used in the wind turbine emulation system.

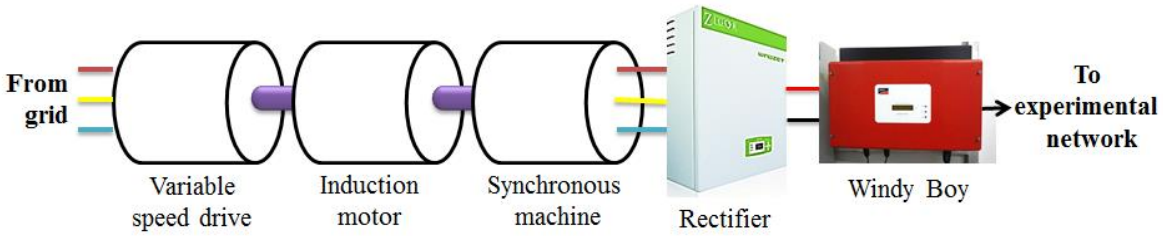

Figure 3.9: Topology of the wind turbine emulation system

(a) (b)

Figure 3.10: (a) Induction motor coupled with synchronous machine driven by (b) VSD of wind turbine emulator

Table 3.3: Specifications of VSD for wind emulator

Characteristics	**Specifications**
Input Voltage	3~ 380…415 V
Input Current	7.9 A
Input Frequency	48…63 Hz
Output Voltage	3~ 0…U_{Input} V
Output Current	8.5 A
Output Frequency	0…300 Hz

Table 3.4: Specifications of SMA Windy Boy 2500

Characteristics	**Specifications**
VDC max	600 V
VDC MPP	224 – 480 V
IDC max	12 A
VAC nom	230 V
fAC nom	50/60 Hz
PAC nom	2300 W
IAC nom	10 A
cos φ	1

(a) (b)

Figure 3.11: (a) Rectifier; (b) SMA Windy Boy 2500

3.2.4 Electric Vehicles

The electric vehicle used is the Proton Wira converted by UTAR students as shown in Figure 3.12. This electric vehicle is designed to use three-phase AC motor and the speed of motor is controlled using the motor controller of Curtis 1239-8501. The motor can be operated at high voltage ranging from 144 V to 170 V. When the current is increased to 500 A, the speed of the motor can reach up to 88 horsepower and 108 lbs of torque. The maximum current output rating of the battery charger used is 15 A, having 93 % of efficiency. When the electric vehicle is plugged to the network, it can be charged up to 12 A practically. It is connected to the network through the LV panel via the 5-pin plug. Figure 3.13 shows the 5-pin connector of the electric vehicle. In this experiment, electric vehicle acts as a significant load to absorb power from the network and causing voltage to drop significantly.

Figure 3.12: Electric vehicle used in the experiment

Figure 3.13: Charging connector of the electric vehicle

3.2.5 Load Emulator

Three phase load bank in Figure 3.14 is designed and built to emulate the consumer load. The load bank consists of 18 units of 500 W power resistors. Each resistor can be controlled by triggering the solid state relay (SSR) and the relay is controlled via Labview control system using NI 9403 Digital Output Module as interface between the supervisory computer (PC) and the controllable load. This NI 9403 is a 37 channel, 7 µs bidirectional digital I/O module for NI Compact DAQ chassis. Each channel is compatible with 5 V/TTL signals and providing 32 digital input or output channels as shown in Figure 3.15. The COM lines will be referred as the common point for the signals. The 5 V digital signals will be channelled to the D2425 SSR as shown in Figure 3.16. This D2425 SSR is silicon controlled rectifier output which is suitable for heavy industrial loads and it is operated with zero switching. The control voltage is 3-32 VDC and the current rating is 25 A. Figure 3.17 shows the configuration of the controllable load bank. Each phase can be loaded up to 3000 W

with an increment of 500 W per step. However, there is limitation for the designed load bank as it is purely resistive. Hence, the load bank is having the unity power factor all the way. In order to emulate a better consumer load, inductive load is connected.

Figure 3.14: Load bank used in the experimental

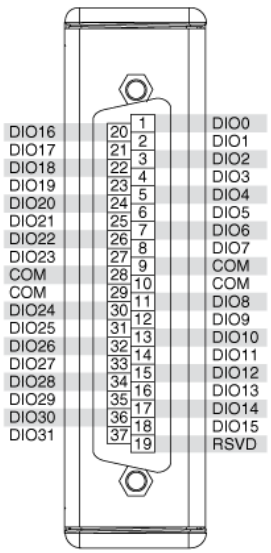

Figure 3.15: NI 9403 37 channels connection diagram

Figure 3.16: D2425 Solid State Relay

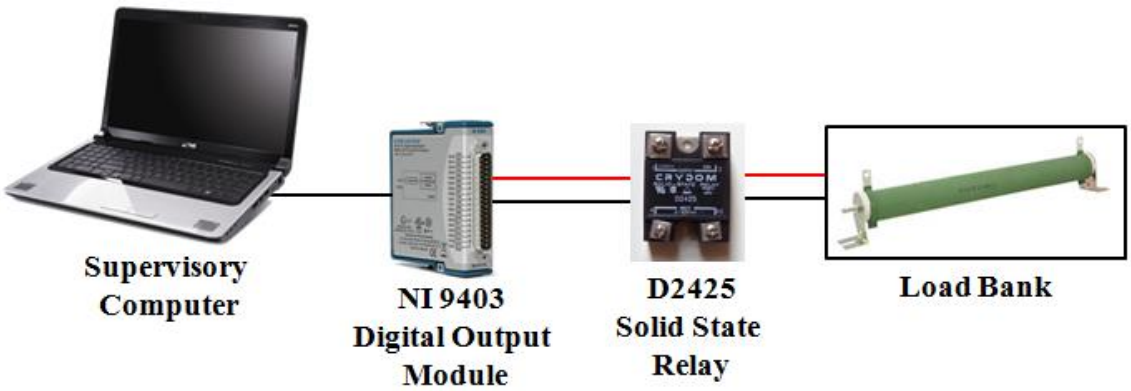

Figure 3.17: Arrangement of controllable load bank

Inductive load used in the experiment is the laboratory equipment from ELWE Germany as shown in Figure 3.18. It is a three-phase variable inductive load consisted of 8 steps. It has 45 - 360 Var and the current rating is 0.2 - 1.56 A. Applying the rating given, inductance calculated using the formula P=IV, $V_L=I_LX_L$ and $X_L=2\pi fL$, inductance, L, is in the range of 0.47 - 3.58 H. However, based on the measurement, inductance calculated is in the range of 0.339 - 2 H. Hence, this inductor load can only contribute maximum of 259 Var for each phase during the

experiment. This inductive load is used to vary the power factor of the emulated network. Power factor will be 0.85 when inductive load is switched to 7 steps.

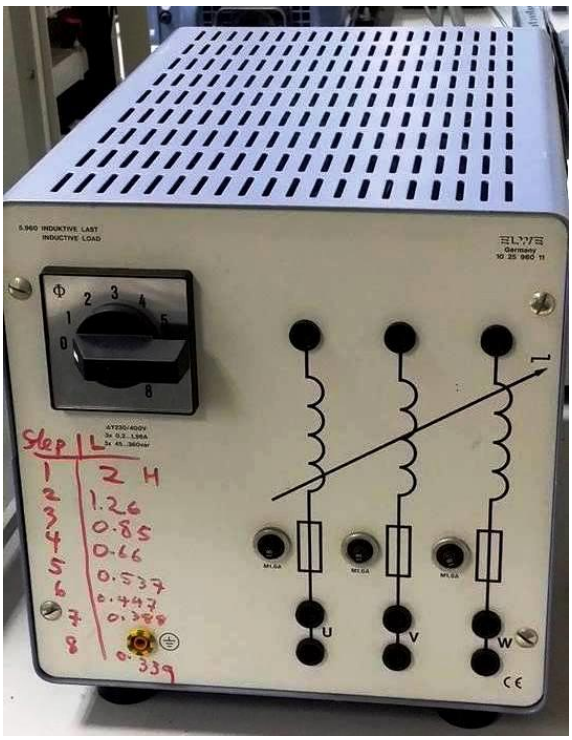

Figure 3.18: Inductive load used in the experiment

3.2.6 Energy Storage System

The proposed energy storage system consists of three bi-directional inverters. Each bi-directional inverter is integrated with four battery banks. A RS232/RS485 converter is the communication link between the supervisory computer and the bi-directional inverter. The structure of the proposed energy storage system is shown in Figure 3.19. The Sunny Island is able to be controlled to maintain the voltage and frequency of the grid at a constant level to mitigate the voltage rise, voltage unbalance and improve the power factor of the networks. This energy storage system

is usually installed at the loads because RE and EV are usually placed at the customer sides.

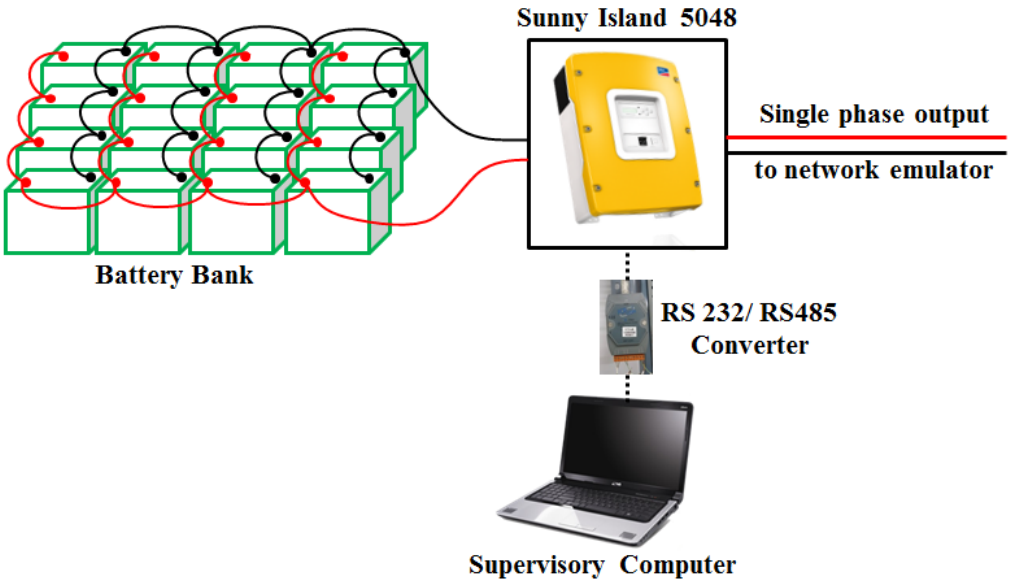

Figure 3.19: Setup of the proposed energy storage system

3.2.6.1 SMA Sunny Island 5048

Sunny Island 5048 is a bi-directional inverter produced by SMA GmbH, Germany. The most advanced technology used in their Sunny Boys is combined with an outstanding feature set for off-grid PV applications to form the SMA's next generation of Sunny Island inverters. The new Sunny Island 5048 shown in Figure 3.20 has incredible surge capabilities and excellent AC output characteristics. It provides a very clean and stable 230 VAC output. Multiple units can be used together for single-phase or three-phase applications. In this project, three Sunny Islands are used for each phases. The power provided by the Sunny Island can be increased by simply adding an additional Sunny Island inverter in parallel. The Sunny Island also has the special ability to facilitate AC coupling of all the power

generation sources. This is kind of efficient use of available AC power and greatly simplifies the system expansion. The overall life of the batteries is optimized with the help of the Sunny Island 5048 through its advanced battery management system. Estimation of state of charge of the batteries can be obtained by this battery management system as criteria for the energy storage system to charge and discharge.

Figure 3.20: Sunny Island 5048 bi-directional inverter

One of the greatest advantages of AC coupling is that it allows any type of power generating device to be integrated to the system, such as solar, wind, hydro, even gas or diesel powered generators. Hence, the chance to take advantage of all the resources available at different location is offered to the system designers. It also allows for easy system expansion by providing a solution for connecting future power sources. AC coupling offers simple system expansion and guarantees that the system will continue to serve the needs of its users safely and reliably over the long term.

As a conclusion for Sunny Island 5048, the settings needed for the operation can be configured in few steps. It is flexible in its application, extendable and takes on all the control processes. In addition, the device is highly efficient and has an ergonomic die-cast aluminum enclosure. For systems, it is flexible from 3 kW to 300 kW, single and three-phase operation. It is connectable in parallel and modularly extendable, AC and DC coupling. It is simple and easy commissioning with the "Quick Configuration Guide" and complete off-grid management. It has high efficiency, intelligent battery management for maximum battery life, charge level calculation to obtain the condition of battery. It has extreme overload capacity, OptiCool active cooling system and 2-year SMA warranty. Sunny Island also offers the highest flexibility where real time active and reactive power controls are possible. With this features, the Sunny Island 5048 integrated with batteries are controlled by the proposed fuzzy controller to mitigate the voltage rise, voltage unbalance and improve the power factor caused by the intermittent RE power output on LV distribution networks. Table 3.5 shows the specifications of SMA Sunny Island 5048 used in this project.

Table 3.5: Specifications of SMA Sunny Island 5048

Output data	
Nominal AC voltage (adjustable)	230 V (202 V – 253 V)
Grid frequency adjustable	45 Hz – 55 Hz
Continuous AC output at 25 °C / 45 °C	5000 W / 4000 W
Continuous AC output at 25 °C for 30 / 5 / 1 min	6500 W / 7200 W / 8400 W
Nominal AC current	21 A
Max. current	100 A (for 100 ms)
Output voltage harmonic distortion factor	< 3 %
Power factor	–1 to +1
Input data	
Input voltage (range)	230 V (172.5 V – 250 V)
Input frequency	50 Hz (40 Hz – 70 Hz)

Max. AC input current (adjustable)	56 A (2 A – 56 A)
Max. input power	6.7 kW /12.8 kW
Battery data	
Battery voltage (range)	48 V
Max. battery charging current	120 A
Continuous charging current	100 A
Battery capacity	100 Ah to 10000 Ah
Charge control	IUoU with automatic full and equalization charge

3.2.6.2 Batteries

Batteries store energy in electrochemical form, creating electrically charged ions. However, batteries consist of varieties of technologies, applying different operation principles and materials. The most important battery concepts are electrochemical and redox flow. For electrochemical batteries, there are lead acid, nickel cadmium, nickel metal-hydride, sodium sulphur, lithium ion and others. Lead acid batteries are commonly used due to its reasonable price.

Battery used in this project is Hoppecke solar.bloc valve-regulated lead acid (VRLA) battery for typical applications of solar or off grid applications, storage for direct consumption of photovoltaic energy, telecommunications and traffic systems. This VRLA battery is reported to have a higher operational efficiency and longer lifetime. Figure 3.21 shows the batteries used in the experiment. Each battery bank consists of four VRLA batteries rated at 48 V, 115 Ah. Four banks are connected in parallel in order to increase the capacity to 460 Ah. The nominal voltage of the battery is 12 V which is having a total capacity of 5.52 kWh. The rated power for the Sunny Island used is 4.0 kW at 45°C and 5.0 kW at 25°C. Figure 3.22 shows the connection of the

energy storage system. This energy storage system acts as one of the energy sources in the experiment.

In terms of sizing of the battery, assumed that 400 W demand is introduced in the network. Using the equation 3. 1, the annual energy consumption is 3504 kWh, while the efficiency is assumed to be 90%, battery size needed for a 1-day supply is 222.22 Ah. In the experiment, 460 Ah battery is connected, however, only 230 Ah is useable due to its 50% of depth of discharge. Hence, the battery used in the experiment is able to sustain the 400 W load in a day, assuming there is no any PV power output for the day. In order to sustain for a week, the battery capacity needed is 1555.55 Ah.

Hence, the rated battery capacity has to be above 3111.1 Ah in order to sustain for a week.

$$Battery\ size\ [Ah] = \frac{Autonomy\ time\ x\ \frac{Annual\ energy\ consumption}{365}}{Efficiency}\ x\ \frac{1000}{Battery\ voltage}$$

----- (3.1)

Figure 3.21: Batteries

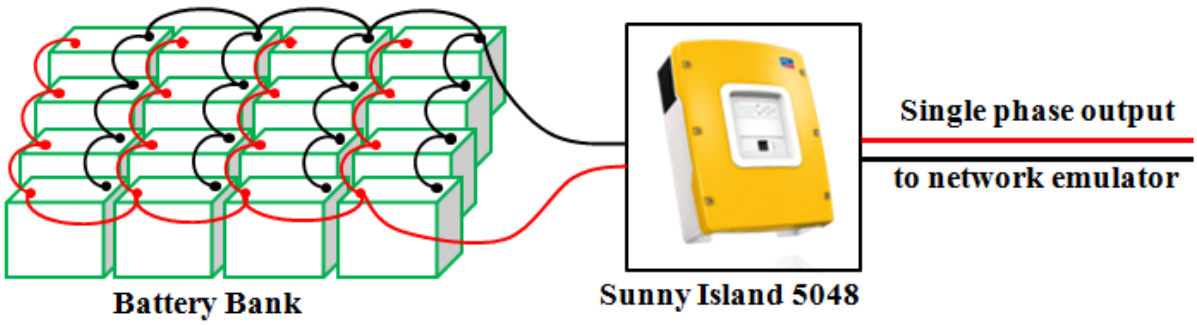

Figure 3.22: Arrangement of energy storage system

The main benefit of the lead–acid battery is its low cost; the main drawbacks are its large size and weight for a given capacity and voltage (Buchmann, 2009). Lead–acid batteries should never be discharged to below 20% of their full capacity, because internal resistance will cause heat and damage when they are recharged. Therefore, 50% is the recommended state of charge (SOC) for the batteries. Figure 3.23 shows the estimated life cycles based on depth of discharge for C_{10} Hoppecke solar.bloc, which is the batteries used in the experiment (Hoppecke, 2012). It is observed that, 1,193 life cycles can be obtained with 48% depth of discharge.

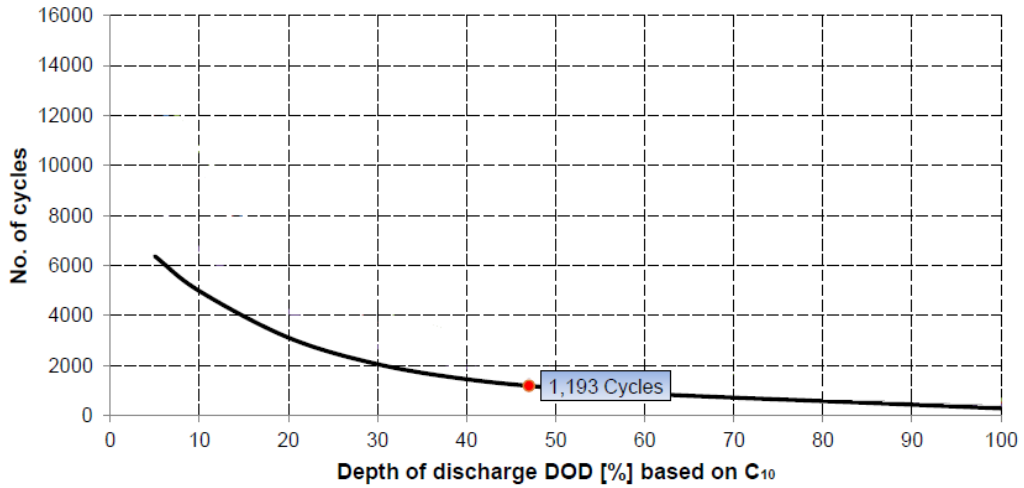

Figure 3.23: Depth of discharge for C_{10} Hoppecke solar.bloc

The higher the conversion efficiency, the less energy is converted into heat and hence, the faster a battery can be charged without overheating. The conversion efficiency of the batteries is better when the batteries are having lower internal resistance. One of the main reasons why lead-acid batteries monopolize the energy storage markets is that the conversion efficiency of lead-acid cells at 85%-95% which is much higher than Nickel-Cadmium (NiCad) at 65%, Alkaline (NiFe) at 60%, or other cheaper battery technologies. Lead-acid is moderately expensive, having moderate energy density, and moderate rate of self-discharge. Higher discharge rates result in considerable loss of capacity. So, lead acid batteries are used in the project for charge and discharge purpose.

3.2.7 Communication and Data Acquisition Using LabVIEW

A data acquisition system is developed for monitoring the power flow of the network. Several 40/5 A current transformers are used to measure current while NI 9225 3 Channels Voltage Measurement Card is used for voltage measurement. Elcontrol STAR 3 power meters are used to measure and display the parameters. All the three-phase voltage and current at the point of connection around the LV distribution network are monitored. The data acquisition device used is the CompactDAQ 9174 Data Acquisition Chassis together with the NI 9225, a 3 Channels Voltage Measurement Card module. Figure 3.24 shows the CompactDAQ 9174. The chassis is connected to the PC to monitor the RMS voltage via Laboratory Virtual Instrument Engineering Workbench (LabVIEW).

Figure 3.24: CompactDAQ 9174 Data Acquisition Chassis

Another data acquisition device used is the Data Taker DT82 as shown in Figure 3.25. It is a stand-alone and real time data logger which is used to acquire every data entry. It can communicate with PC through Ethernet, USB, or RS232. Ethernet is used in this project. A web based program developed by the manufacturer can be accessed by the internet protocol (IP) address assigned to the data logger. Therefore, Data Taker is configured to acquire the data needed and the PC is used to record the

data collected via LabVIEW. The program written in the data logger to acquire data from the power meters is shown in Appendix A.

Figure 3.25: Data Taker DT82 Intelligent Data Logger

The PC is connected to the three single-phase energy storage system using RS232/ RS485 converter of ICP CON 7563. Signals sent are interpreted into a standard open process control (OPC) format via YAOPC server which is under SMA possession protocol. Hence, the energy storage system can be controlled through the control algorithm developed in LabVIEW. Figure 3.26 shows the flow of data measurement and the instruction between PC and the three-phase energy storage system.

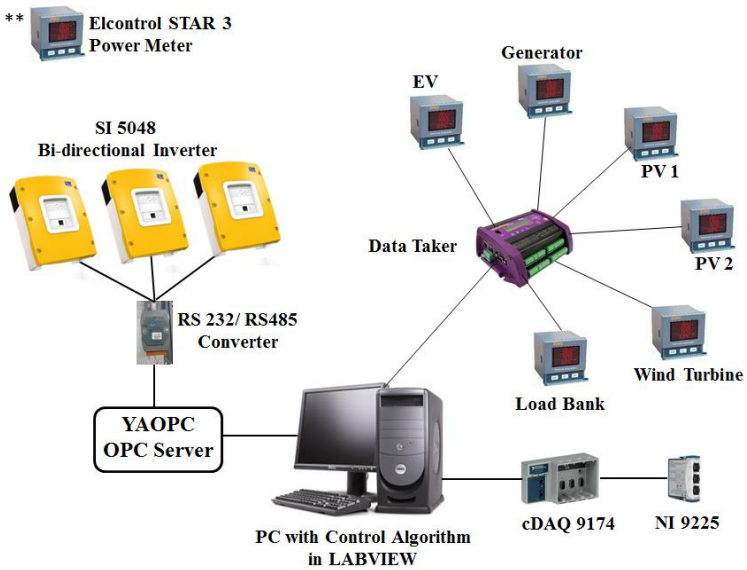

Figure 3.26: Data acquisition between PC, Data Taker, cDAQ 9174, and the bi-directional inverter

LabVIEW is used in this project to develop the control algorithm. The programming language applied in LabVIEW is a dataflow programming language. By connecting the wires, the structure of a graphical block diagram on different function-nodes is used to control the execution. Variables are propagated with these wires and all the nodes can be carried out once all the input information is ready. It is capable to execute in parallel since multiple nodes can be run at the same time.

The configuration of user interfaces is tied into the development cycle which known as a front panel. The LabVIEW programs are named as virtual instruments (VIs). There are three elements in each VI, namely: front panel, block diagram, and connector panel. The controls and indicators on the front panel can input data or export data from an executing VI. The VI can be used as a subVI. Hence, a VI can either be executed as a normal program with its front panel or dropped as a node onto the block diagram as subVI. The connector panel is used to determine the inputs and outputs node. This means that each VI can be easily tested and troubleshooting work can be done before being embedded into a larger program.

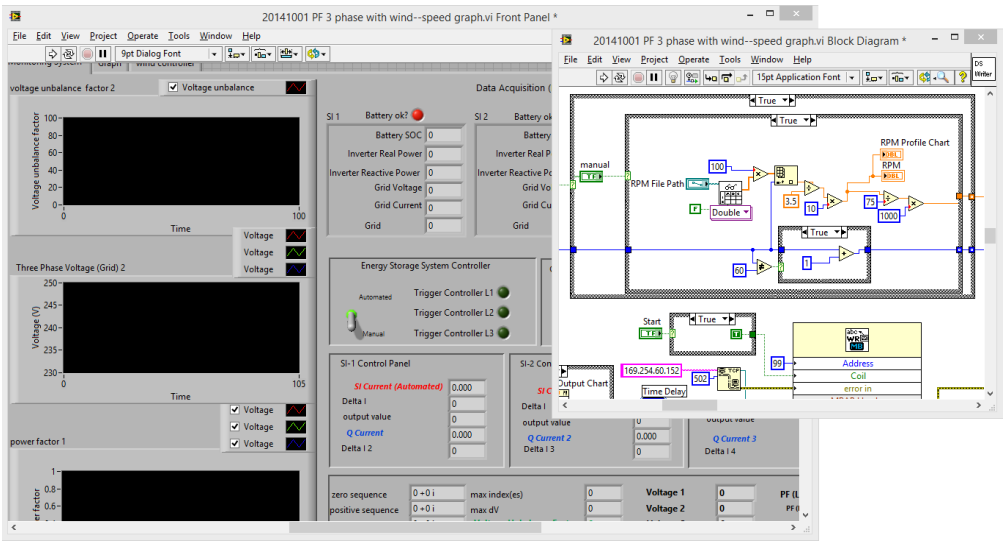

Figure 3.27: Screenshot of LabVIEW program

Figure 3.27 is a LabVIEW program illustrating the necessary elements in LabVIEW programming, which is the dataflow of block diagram in the right frame and the I/O variables in graphical objects in the left frame. The entire algorithm will be designed and constructed in the block diagram while the front panel is the graphical user interface presented.

The main benefit of LabVIEW as compared to other programming tools such as C++, C#, and FORTRAN, is their wide-ranging support for accessing instrumentation hardware. It also contains drivers and abstraction layers for many different types of instruments and buses. The abstraction layers provide standard software interfaces to communicate with the hardware devices. Hence, the provided driver interfaces can save the program development time. The National Instrument is much user friendly as compared to other traditional or competing systems because people who are having limited knowledge in writing a program can write programs and set up test solutions in a shorter time period with LabVIEW.

3.3 Summary

The LV distribution network is set up to study the loading and generation conditions. This network consists of a network emulator, photovoltaic systems, wind turbine emulation systems, electric vehicles, load emulator, and energy storage system with SMA Sunny Island 5048 and batteries. The network emulator is a 15 KVA synchronous machine coupled with an induction motor driven by a variable speed drive to regulate the system at 240 V, 50 Hz. Two PV systems, a wind emulator and an electric vehicle are installed on the experimental LV network. All the devices are single-phase and phases to connect can be selected freely by switching the phase selector. Besides, a 9.0 kW three-phase controllable purely resistive load bank is developed. A laboratory equipment of three-phase inductive load is also used to vary the power factor of the networks. The data acquisition system is formed by several current transformers, power meters, data logger, NI CompactDAQ chassis with measurement cards, and a supervisory computer. All the measurements are displayed and recorded using LabVIEW. Performance of the experimental LV distribution network is tested. It is similar to the Malaysia's LV distribution networks.

CHAPTER 4

Design of Control Algorithm

4.1 Introduction

The details of the control strategy of the proposed fuzzy controlled energy storage system are presented in this chapter. Fuzzy logic is selected as the strategy of the controller because it can produce an appropriate output based on the needs and changes of the network parameters, which is different from the conventional Boolean method as controller. Hence, the amount of real and reactive power can be manipulated based on the changes of network parameters effectively. The coding in LabVIEW is also explained in this chapter.

4.2 Fuzzy Controller for the Energy Storage System

Load demand, resistance, and reactance of the distribution network are usually unknown and varying time by time, imply voltage unbalance, voltage fluctuation and power factor also varying simultaneously. Particular measure of real power that energy storage system needed to supply or absorb, to maintain the network voltage

level, is hard to be estimated by using the analytical method as voltage magnitude is dynamic. The equation of voltage variation is expressed as follow:

$$V = V_{nominal} + \frac{RP_{PV-L} + XQ_{PV-L}}{V_{nominal}} + j\frac{XP_{PV-L} - RQ_{PV-L}}{V_{nominal}} \quad \text{---------- (4.1)}$$

where R and X are the line resistance and reactance, $V_{nominal}$ is the rated voltage at the PCC. While $P_{PV\text{-}L}$ and $Q_{PV\text{-}L}$ are denoted as

$$P_{PV-L} = P_{Load} - P_{PV} \pm P_{Inverter} \quad \text{---------- (4.2)}$$

$$Q_{PV-L} = Q_{Load} - Q_{PV} \pm Q_{Inverter} \quad \text{---------- (4.3)}$$

where P_{Load} and Q_{Load} are the real and reactive power of the load, P_{PV} and Q_{PV} are the real and reactive power output of PV, $P_{Inverter}$ and $Q_{Inverter}$ are the real and reactive power output of the bi-directional inverter. Voltage at the PCC is maintained within the tolerance boundary when $P_{Inverter}$ and $Q_{Inverter}$ are determined provided other parameters are recognized. However, it is unknown for R and X. In addition, $P_{Inverter}$ and $Q_{Inverter}$ is in constantly changing power flow condition. Therefore, fuzzy logic control is much appropriate to solve the dynamic voltage problems due to uncertainty of parameters needed.

The extended fuzzy control algorithm is developed using LabVIEW in a PC which is linked to the bi-directional inverters. Real time measurements will be collected and manipulated by the controller such that an appropriate instruction can be sent to the inverters for any remedial actions. The real and reactive power output of the energy storage system can influence the network voltage. However, real power is more influential than the reactive power on the distribution network because the resistance is greater than the reactance of the lines. Therefore, real power is used to correct the

voltage on the network. Below is the equation showing how the voltage change (ΔV) is related to the real (P) and reactive power (Q) output of the energy storage (Jenkins, 2000).

$$\Delta V = \frac{RP + XQ}{V} \approx \frac{RP}{V} \qquad \text{---------- (4.5)}$$

where R and X are the resistance and reactance of the distribution line. On the other hand, reactive power is used to correct the power factor because the resistance is greater than the reactance of the distribution lines as shown in Eq. (4.6) (Jenkins, 2000). However, the real power can still influence the power factor because the amount of real power involved to correct the voltage is significant. The power factor correction cannot be achieved satisfactory if it is carried out simultaneously with the voltage correction. This is because the energy storage is not able to identify the right amount of reactive power to be injected to correct the power factor if the energy storage is still adjusting its real power injection. Therefore, it is proposed to correct the voltage before the power factor.

$$\delta V = \frac{XP + RQ}{V} \qquad \text{---------- (4.6)}$$

Figure 4.1 shows the flow chart of the control algorithm. The controller begins with the collection of the measured three individual phase voltages (V_{phx}) and three individual phase power factors (PF_{phx}) in real time from the monitoring system. V_{phx} is the measured voltage at the PCC. The controller will check whether the voltage is within the acceptable range of 238 V and 243 V or not. Park's transformation is used to determine the phase with the maximum voltage deviation. Voltage deviation, ΔV_y, is computed by using $V_{yphx}–V_{ref}$, where V_{yphx} is the measured voltage of the most severe phase at the PCC and V_{ref} is the nominal voltage rated at 240 V.

The fuzzy controller uses ΔV_y as one of the linguistic variables to create seven linguistic terms through fuzzification in order to generate one output (ΔI_p) as the instruction to the bi-directional inverter through defuzzification. The bi-directional inverter will adjust its real power output accordingly. This process will continue until the voltage magnitude is within the statutory limit. Once the voltage magnitude is restored, the voltage unbalance factor will also reduced.

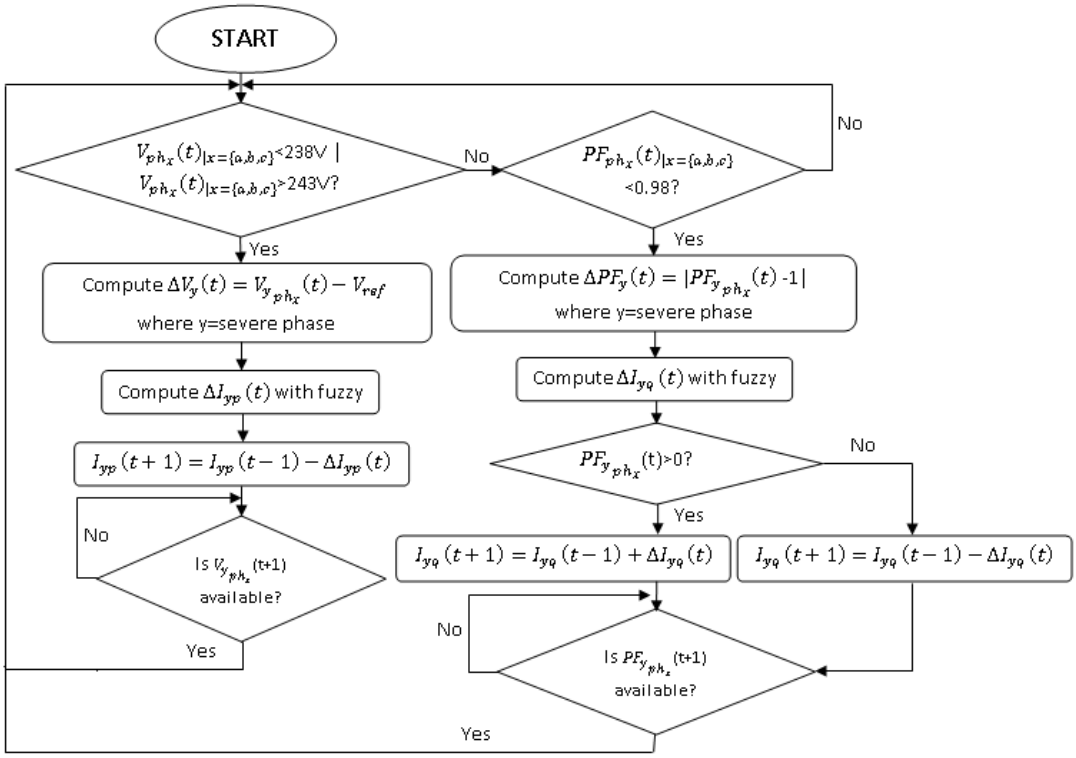

Figure 4.1: Flowchart of control algorithm

Figure 4.1 shows that the controller will correct the power factor if the voltage magnitude is with the acceptable range of 238V and 243 V. If the voltage is out of the acceptable range of 238 and 243 V, then the controller will correct the voltage first before the power factor. Similarly, should the measured power factor is below

0.98, ΔPF_y is computed by using $|PF_{yphx}-1|$, where PF_{yphx} is the power factor of the severe phase at the PCC. The fuzzy controller uses ΔPF_y in the fuzzy system to create one output (ΔI_q) as the instruction to the bi-directional inverter. The instruction I_q is used to manipulate the reactive power flow of the energy storage system in order to improve the power factor of the network. The details of how ΔI_p and ΔI_q are generated will be discussed in the following. The meaning of the inequality of $PF_{yphx}(t)$ is to check whether the power factor is leading or lagging at time t. If $PF_{yphx}(t)$ is greater than 0, then the power factor is leading. If it is not greater than 0, then the power factor is lagging.

4.2.1 Details of the Fuzzy Controller

As mentioned above, ΔV_y used as the input parameter for the predefined fuzzy membership includes seven linguistic terms of voltage condition. It is necessary to convert the voltage deviation and power factor into linguistic variables. This is because the fuzzy controller takes the linguistic variables as the inputs that describe the conditions of voltage and power factor with continuous values starting from 0 to 1. Therefore, the control signal derived from the de-fuzzification is a precise instruction to the energy storage system to restore the voltage and power factor in a relatively short period as compared to any basic control algorithm. They are extremely undervoltage (EUV), very undervoltage (VUV), undervoltage (UV), normal (Normal), overvoltage (OV), very overvoltage (VOV), and extremely overvoltage (EOV) as shown in Figure 4.2. While the predefined fuzzy membership for ΔPF_y also includes seven different envelopes of power factor condition. Two of

the input parameters are not linked together. They will be triggered by different condition and criteria. They are negative extremely high power factor (-EHPF), negative high power factor (-HPF), negative power factor (-PF), undefined (Undefined), positive power factor (+PF), positive high power factor (+HPF), and positive extremely high power factor (+EHPF) as shown in Figure 4.3. These memberships functions will be mapped to determine the types of instructions.

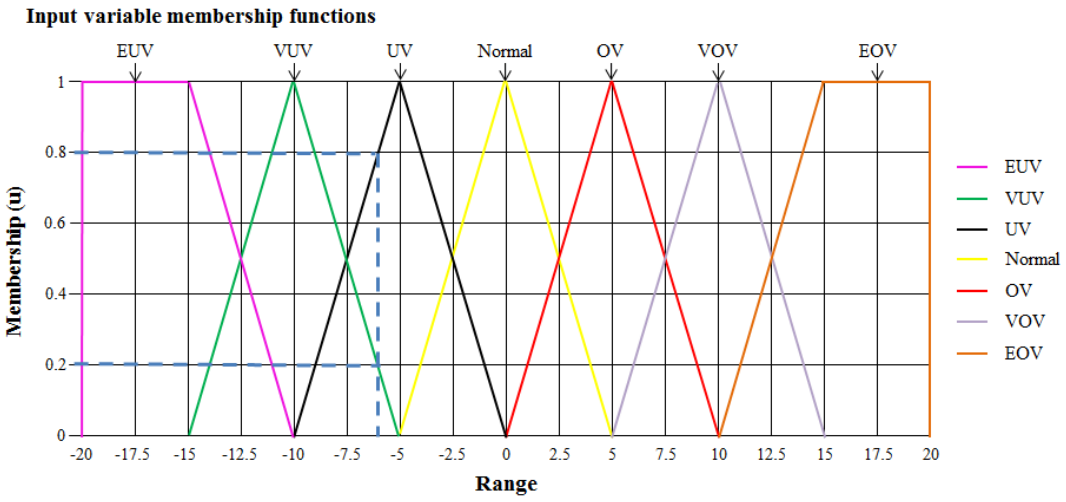

Figure 4.2: Fuzzy logic input variable membership for voltage change (ΔV_y)

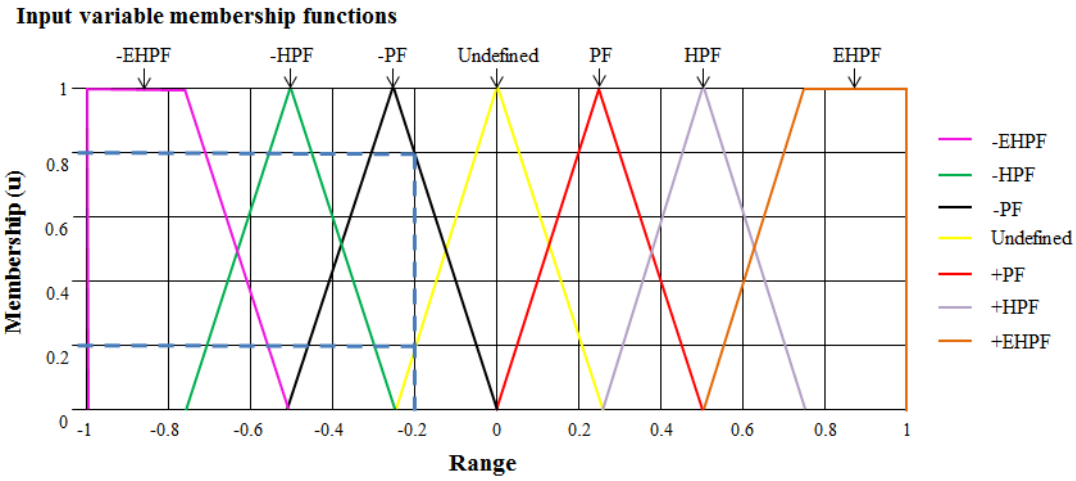

Figure 4.3: Fuzzy logic input variable membership for power factor change (ΔPF_y)

For the defuzzification, there is also seven types of predefined membership functions, namely extremely high supply power (EHSupply), high supply power (HSupply), supply power (Supply), normal (Normal), absorb power (Absorb), high absorb power (HAbsorb), and extremely high absorb power (EHAbsorb). The rules for the defuzzification in terms of voltage change to be done are as shown in Table 4.1, while Table 4.2 is due with the rules for defuzzification of power factor change. The rules are designed in such a way to obtain the results oriented. After the membership functions mapped each other, the centroid of defuzzification is used. The types and the membership of the instructions are used to justify the area encircled in the fuzzy output membership in Figure 4.4 and Figure 4.5. The changes needed for real current (ΔI_p) to minimize the unbalance voltage is sent as instruction to the bi-directional inverter by using the center of area (CoA) deffuzification method. In the same way, the change of reactive current (ΔI_q) is needed to improve the power factor. The linguistic variable ΔV_y can vary in the range of -20 V to 20 V as the voltage regulation is ±10% of the nominal value while the power factor can only vary from -1 to 1.

Table 4.1: Rules of defuzzification for voltage change (ΔV_y)

IF Delta Voltage =	**THEN Delta I =**
EUV	EHSupply
VUV	HSupply
UV	Supply
Normal	Normal
OV	Absorb
VOV	HAbsorb
EOV	EHAbsorb

Table 4.2: Rules of defuzzification for power factor change (ΔPF_y)

IF Delta Voltage =	THEN Delta I =
-EHPF	EHSupply
-HPF	HSupply
-PF	Supply
Undefined	Normal
+PF	Absorb
+HPF	HAbsorb
+EHPF	EHAbsorb

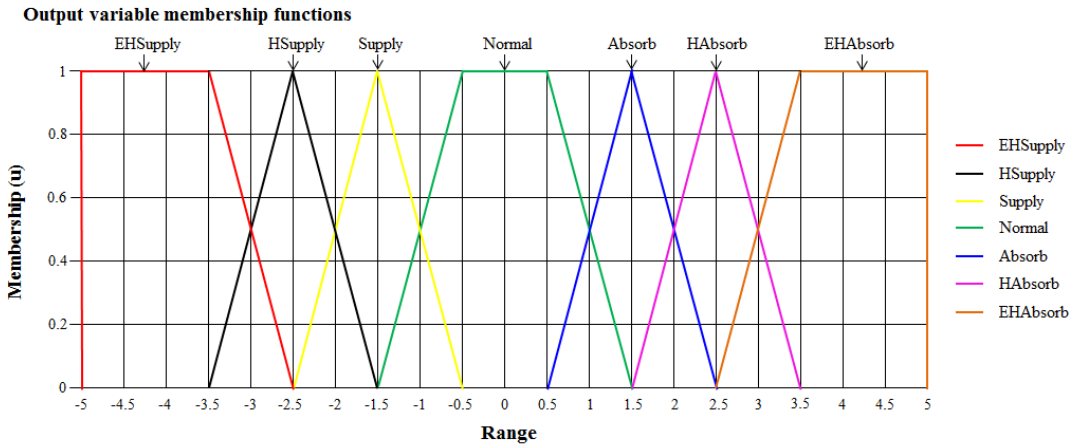

Figure 4.4: Fuzzy output membership of instruction (ΔI_p)

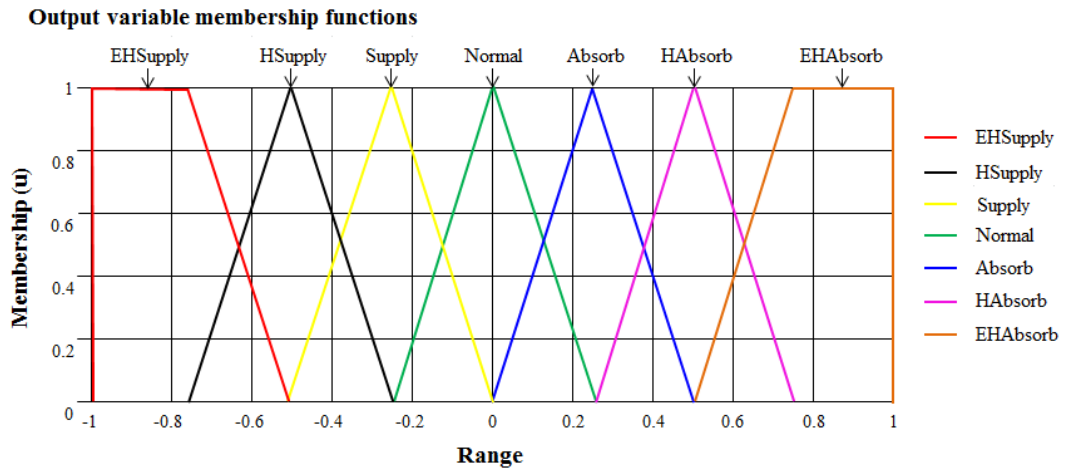

Figure 4.5: Fuzzy output membership of instruction (ΔI_q)

For an example, if ΔV_y is -6 V, it will generate two outputs:

1. 0.2 of very undervoltage (VUV)
2. 0.8 of undervoltage (UV)

Hence, the invoked rules for -6 V is "if delta voltage is VUV, then delta I is Hsupply" and "if delta voltage is UV, then delta I is Supply" with the weight of 0.2 and 0.8 respectively. The instruction (ΔI_p) sent to the bi-directional inverter can be calculated through the CoA defuzzification method as shown in Figure 4.6. Therefore, the output value will be -1.7. For the power factor, it is exactly similar to the example above, if ΔPF_y is -0.2, it will create two outputs:

1. 0.2 of undefined (Undefined)
2. 0.8 of negative power factor (-PF)

Therefore, the antecedents and consequences for -0.2 is "if delta power factor is Undefined, then delta I is Normal" and "if delta power factor is -PF, then delta I is Supply" with the weight of 0.2 and 0.8 respectively. The command (ΔI_q) is delivered after the calculation using the CoA defuzzification method and it is found to be -0.2 as shown in Figure 4.7.

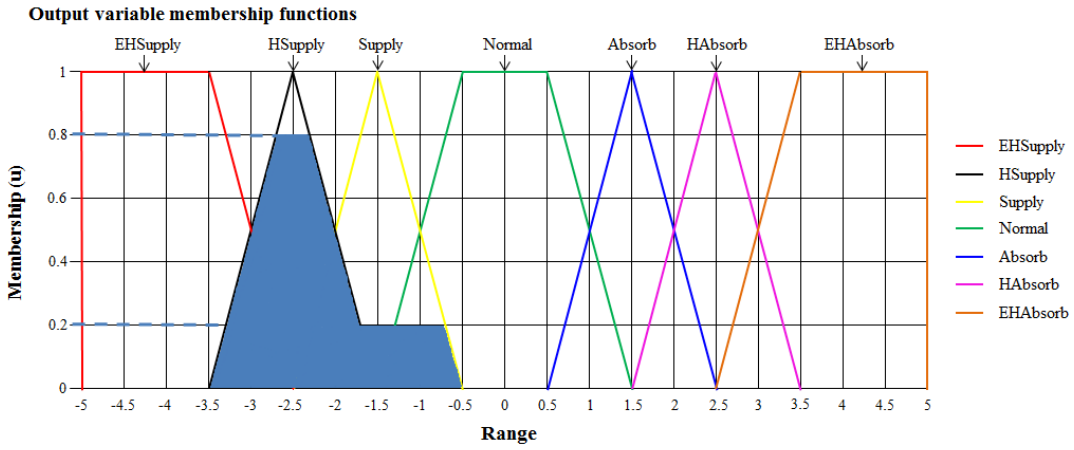

Figure 4.6: CoA defuzzification method for real current change (ΔI_p)

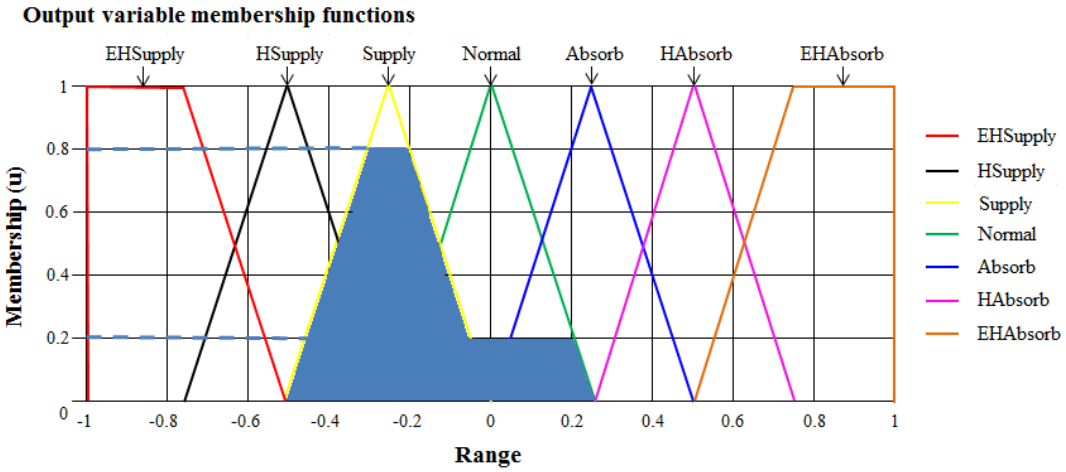

Figure 4.7: CoA defuzzification method for reactive current change (ΔI_q)

4.2.2 Implementation of fuzzy Control Algorithm using LabVIEW

In LabVIEW, there is front panel and block diagram panel. Figure 4.8 shows the developed graphical user interface of the energy storage system. Front panel is the interface for the user to observe the changes of network parameters. From the front panel, the user can monitor and control the network condition. It consists of the data

acquisition from the Data Taker with the basic parameters such as voltage, real and reactive power, power factor, frequency, and current. The phase selection, VUF, divergence, voltage sequence and other necessary parameters are also shown in the interface for the purpose of inspection. Besides, the users can monitor and control the three Sunny Islands through the interface manually or automatically. For manual control, the user is allowed to control the amount of absorption and injection of power in the Sunny Island. In automated mode, the fuzzy control algorithm will trigger the energy storage system when the voltage is out of the acceptable range. There are 15 buttons in the load bank controller to control the emulated consumer load. Graphs will demonstrate the dynamic change of voltage, VUF and power factor.

Figure 4.8: Graphical User Interface of the Energy Storage System

The block diagram contains a lot of wired functional blocks. They are divided into a few parts, which are the data acquisition section, fuzzy control section, computing section, control of Sunny Island, and others. The details of the parts will be further elaborated in the following paragraphs. Figure 4.9 shows a simple load bank control

where it controlled by the 15 buttons shown on the monitoring interface in Figure 4.8. The 15 buttons are clustered as a whole in order to arrange them properly.

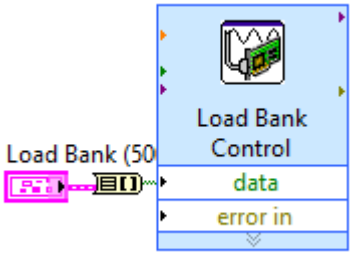

Figure 4.9: Load bank control

4.2.2.1 Coding of the Data Acquisition

The functional blocks used to read the measurement data from the Data Taker is shown in Figure 4.10. In order to establish a working connection, the TCP open connection with the IP address 169.254.60.152 is used to connect the Data Taker and read the input registers of the 5 power meters of PV1, PV2, load bank, generator, and wind turbine. Since the data read from the registers are encoded values, all the data are decoded as shown in Figure 4.11 in order to obtain the parameters correctly.

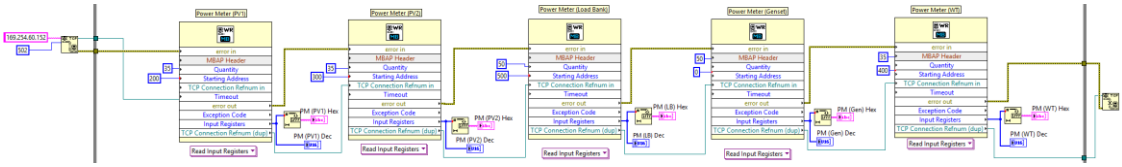

Figure 4.10: Values read from the input registers

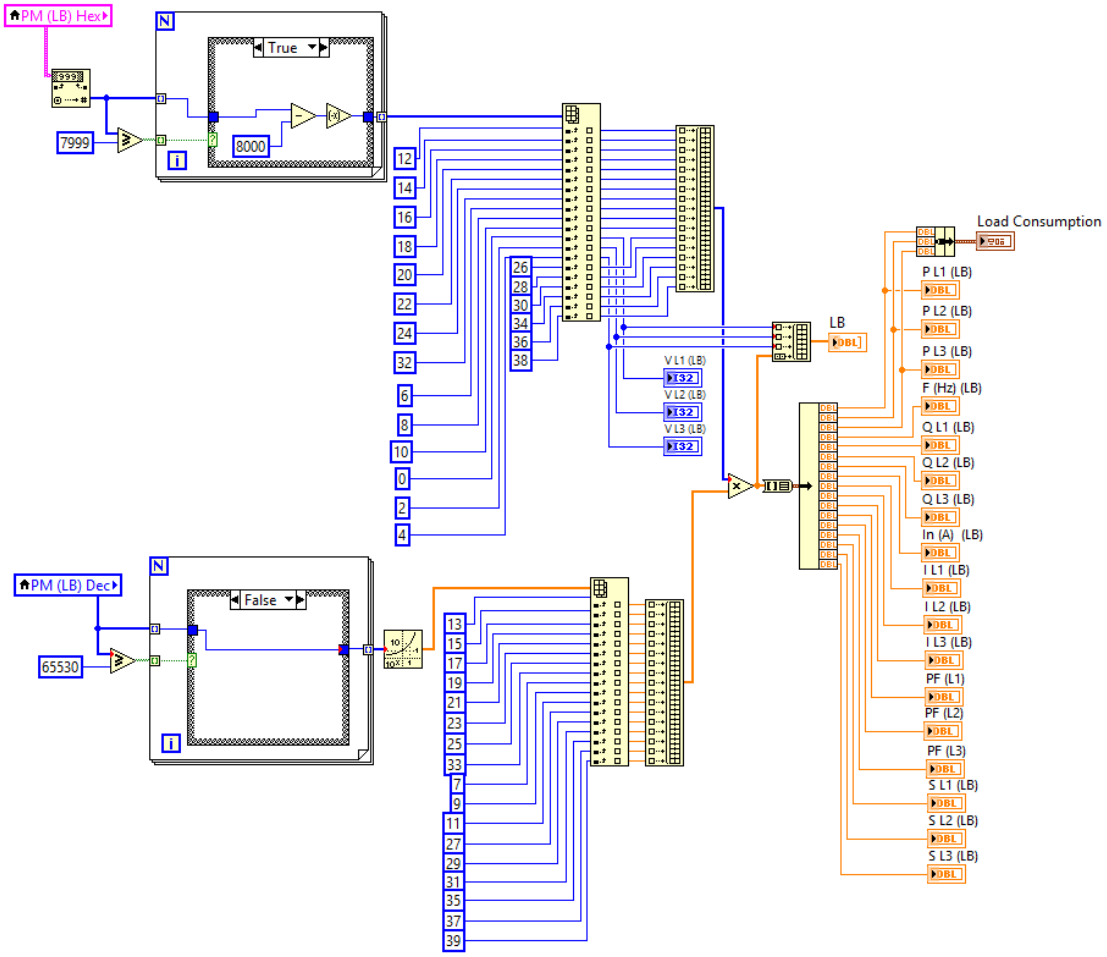

Figure 4.11: Way to decode the encoded the parameters obtained

4.2.2.2 Saving of the data collected

After all the data acquisition, data obtained will be saved in TDMS format in the desired location. For TDMS format file, it can be generated in the template excel file with all the group names (sheet) and channel names (column) are given. Hence, the data will be grouped and displayed in different sheets as desired. The user can review and analyse the data loaded from the file directly as shown in Figure 4.12. Figure 4.13 shows the coding for storing of the data. The data measured by the Sunny

Islands and power meters will be saved accordingly. The specified TDMS file will be created or replaced to the specific file path.

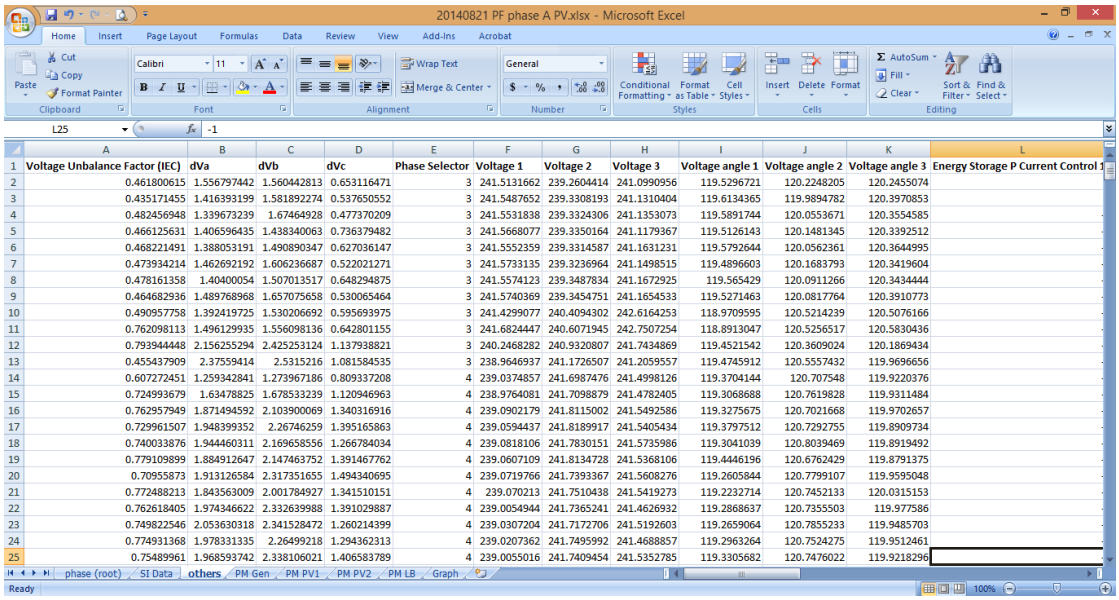

	A	B	C	D	E	F	G	H	I	J	K	L
1	Voltage Unbalance Factor (IEC)	dVa	dVb	dVc	Phase Selector	Voltage 1	Voltage 2	Voltage 3	Voltage angle 1	Voltage angle 2	Voltage angle 3	Energy Storage P Current Control 1
2	0.461800615	1.556797442	1.560442813	0.653116471	3	241.5131662	239.2604414	241.0990956	119.5296721	120.2248205	120.2455074	
3	0.435171455	1.416393199	1.581892274	0.537650552	3	241.5487652	239.3308193	241.1310404	119.6134365	119.9894782	120.3970853	
4	0.482456948	1.339673239	1.67464928	0.477370209	3	241.5531838	239.3324306	241.1353073	119.5891744	120.0553671	120.3554585	
5	0.466125631	1.406596435	1.438340063	0.736379482	3	241.5668077	239.3350164	241.1179367	119.5126143	120.1481345	120.3392512	
6	0.468221491	1.388053191	1.490890347	0.627036147	3	241.5552359	239.3314587	241.1631231	119.5792644	120.0562361	120.3644995	
7	0.473934214	1.462692192	1.606236687	0.522021271	3	241.5733135	239.3236964	241.1498515	119.4896603	120.1683793	120.3419604	
8	0.478161358	1.40400054	1.507013517	0.648294875	3	241.5574123	239.3487834	241.1672925	119.565429	120.0911266	120.3434444	
9	0.464682936	1.489768968	1.657075658	0.530065464	3	241.5740369	239.3454751	241.1654533	119.5271463	120.0817764	120.3910773	
10	0.490957758	1.392419725	1.530206692	0.595693975	3	241.4299077	240.4094302	242.6164253	118.9709595	120.5214239	120.5076166	
11	0.762098113	1.496129935	1.556098136	0.642801155	3	241.6824447	240.6071945	242.7507254	118.8913047	120.5256517	120.5830436	
12	0.793944448	2.156255294	2.425253124	1.137938821	3	240.2468282	240.9320807	241.7434869	119.4521542	120.3609024	120.1869434	
13	0.455437909	2.37559414	2.5315216	1.081584535	3	238.9646937	241.1726507	241.2059557	119.4745912	120.5557432	119.9696656	
14	0.607272451	1.259342841	1.273967186	0.809337208	4	239.0374857	241.6987476	241.4998126	119.3704144	120.707548	119.9220376	
15	0.724993679	1.63478825	1.678533239	1.120946963	4	238.9764081	241.7098879	241.4782405	119.3068688	120.7619828	119.9311484	
16	0.762957949	1.871494592	2.103900069	1.340316916	4	239.0902179	241.8115002	241.5492586	119.3275675	120.7021668	119.9702657	
17	0.729961507	1.948399352	2.26746259	1.395165863	4	239.0594437	241.8189917	241.5405434	119.3797512	120.7292755	119.8909734	
18	0.740033876	1.944460311	2.169658556	1.266784034	4	239.0818106	241.7830151	241.5735986	119.3041039	120.8039469	119.8919492	
19	0.779109899	1.884912647	2.147463752	1.391467762	4	239.0607109	241.8134728	241.5368106	119.4446196	120.6762429	119.8791375	
20	0.70955873	1.913126584	2.317351655	1.494340695	4	239.0719766	241.7393367	241.5608276	119.2605844	120.7799107	119.9595048	
21	0.772488213	1.843563009	2.001784927	1.341510151	4	239.070213	241.7510438	241.5419273	119.2232714	120.7452133	120.0315153	
22	0.762618405	1.974346622	2.332639988	1.391029887	4	239.0054944	241.7365241	241.4626932	119.2868637	120.7355503	119.977586	
23	0.749822546	2.053630318	2.341528472	1.260214399	4	239.0307204	241.7172706	241.5192603	119.2659064	120.7855233	119.9485703	
24	0.774931368	1.978331335	2.26499218	1.294362313	4	239.0207362	241.7495992	241.4688857	119.2963264	120.7524275	119.9512461	
25	0.75489961	1.968593742	2.338106021	1.406583789	4	239.0055016	241.7409454	241.5352785	119.3305682	120.7476022	119.9218296	

Figure 4.12: Data saved in excel format

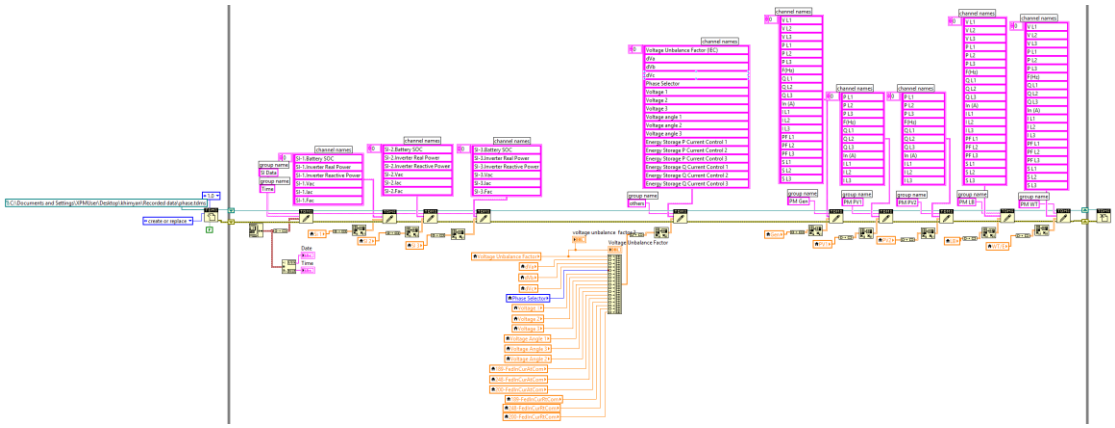

Figure 4.13: Data Collection coding

4.2.2.3 Control of the Sunny Island

Figure 4.14 illustrates the way to turn ON and OFF the Sunny Island with either signal '1' or '2' is sent. Once the signal is sent to turn ON, IO server variable pre-set in the IO server library will connect with the YAOPC server which is under the SMA possession protocol. Next, true and false selector is used by the controller to identify whether the instruction sent to the Sunny Island is taken from the automated control or manual control as shown in Figure 4.15. When the instruction transmitted is the same as the previous iteration, it flows into the false case and no action is taken in the Sunny Island. This can prevent the communication port from doing the extra job and avoiding the delayed problem. As shown in Figure 4.16, the parameters of the Sunny Island are read from the IO server variable. Batteries of each phases within a range of 60% - 90% is set as healthy condition. Power output of the Sunny Island is plotted to have a better view on monitoring.

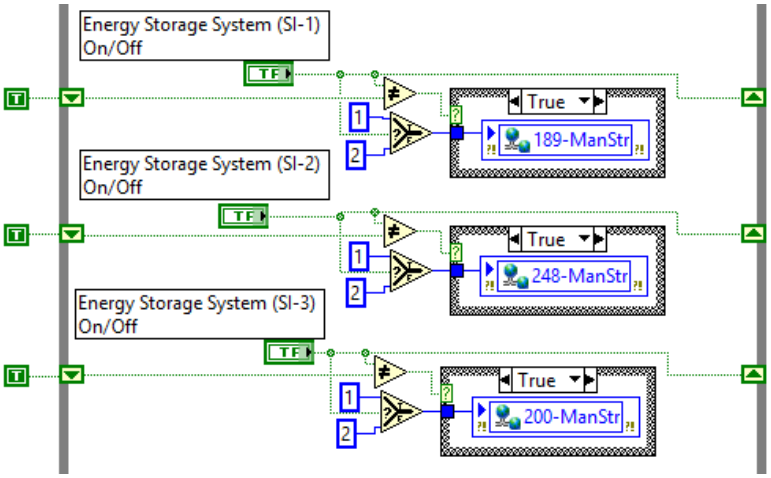

Figure 4.14: Turning ON and OFF of the Sunny Island

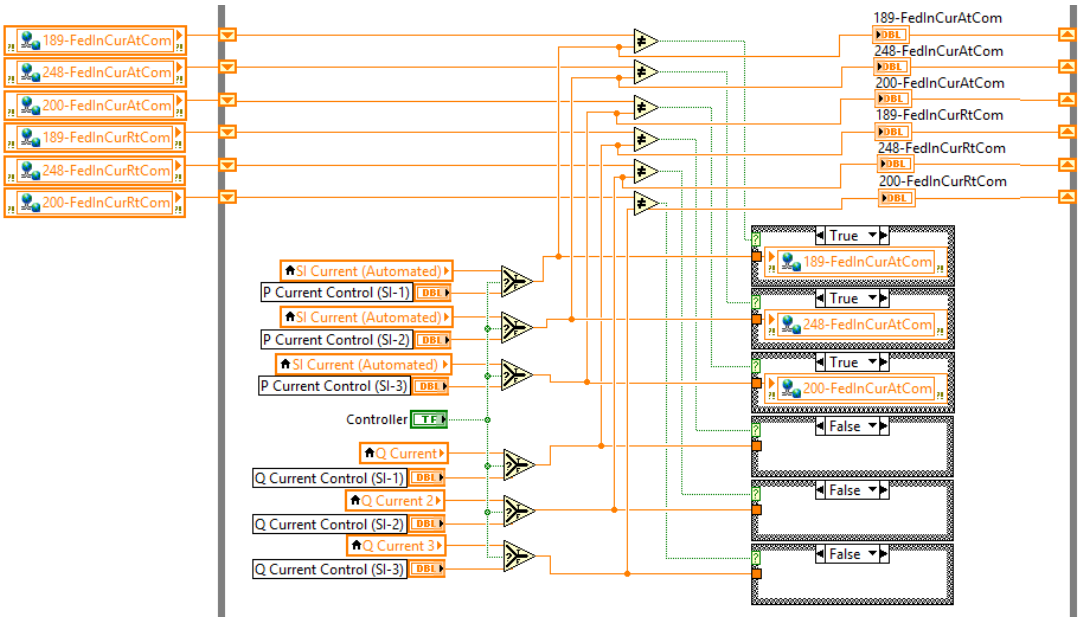

Figure 4.15: Controlling of Sunny Island

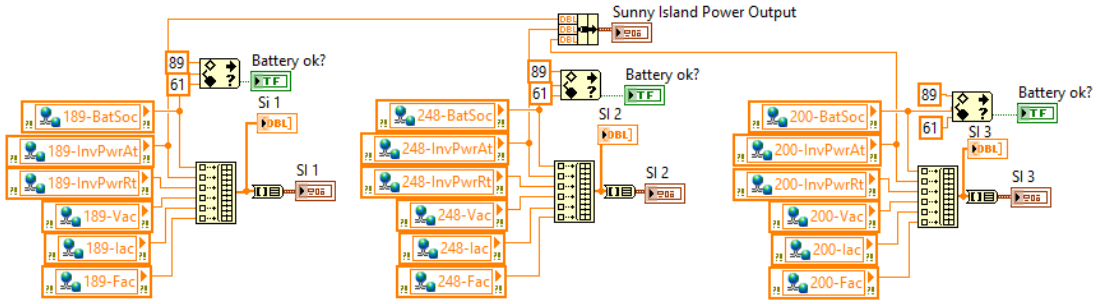

Figure 4.16: Reading parameters from Sunny Island

4.2.2.4 Coding of the Main Fuzzy Controller

For the programming of the main fuzzy controller, it is put into a sequence structure. Firstly, the voltage and current are obtained by DAQ Assistant and the fundamental of voltage and current signals for N channels are calculated. By using the complex to polar function, the output received will be converted to the magnitude and phase components. Hence, the voltage and current magnitude can be obtained while the voltage angle and the current angle can be calculated from the phase component.

Therefore, VUF can be calculated when the negative sequence is divided by positive sequence and times 100. Figure 4.17 shows the block diagram for the calculation of VUF.

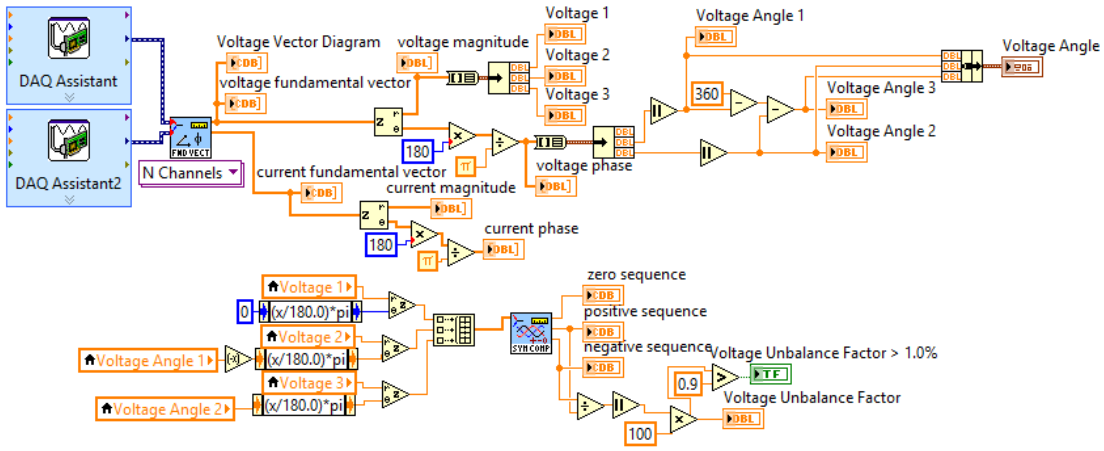

Figure 4.17: Calculation of VUF

By utilizing the symmetrical components, maximum divergence can be determined and phase with the maximum divergence will be corrected by the energy storage system. Park's Transformation as shown in Figure 4.18 will be adopted as the phase selection for the fuzzy controller. Park's transformation is used to determine the maximum divergence of phase, while the phase selection for low power factor is shown in Figure 4.19. The condition to trigger the case is when the power factor is lower than 0.98. The phase with the lowest power factor will be selected as the severe phase. However, when the voltage unbalance and the power factor are within the tolerance, it will go to the default case, hence, the fuzzy controller will maintain the previous instruction with no increment or deduction of current output towards the Sunny Islands. Figure 4.20 and Figure 4.21 show the fuzzy logic for voltage unbalance and power factor used respectively. It is explained in the section 4.2.1

which describes the details of the fuzzy controller. The output of the fuzzy logic is the current value that needed by the energy storage system for adjustment of the power output.

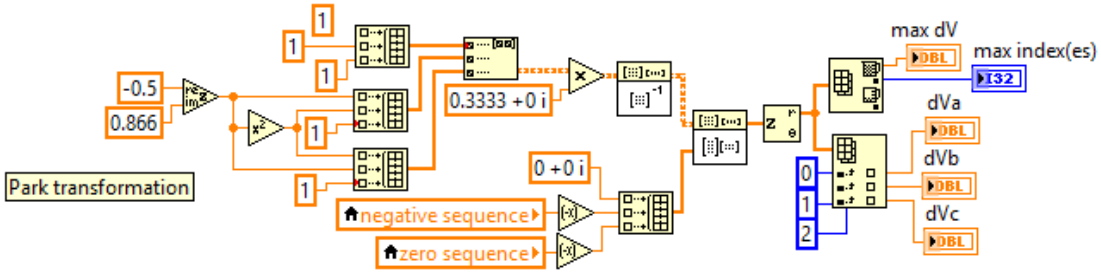

Figure 4.18: Park's Transformation

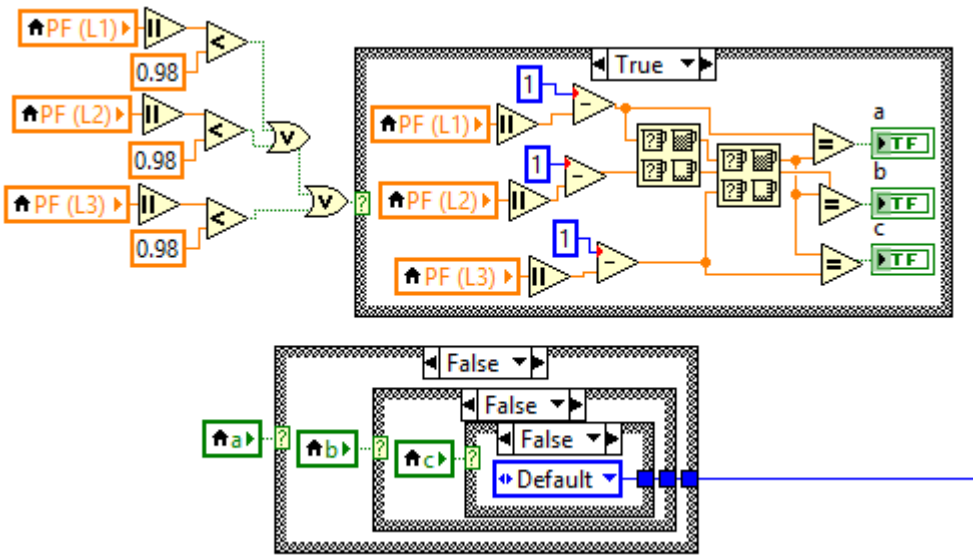

Figure 4.19: Phase selection for low power factor

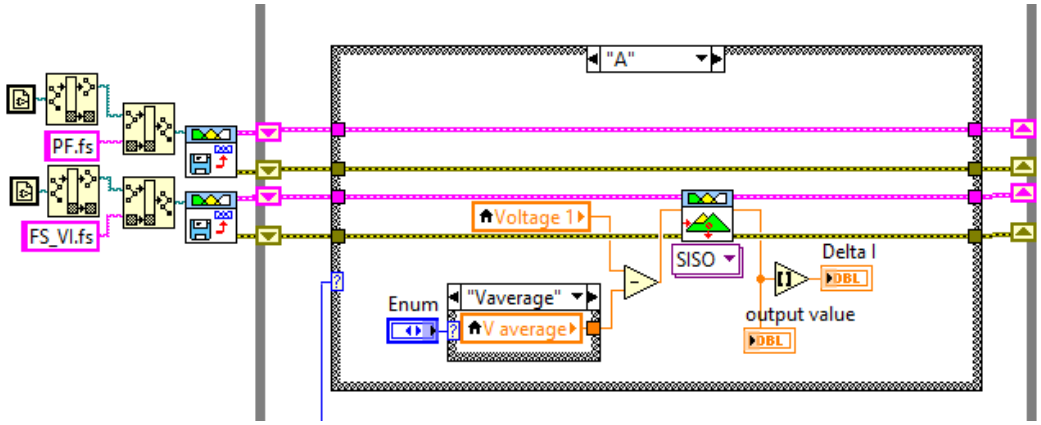

Figure 4.20: Fuzzy logic for voltage unbalance

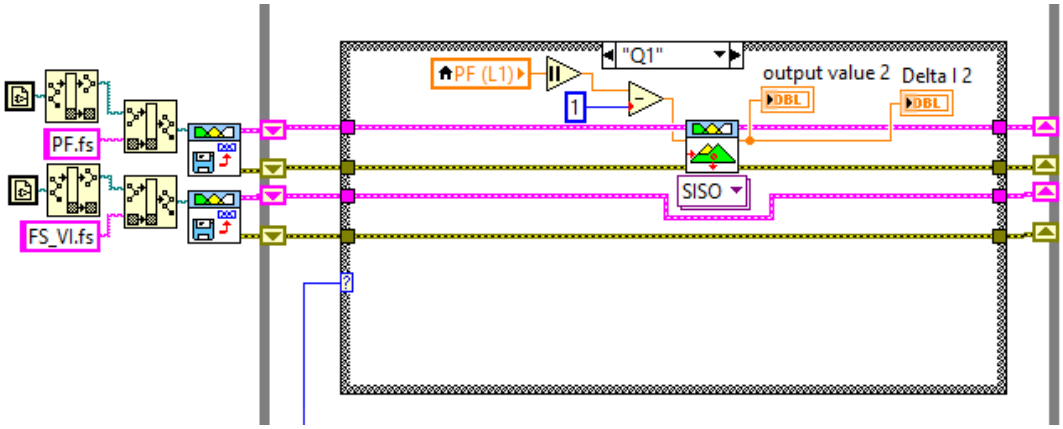

Figure 4.21: Fuzzy logic for power factor

4.2.2.5 Network Operating Conditions Causing the Operation of the Energy Storage System

For the energy storage system to supply or absorb power from the networks, the following situations must be fulfilled. First, the voltage must be greater than 230 V and updated in the following iteration for the case to be triggered. The case will check the active current value whether it is within the defined safety range which is -16 A to 16 A. Another condition that needs to be fulfilled is that the voltage of the distribution network must be higher than 1 which is set in the controller in order to

make sure that the network is always energised; otherwise the energy storage system can continue to operate on the dead network. Then, the present current value will subtract the output current specified by the fuzzy logic. If the current value after subtraction is equals to 0 A, the case will check for the present voltage whether it is smaller than the average voltage. If it is smaller than the average voltage, the current will be added by 1 A. In vice versa, current will become -1 A. This is to prevent the energy storage system to stop working. Finally, the current value will be sent to the energy storage system in order to mitigate the voltage unbalance of the network. Figure 4.22 shows the cases as mentioned above.

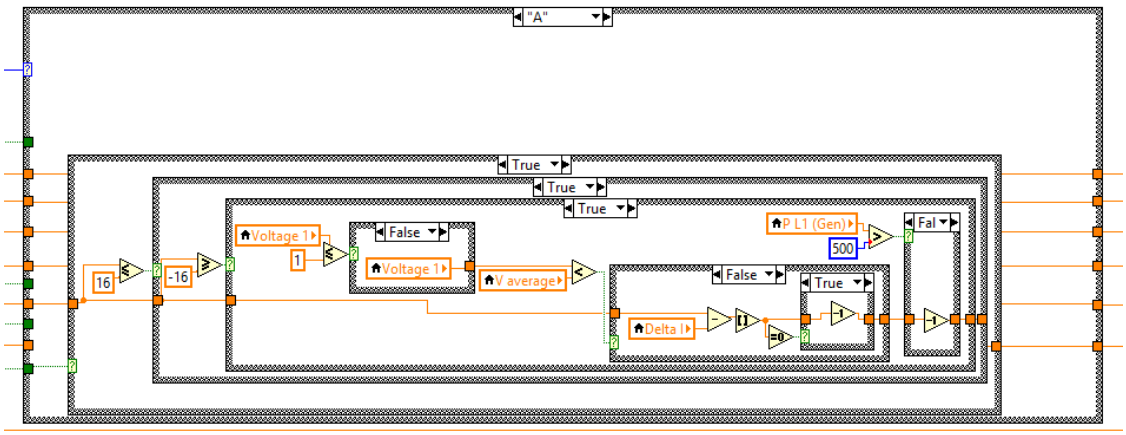

Figure 4.22: Condition of active current before sent to the energy storage system

On the other hand, the conditions for reactive current are slightly different. First, the reactive current is checked to be within the range of -16 A to 16 A. The acceptable voltage range for the case is within 238 V to 243 V. If the power factor is in the range of 0.3 to 0.98, the present current value will be added by the current output of the fuzzy logic. However, if the power factor is in the range of -0.3 to -0.98, the output of fuzzy logic will be subtracted by the current value. After all, the reactive current instruction will be sent to the energy storage system to improve the power

factor of the network. Figure 4.23 shows the situation and the way for the reactive current to process before sent to the energy storage system.

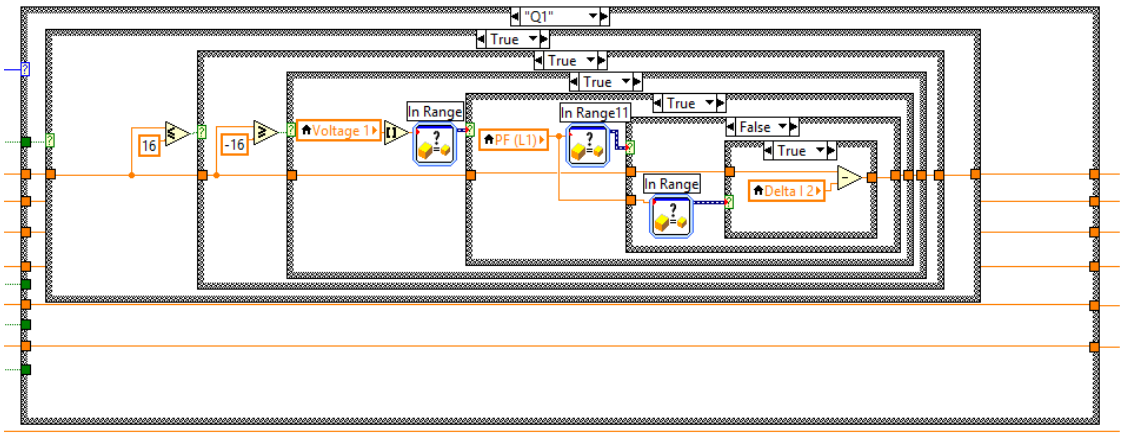

Figure 4.23: Processing of reactive current before sent to the energy storage system

After all, the energy storage system will operate by adjusting the power output from the bi-directional inverter after the amount of the real and reactive current needed to inject or absorb had been determined. Hence, voltage rise, voltage unbalance, and low power factor can be mitigated by this fuzzy logic controlled energy storage system effectively.

4.3 Summary

Fluctuations of RE output and random plugged-in EVs are unpredictable, causing voltage rises, voltage sags, voltage unbalance, and low power factor. Therefore, an effective active control algorithm is needed to mitigate the fluctuating voltage rises, voltage unbalance and improve power factor. This chapter presents a fuzzy control method implemented with the energy storage system. The fuzzy control algorithm is

developed using LabVIEW in a supervisory personal computer. The fuzzy control would determine and send the appropriate instruction to the energy storage system and instruct the energy storage system to carry out the necessary action to prevent the network parameters exceed their statutory limits. The Park's transformation is used in the algorithm to identify the affected phase that causing high degree of voltage unbalance factor and hence to coordinate with the three-phase energy storage system to mitigate the voltage rise, voltage sags and voltage unbalance issues. Hence, the particular affected phase can be addressed and balance the voltage effectively. Meanwhile, only the lowest power factor will be addressed for each phases to improve the power factor.

CHAPTER 5

RESULTS AND DISCUSSIONS

5.1 Introduction

The performance of the fuzzy controlled energy storage system is verified by setting up the energy storage system on the experimental LV distribution network with two single-phase PV systems, a wind turbine emulation system, and an electric vehicle. A number of case studies under different generations load demands are designed to investigate the performance of the three single-phase fuzzy controlled energy storage systems. The discussion of the results and conclusions are presented in this chapter.

5.2 Experimental Result and Discussion

The renewable energy used in this system is the 3.6 kW_p PV system and 2.3kW_p wind emulation system. When the RE is connected to the network, it causes VUF to fluctuate and increase. The statutory limit of VUF set by Malaysian Grid Code is 1 %. Hence, the fuzzy logic controlled energy storage system is designed to react in such a way to prevent the network VUF from exceeding 1 %. In addition, penalty will be charged when power factor is lower than 0.85. Hence, this energy storage system is

also designed in such a way to improve the power factor. Several case studies are conducted to represent the different scenarios.

5.2.1 Case Study 1: Impacts of high PV power output on the experimental LV distribution network

The idea of this case study is to investigate the impact of the intermittent PV power output on the experimental network. A constant load of 700 W and a 3.6 kW_p PV system are connected at phase A of the experimental network. Figure 5.1 shows the load profile, PV power output and the power factor of the experimental case study. Figure 5.2 shows the voltage and VUF at the PCC.

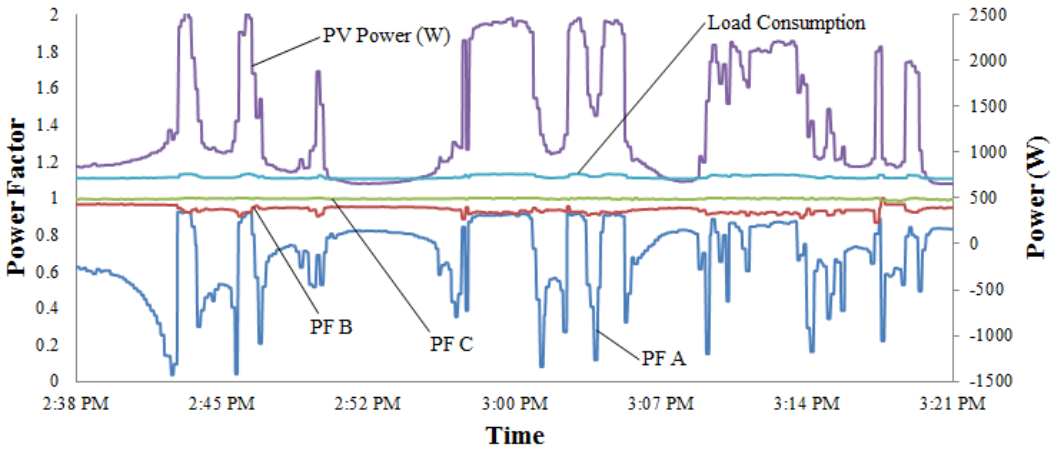

Figure 5.1: PV power output at Phase A, load at Phase A and power factor of all three phases of the experimental case study 1

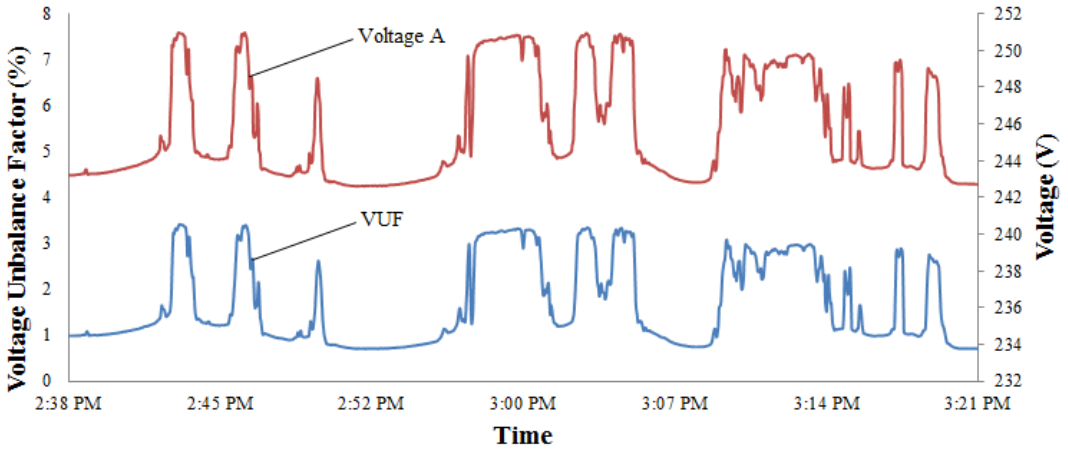

Figure 5.2: VUF and voltage at phase A of the experimental case study 1

Initially, the PV system generates 800 W which is slightly greater than the 700 W load. The VUF is recorded at 1% while the voltage is approximately 243 V. However, at 2:45 pm, the PV power output starts to increase, causing the system voltage to rise above 251 V and the VUF to be 3.4%. It is noticed that the power factor is fluctuating all the time. This is due to the intermittent PV power output.

5.2.2 Case study 2: Power factor of a university's building

The second case study is carried out to study the power factor profile at the tutorial block (SE Block) in the university. This data was collected on the 1st July 2013 from 12 am to 11.59 pm. This one day data was taken at the switch room of SE Block using TES-3600 3-phase power analyzer.

Figure 5.3 is the power factor profile on Monday, a working day. It is shown that the power factor is in the range of 0.75 and 0.85 early in the morning. However, the power factor begins to increase to the range of 0.8 and 0.9 starting at 8 am. This is because the occupants started to switch on many electronic devices in SE Block such as lighting, air conditioner, fans, computers and even some of the laboratory equipment.

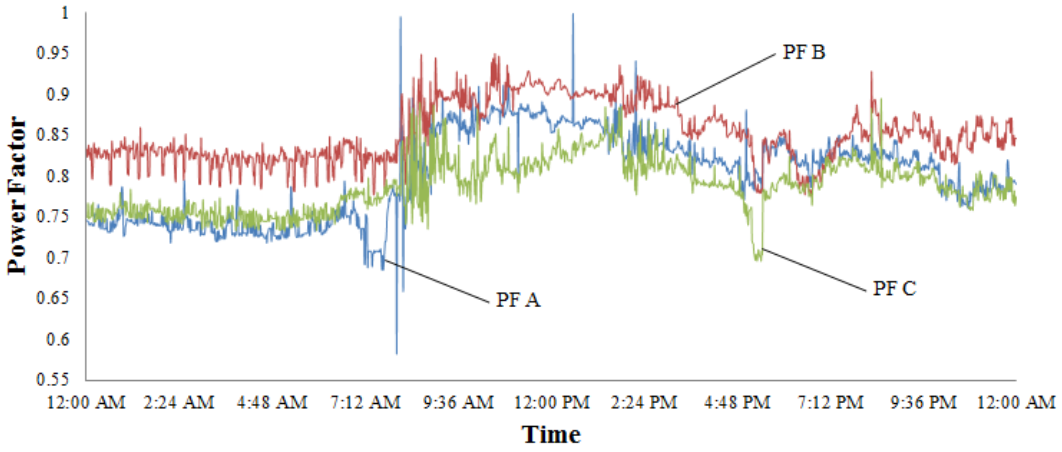

Figure 5.3: Power factor profile on 1st July 2013, Monday

Figure 5.4 shows the power factor profile on a non-working day, Saturday. It is shown that the power factor stays within the range of 0.75 and 0.85 throughout the day. This is because the occupants didn't switch on many electronic devices. Case study 2 shows that the power factor at the building of the university is always low. However, if the energy storage system is used, the power factor of the building is improved.

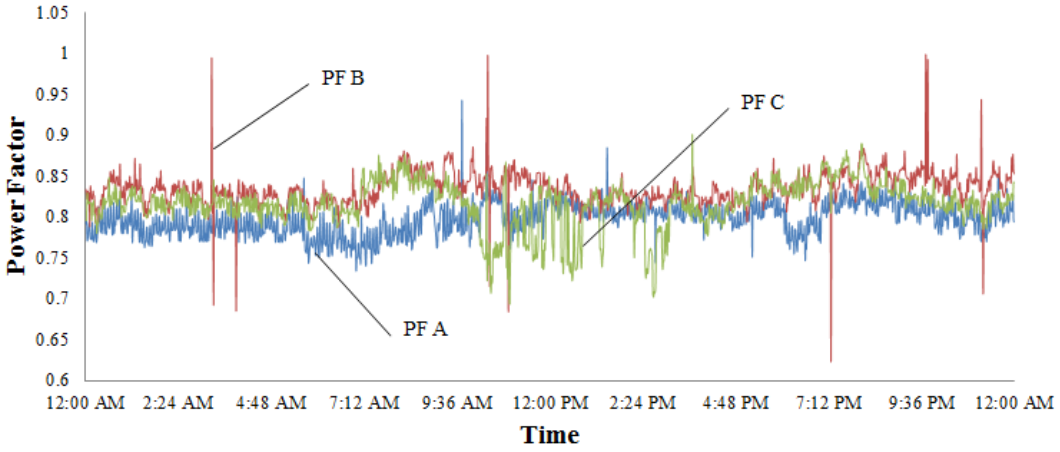

Figure 5.4: Power factor on 6th July 2013, Saturday

5.2.3 Case Study 3: Effect of using fuzzy controlled energy storage on the network with PV

This case study is to study the response of the fuzzy controlled energy storage system with respect to the changes of PV power output under a balanced load condition. A fixed load of 400 W is introduced to every phases. A 3.6 kW_p PV system is connected to phase B of the network.

Figure 5.5 shows that, the increment of PV power output affects the three-phase voltages at 3.38 pm. Due to the coupling effect, voltage at phase C reduces to 230 V although the PV exports power to phase B. The fuzzy control system detects the sudden change and instructs the bi-directional inverter to absorb the excess power from the PV system at phase B. The three-phase voltages are then restored to their nominal values once the excess power is stored into the energy storage system. At

3.45 pm, the control algorithm detects that the voltage at phase C is out of range. Therefore, the controller instructs the energy storage system to restore the voltage.

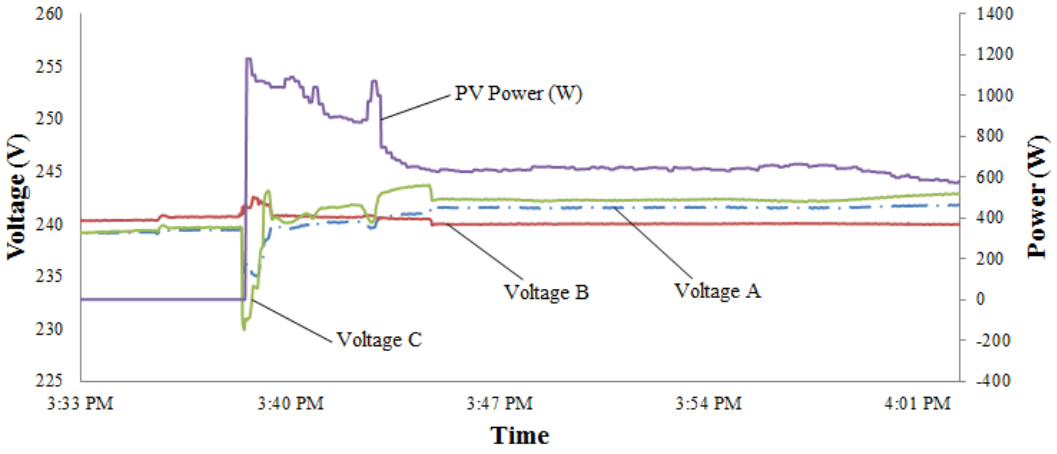

Figure 5.5: Three-phase voltages and PV power output of the experimental case study 3

Figure 5.6 shows the response of the energy storage system and the VUF of the experimental network. The VUF is recorded at 2% when the PV system exports power to the network. It is noticed that VUF is reduced to 0.5% in 1 minute when the energy storage system absorbs the excess power from the network. As compared to the results of (Wong, Lim, & Morris, 2014) in Figure 5.7, VUF is found mitigated from 1.9% to 0.9% in 5 minutes. Table 5.1 shows the improvement of power quality with the integration of the fuzzy controlled energy storage system.

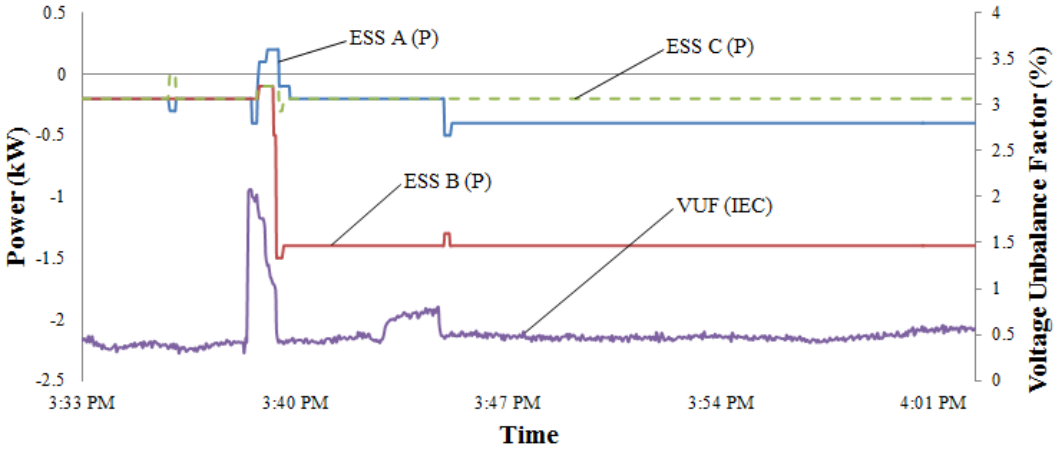

Figure 5.6: VUF and power output of the energy storage system of the experimental case study 3

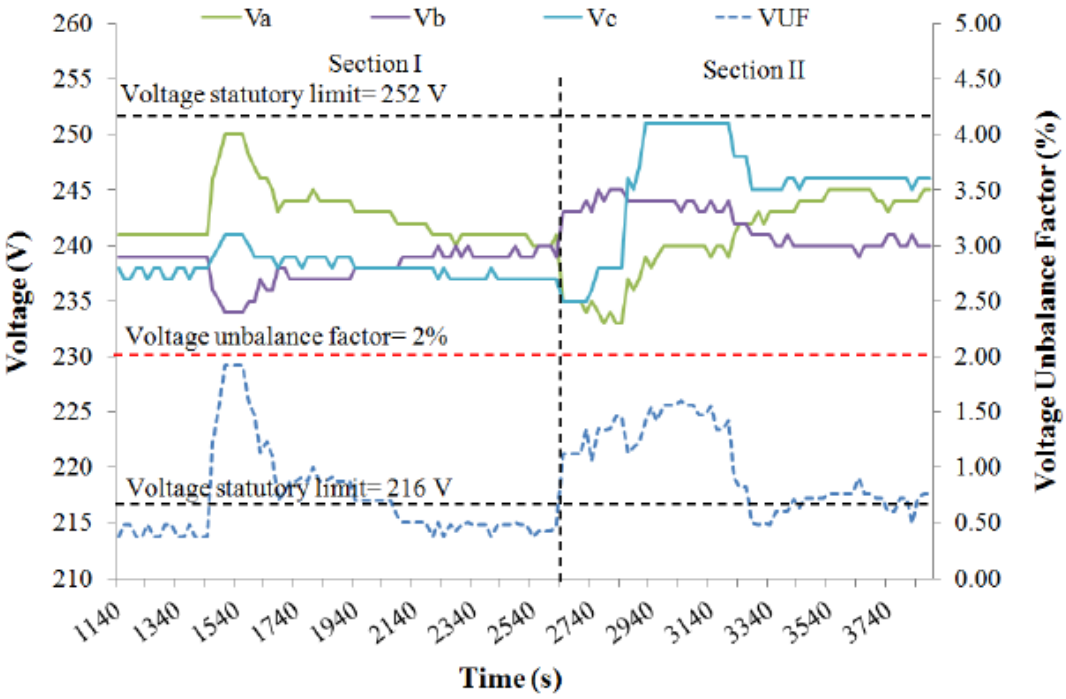

Figure 5.7: Corresponding VUF of the energy storage system using the control strategy of (Wong, Lim, & Morris, 2014)

Table 5.1: Comparison of the improvement of VUF with the integration of the energy storage system

Methods	VUF Before	VUF After	VUF Improvement	Time Needed
Fuzzy Control (Wong, Lim, & Morris, 2014)	1.9	0.9	52.6%	5 mins
My method	2.0	0.5	75%	1 mins

Figure 5.8 shows that the power factor of the network. There is a drop in power factor at 3.38 pm because the PV inverter begins to be connected to the network, exporting real power to the network at that time and hence causing a reduction on the power factor. The reduction in the power factor happens only for a brief period of time after the connection of the PV system at phase B at 3.37 pm. The power factor is restored automatically to the normal level without any corrective effort from the energy storage system because the PV inverter has the built-in feature to bring up the power factor to 0.85 or above at its terminal once it is connected. However, the power factor can still be easily reduced if any electrical vehicles or electrical machines are plugged to the network. Therefore, the energy storage has to be used in conjunction with the PV inverter so that the power factor can be increased up to 1.00.

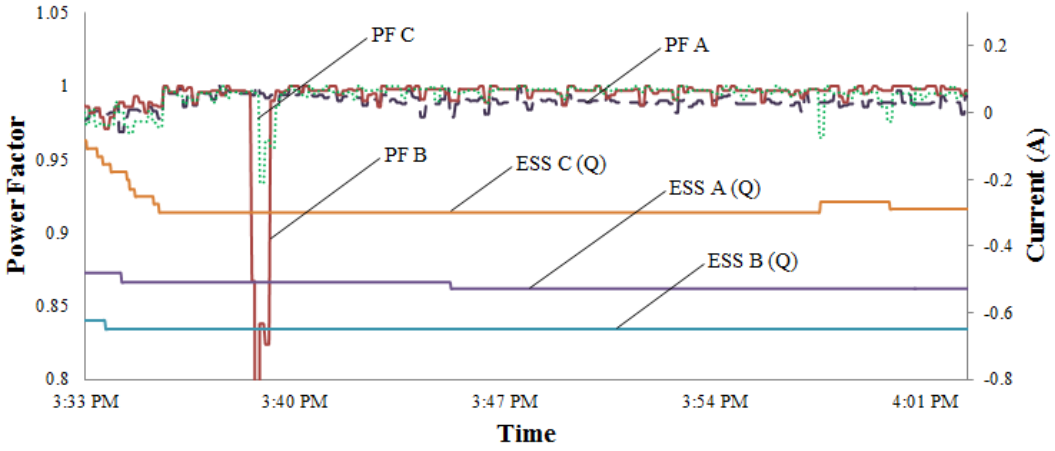

Figure 5.8: Power factor of all three-phases and reactive power output of the energy storage system

5.2.4 Case Study 4: Effect of using energy storage when inductive load is connected.

This case study is to investigate the effectiveness of the fuzzy controlled energy storage system in improving the power factor of the experimental network. In this experiment, a 2600 mH inductive load is connected to phase A. Figure 5.9 shows the VUF, voltage and its angle, power factor, reactive current control of the energy storage system and reactive power flow of the experimental network. It is noticed that VUF is reduced from 0.8% to 0.5% after the energy storage system supplies 192 Var to compensate the inductive load in the experimental network. The fuzzy control algorithm is used to manipulate the amount of reactive current flow from the energy storage system to the network based on the network power factor. It is noticed that the power factor is maintained within 0.98 and unity power factor. Table 5.2 shows the improvement of power factor and VUF with the integration of the fuzzy

controlled energy storage in this case study. Reactive power is not only able to improve the power factor; it can also provide a support to the network voltage. This indicates that reactive power supplied by the energy storage system can improve power factor, VUF, and voltage.

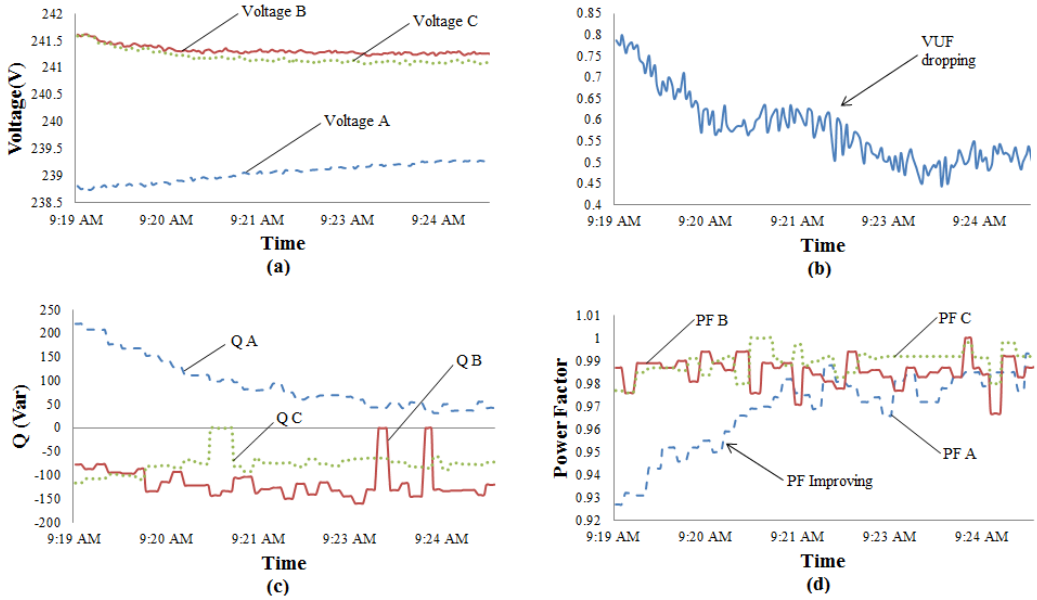

Figure 5.9: (a) Three-phase voltages, (b) VUF, (c) Reactive power flow and, (d) Power factor of the experimental case study 4

Table 5.2: Improvement of power qualities with the integration of the fuzzy controlled energy storage system

Power Quality	Before	After	Improvement
Power Factor	0.93	0.98	5%
VUF	0.8	0.5	37.5%

5.2.5 Case study 5: Effect of using energy storage when electric car (EV) and photovoltaic system (PV) are connected to the network

This case study is to study the response of the proposed energy storage system when EV and PV system are connected at the same time. Figure 5.10 shows the VUF, EV power, PV power output and voltage at phase A. At 3.16 pm, EV is charged at 2.4 kW, hence causing the voltage at phase A to drop below 230 V. It is noticed that the fuzzy controller detects the sudden change and instructs the energy storage system to inject power to the network. At 3.19 pm, PV is connected to phase A of the network, hence causing the voltage at phase A to increase. It is noticed that the fuzzy control algorithm is able to manipulate the power output of the energy storage system so to mitigate the VUF and voltage of the experimental network. At 3.25 pm, the PV and EV are disconnected on a purpose and it is shown that the fuzzy controller is able to regulate the voltage and mitigate the VUF in a very short period.

Figure 5.11 shows the power factor at Phase A, B and C with the reactive current from ESS. The power factor at phase A starts to drop at 3.17 pm because EV begins to draw reactive power only from the grid emulator after ESS supplies real power to EV at 3.17 pm to improve the voltage level. However, the fuzzy controller detects the reduction of the power factor and then supplies reactive power to the network to improve the power factor. At 3.19 pm, the power factor at Phase A drops again. This is because the PV starts to supply real power to the load at 3.19 pm, hence causing the power factor to drop. However, the reduction happens for a brief period of time because the inverter has the built-in feature to correct the power factor at its terminal. At 3.25 pm, the power factor drops again after PV and EV are disconnected from the

network. However, the fuzzy controller senses the reduction and then supplies reactive power to the network to restore the power factor.

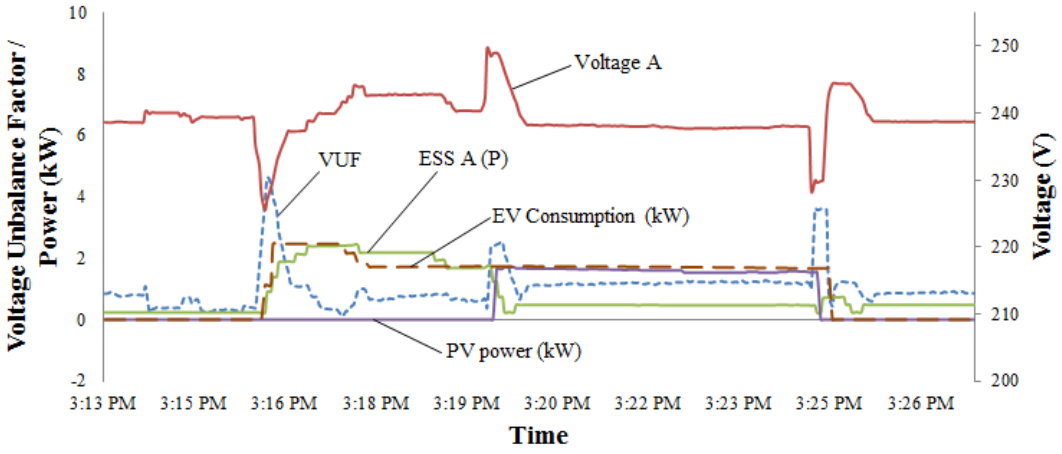

Figure 5.10: VUF, voltage, active power output of energy storage system, and PV power of the experimental case study 5i

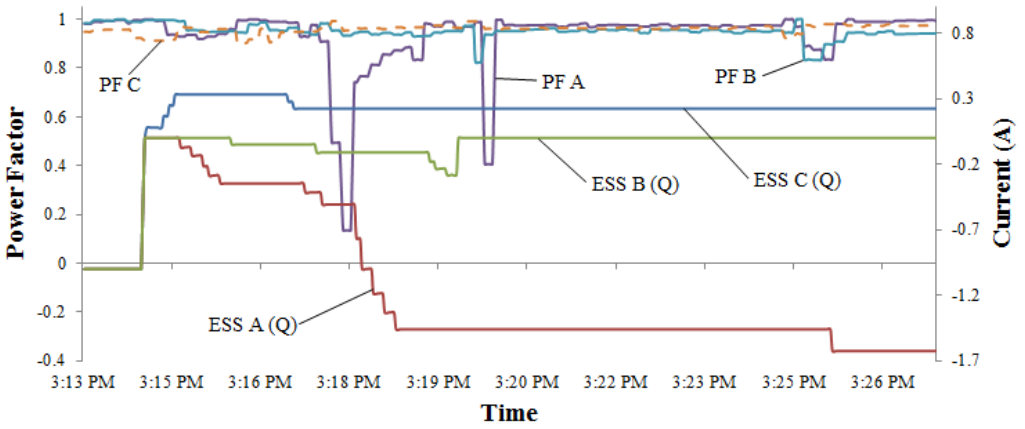

Figure 5.11: Power factors of all three phases and reactive current output from the energy storage system

5.2.6 Case Study 6: Impacts of wind power on the experimental LV distribution network

In this case study, emulated wind energy is injected in order to study its impact to the experimental LV distribution network. The wind speed is emulated based on the wind speed graph of Kuala Terengganu for the year of 1995 in Figure 5.12 (Shamshad Ahmad, 2009). The graph shows that the wind speed is fluctuating. A constant load of 370 W is connected to each of the phases while wind emulator is connected to phase A of the experimental network. This wind emulator is designed to fluctuate along the time in order to emulate the harvested wind energy. However, the wind power that can be generated is around 600 W only. Figure 5.13 shows the wind power output and the power factor of the experimental case study.

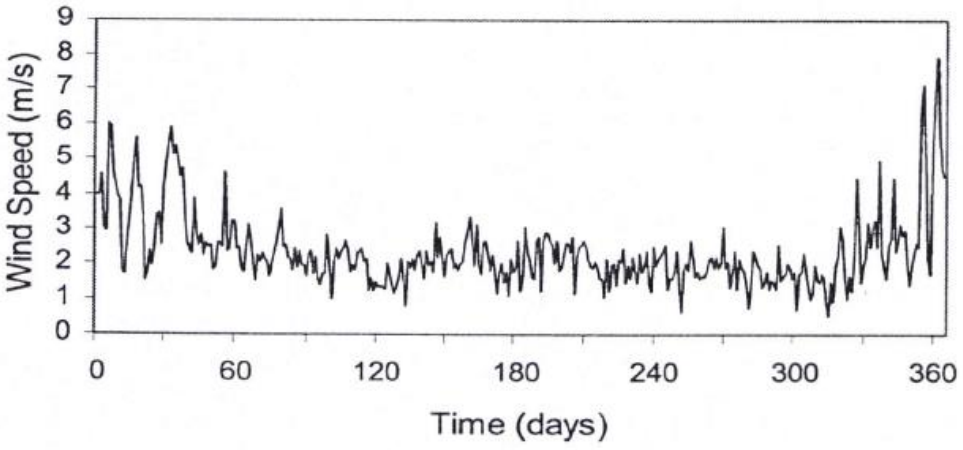

Figure 5.12: Mean daily wind speed values at Kuala Terengganu (Shamshad Ahmad, 2009)

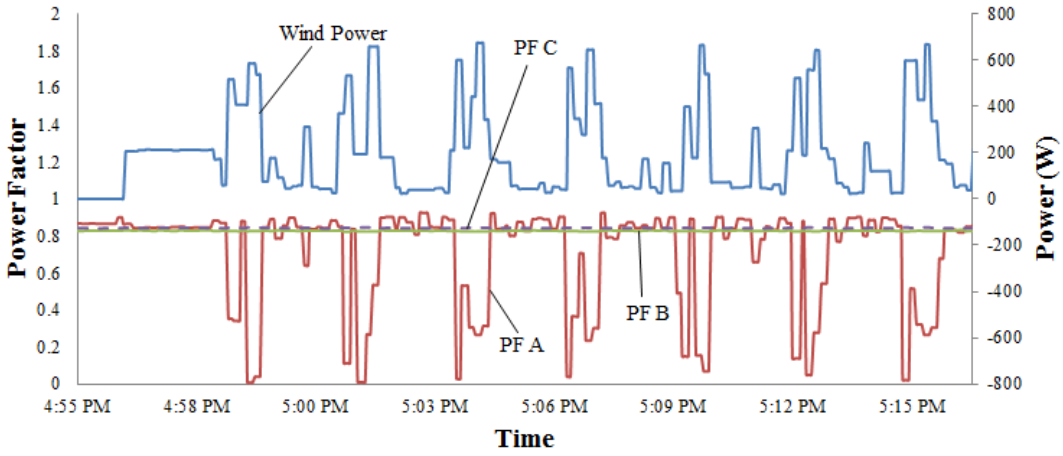

Figure 5.13: Wind power output at phase A and power factor of three-phases in experimental case study 6

When wind power output is fluctuating, the power factor of phase A is also fluctuating according to the wind power. Due to the network is highly loaded with inductance load; power factor is only 0.8 for all the three phases. It is noticed that the power factor drops tremendously during high wind power output. This is because the induction machine is absorbing the reactive power from the network.

Figure 5.14 shows the VUF and voltages of three-phases of the experimental network. It can be noticed that VUF and voltages are affected by the fluctuating wind power output. Due to small wind power output, VUF hits only 0.9% which is still under the statutory limit. However, when this situation is applied to the higher wind power output, VUF and voltages can be out of the range hence creating power quality issues.

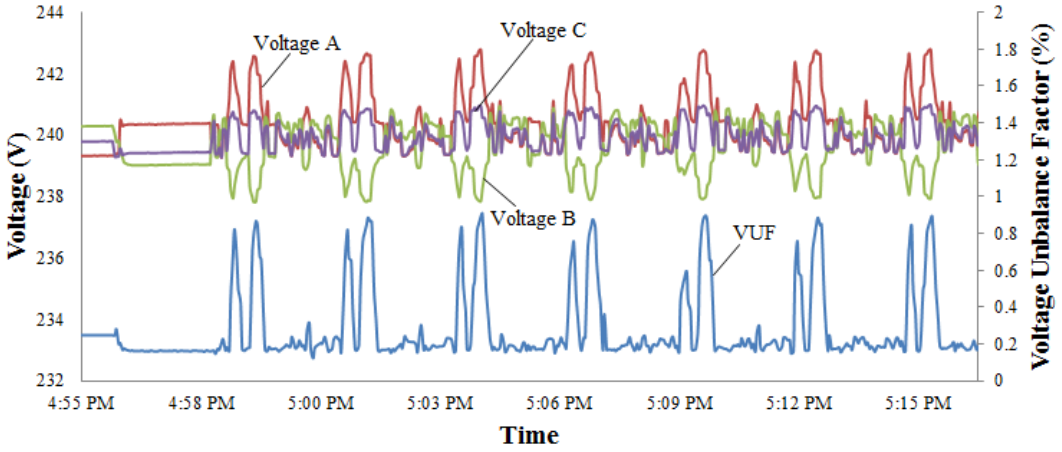

Figure 5.7: VUF and three-phase voltages of the experimental case study 6

5.2.7 Case Study 7: Effect of using fuzzy controlled energy storage on the network with wind emulator.

This case study is to study the response of the fuzzy controlled energy storage system with respect to the changes of wind power output under a balanced load condition. A fixed load of 370 W is connected to every phase and wind emulator is connected to phase A of the network.

Figure 5.15 shows the fluctuating of wind power output affecting the three-phase voltages. Figure 5.16 shows the response of the energy storage system and the VUF of the experimental network. Since the wind power output is around 600 W only, VUF hardly to reach the statutory limit of 1%. For the fuzzy logic control, if VUF hits 0.9%, the energy storage system will react to reduce the hazard of high VUF. At 11.06 am, it can be noticed that, the energy storage system responses to the high VUF.

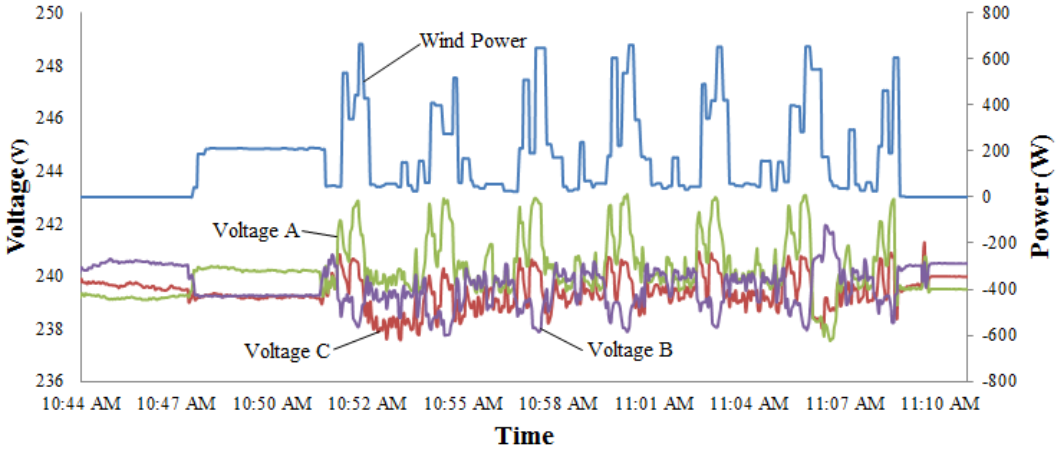

Figure 5.8: Three-phase voltages and wind power output of the experimental case study 7

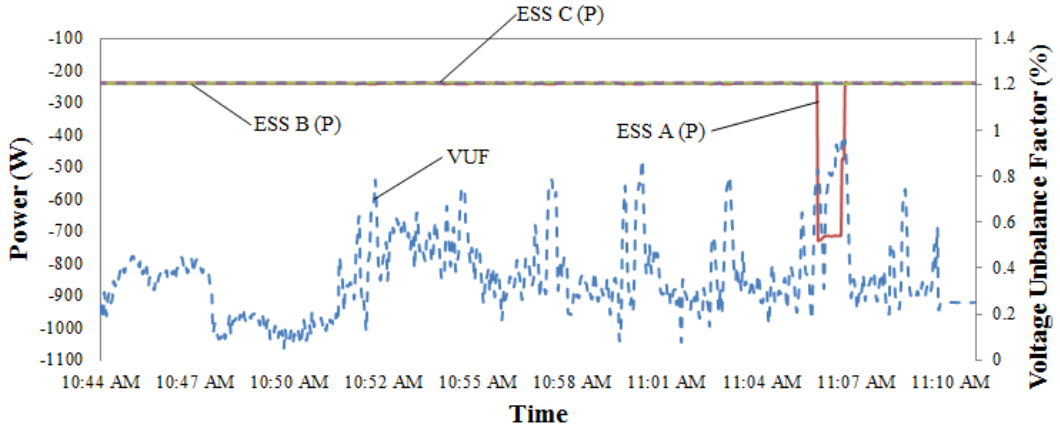

Figure 5.9: VUF and power output of the energy storage system of the experimental case study 7

Figure 5.17 shows the response of the energy storage system and the power factor of the experimental network. Since the inductive load is connected to the network, the power factor is around 0.9. It can be observed that when the energy storage system is used to improve the power factor, the power factor is improved to unity. However,

the wind emulator exporting power to the network causes the power factor to drop. It is because the induction machine absorbs the reactive power from the network. The fuzzy logic control then injects reactive power to the network to improve the power factor.

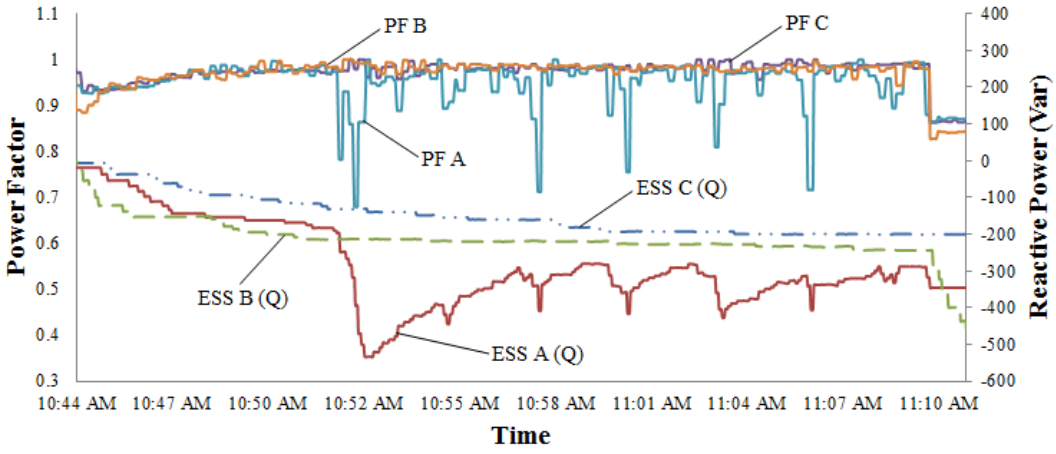

Figure 5.10: Power factor of all three-phases and reactive power output of the energy storage system for experimental case study 7

5.3 Summary

Several scenarios under different generations and loading conditions were outlined in this chapter. The performance of the fuzzy controlled energy storage is verified by setting up the energy storage system on the experimental LV distribution network. The responses of the fuzzy control system under different conditions were investigated. The experimental results show that the fuzzy controlled energy storage system is able to restore the voltage fluctuation, reduce the voltage unbalance factor, and improve the low power factor under rapid changes of RE output and EV integration. Therefore, the developed control algorithm is found satisfy to limit the

desired network parameters within the level under intermittent RE and integration of EV. At the same time, the fuzzy controlled energy storage can increase the use of the RE without limiting the generation effectively.

CHAPTER 6

CONCLUSION

6.1 Conclusion

The utilities of the world are taking solid steps towards incorporating new technologies to evolve the traditional grid systems into smart grid systems. As a promising renewable alternative, the wind and solar power is highly expected to contribute a significant part of generation in power systems in the future, but this also brings new integration related power quality issues. In line with this, this thesis presents a fuzzy controlled energy storage system to mitigate the VUF, voltage rise, and improve the power factor by manipulating the real and reactive power flow. Several scenarios under various generating and loading conditions have been carried out to investigate the performance of the fuzzy controlled energy storage system. It is noticed that the energy storage system which allows real power control only has its limited capability. With the aid of reactive power in the distribution network, it can provide voltage support and also improve power factor. The experimental results show that the proposed fuzzy controlled energy storage system not only mitigates the

voltage rise and VUF caused by intermittent PV power output, but also improves the network power factor effectively.

The majority of the existing control methods are used to solve steady state voltage fluctuation, voltage unbalances and power factor. The fuzzy control method is different from the existing control methods as it is able to adjust the supply of its real and reactive power appropriately and effectively based on the changes in voltage magnitude and power factor at a point of concern. As a result, the voltage magnitude and power factor can be maintained well within the required tolerance under the high intermittency of photovoltaic systems which happened predominantly in Southeast Asia or other regions with cloudy skies. In the developed control algorithm, VUF can be reduced from 2% to 0.5%, which is a 75% of reduction in 1 minute. Power factor is also improved from 0.93 to 0.98. Therefore, this method is an appropriate choice when dealing with dynamic voltage fluctuations, voltage unbalances and power factor. Also, this fuzzy control solution is definitely a new and powerful approach for the energy storage system.

6.2 Future Works

Further work is necessary to study how the energy storage system can solve power quality issues caused by the random penetration of EV, ESS and PV across the real distribution network. Also extra work is required to establish the appropriate size of the energy storage system with respect to the capacity of the RE systems. This is

because the cost of the energy storage system is also an important aspect to be considered for the implementation.

PUBLICATIONS

Journal Paper Published:

Lim, K. Y., Lim, Y. S., Wong, J. & Chua, K. H., 2015. Distributed Energy Storage with Real and Reactive Power Controller for Power Quality Issues Caused by Renewable Energy and Electric Vehicles. *ASCE Journal of Energy Engineering.*

Conference Paper Published:

Lim, K. Y., Lim, Y. S., Wong, J. & Chua, K. H., 2014. *Energy Storage with Fuzzy Controller for Power Quality Improvement on Distribution Network on Distribution Network with Renewable Energy.* Tunisia, Setcor.

REFERENCES

Aarathi A.R, D. M. J., 2014. *Grid Connected Photovoltaic System with Super Capacitor Energy Storage and STATCOM for Power System Stability Enhancement.* Thiruvananthapuram, IEEE, pp. 26-32.

Abba-Aliyu, S., 2009. *Voltage Stability and Distance Protection Zone3,* Göteborg, Sweden: CHALMERS UNIVERSITY OF TECHNOLOGY .

Abdul Rahman Mohamed, K. T. L., 2006. Energy for sustainable development in Malaysia: Energy policy and alternative energy. *ELSEVIER,* pp. 2388-2397.

Alvarez, R. A. et al., 2012. *Greater focus needed on methane leakage from natural gas infrastructure.* s.l., s.n., p. 6435–6440.

Andreas Poulikkas, S. P. G. K. I. H., 2014. Storage Solutions for Power Quality in Cyprus' Electricity Distribution Network. *AIMS's Energy, Volume 2, Issue 1, DOI: 10.3934/energy.2014.1.1,* pp. 1-17.

Anon., 2005. *Overview of Policy Instruments for the Promotion of Renewable Energy and Energy Efficiency in Malaysia.* [Online] Available at: http://1solar.ecosensa.com/images/Overview%20of%20Policy%20for%20the%20Promotion%20of%20Renewable%20Energy%20and%20Energy%20Efficiency%20in%20Malaysia.pdf

Anon., 2014. *Local Automotive News.* [Online] Available at: http://mai.org.my/v3/index.php?option=com_k2&view=item&id=490:rm3-million-fund-set-up-for-300-ev-charging-stations
[Accessed 16 December 2014].

Bajo, C. G. et al., 2015. *Voltage Unbalance Mitigation in LV Networks Using Three-Phase PV Systems.* s.l., IEEE, pp. 1-5.

Bishop, T. H., 2008. *Unbalanced Voltages and Electric Motors.* [Online] Available at: http://www.industrialekg.com/Library/Technical%20Papers%20by%20Third%20Parties/unbalanced-voltages-and-electric-motors.html

Bollen, M., 2002. Definitions of Voltage Unbalance. *Power Engineering Review, IEEE,* pp. 49-50.

Buchmann, I., 2009. *Non-correctable Battery Problems.* [Online] Available at: http://batteryuniversity.com/learn/article/non_correctable_battery_problems [Accessed 2013].

Calstart, 2010. *ALLCARINDEX.* [Online] Available at: http://www.allcarindex.com/auto-car-model/United-States-Calstart-Showcase-Electric-Vehicle-SEV/ [Accessed 2 September 2014].

Canada, M. o. N. R., 2004. *Final Report on the August 14, 2003 Blackout in the United States and Canada: Causes and Recommendations,* Canada: U.S.-Canada Power System Outage Task Force.

Castillo, M. D., Jr., G. P. L., Yoon, Y. & Chang, B., 2014. Application of Frequency Regulation Control on the 4MW/8MWh Battery Energy Storage System (BESS) in Jeju Island, Republic of Korea. *Journal of Energy and Power Sources,* 1(6), pp. 287-295.

Chen, T.-H., Yang, C.-H. & Hsieh, T.-Y., 2009. *Case Studies of the Impact of Voltage Imbalance on Power Distribution Systems and Equipment.* United States, WSEAS, pp. 461-465.

Chua, K. H. et al., 2012. Energy Storage System for Voltage Unbalance Mitigation in Low Voltage Distribution Networks with Photovoltaic Systems. *IEEE Transactions on Power Delivery*, October, 27(No.4), pp. 1783-1790.

Chua, K. H. et al., 2012. Voltage Unbalance Mitigation in Low Voltage Distribution Networks with Photovoltaic Systems. *Journal of Electronic Science and Technology,* March.10(No 1).

Chuang, A. S. & Gellings, C., 2008. *Demand-side Integration in a Restructured Electric Power Industry.* France, Electric Power Research Institute, pp. 1-9.

Dabur, P., Singh, G. & Yadav, N. K., 2012. Electricity Demand Side Management:Various Concept and Prospects. *International Journal of Recent Technology and Engineering (IJRTE),* pp. 1-6.

Divya, K. & Østergaard, J., 2008. Battery energy storage technology for power systems—An overview. *Electric Power Systems Research*, 79(4), p. 511–520.

E. Ghahremani, I. K., 2014. *Optimal Allocation of STATCOM with Energy Storage to Improve Power System Performance.* Chigago, IL, USA, IEEE, pp. 1-5.

E.A. Mertens Jr, L. F. B. J. H., 2007. *Evaluation and tends of power quality indices in distribution system.* Barcelona, IEEE, pp. 1-6.

Farhoodnea, M., Mohamed, A., Shareef, H. & Zayandehroodi, H., 2013. Power quality impacts of high-penetration electric vehicle stations and renewable energy-based generators on power distribution systems. *Measurement, Volume 46, Issue 8, October 2013,* pp. 2423-2434.

Feldman, D. & Barbose, G., 2014. *Photovoltaic (PV) Pricing Trends: Historical, Recent, and Near-Term Projections (2014 Edition),* United State: National Renewable Energy Laboratory (NREL).

Ferry A. Viawan, S. M. I. D. K. S. M. I., July 2008. *Coordinated Voltage and Reactive Power Control in the presence of distributed generation.* Pittsburgh, PA, IEEE, pp. 1-6.

Forster, F., 2010. *EE Times Europe Automotive.* [Online] Available at: http://www.automotive-eetimes.com/en/digital-isolation-in-hybrid-and-electric-vehicles.html?cmp_id=71&news_id=222901126&page=0
[Accessed 17 September 2015].

Ghavameddin Nourbakhsh, B. T. G. M. A. G., 2013. *Distribution Tap Changer Adjustment t Improve Small-Scale Embedded Generaor Penetration and Mitigation Voltage Rise.* Hobart, TAS, IEEE, p. 5.

Gosbell, V. J., 2002. *Voltage Unbalance.* [Online] Available at: http://www.elec.uow.edu.au/apqrc/content/technotes/technote6.pdf

GreenTech, M., 2013. *Standards for Electric Vehicles.* [Online] Available at: http://www.greentechmalaysia.my/content.asp?zoneid=2&articleid=243&cmscategoryid=407#.VcLeafmqqko

H.M.S.Chandana Herath, S. M., 2008. *Power Quality Trends in Energy Australia Distribution Network.* Wollongong,NSW, IEEE, pp. 1-6.

Hendri Masdi, N. M. S. M. A. M. a. S. Y., 2004. *Design of a Prototype D-Statcom for Voltage Sag Mitigation.* Malaysia, IEEE, pp. 61-66.

Hoppecke, 2012. *Sizing of lead acid batteries for solar application,* Germany: Hoppecke.

IEEE, 2005. *IEEE Recommended Practice for Powering and Grounding Electronic Equipment.* United States of America: Institute of Electrical and Electronics Engineers, Inc..

International Monetary Fund, 2016. *Commodity Prices of Natural Gas.* [Online] Available at: http://www.indexmundi.com/commodities/?commodity=natural-gas&months=60&currency=myr

International Renewable Energy Agency (IRENA), 2015. *Battery Storage for Renewables: Market Status and Technology Outlook,* s.l.: International Renewable Energy Agency (IRENA).

Jenkins, N. e. a., 2000. *Embedded Generation.* London: IET.

Jiménez, A. & García, N., 2012. *Unbalanced three-phase power flow studies of distribution systems with plug-in electric vehicles.* North American, IEEE, pp. 1-6.

Johnson, K., 2007. *The Fundamentals of Linking Demand Side Management Strategies with Program Implementation Tactics,* Strategies Newsletter: Association of Energy Services Professional.

KeeGan Dorai, L. K. B. A., 2012. *Motor Trader.* [Online] Available at: http://www.motortrader.com.my/news/first-public-ev-charging-stations-in-malaysia/
[Accessed 22 September 2015].

Kenneth Gillingham, R. G. N. a. K. P., 2004. *Retrospective Examination of Demand-Side Energy Efficiency Policies,* Washington: Resources for the future.

Kottick, D., Res. & Dev. Div., I. E. C. L. H. I., Blau, M. & Edelstein, D., 2002. Battery energy storage for frequency regulation in an island power system. *IEEE Transactions on Energy Conversion (Volume:8 , Issue: 3),* 8(3), pp. 455 - 459.

Lee, C.-Y., 1999. Effects of unbalanced voltage on the operation performance of a three-phase induction motor. *IEEE Transaction Energy Conversion,* pp. 202-208.

Liang, L., Zhong, J. & Jiao, Z., 2012. *Frequency Regulation for a Power System with Wind Power and Battery Energy Storage.* Auckland, IEEE, pp. 1-6.

Li, F. et al., 2008. A Framework to Quantify the Economic Benefit from Local VAR Compensation. *International Review of Electrical Engineering (IREE),* pp. 989-998.

Li, K., Liu, J., Wang, Z. & Wei, B., 2007. Strategies and Operating Point Optimization of STATCOM Control for Voltage Unbalance Mitigation in Three-Phase Three-Wire Systems. *Power Delivery, IEEE Transactions, Volume:22, Issue:1,* pp. 413-422.

Lim Yun Seng, P. T., 2006. *Innovative Application of Demand Side Management to Power Systems.* Sri Lanka, IEEE Conference Publications, pp. 185-189.

Lim, Chia Ying, 2015. *Electric vehicles are the face of future mobility.* Malaysia: Star Media Group Berhad.

Lim, Y. S., WHITE, S., NICHOLSON, G. & TAYLOR, P., 6-9 June 2005. *Additional applications of demand side management techniques in power systems integrated with distributed generation.* Turin, Italy, IEEE, pp. 1-5.

Lu, C.-F., Liu, C.-C. & Wu, C.-J., 2002. Effect of battery energy storage system on load frequency control considering governor deadband and generation rate constraint. *IEEE Transactions on Energy Conversion (Volume:10 , Issue: 3),* 10(3), pp. 555 - 561.

Lyons, P. F., Trichakis, P., Taylor, P. C. & Coates, G., 2010. A Practical Implementation of A Distributed Control Approach for Microgrids. *Intelligent Automation & Soft Computing,* pp. 319-334.

Malaysia Building Integrated Photovoltaic, M., 2010. *PV System Cost.* [Online] Available at: http://www.mbipv.net.my/content.asp?zoneid=4&categoryid=12 [Accessed 27 August 2012].

Marcos, J., Marroyo, L., Lorenzo, E. & García, M., 2012. *Power output fluctuations in large PV plants.* Santiago de Compostela (Spain), European Association for the Development of Renewable Energies, Environment and Power Quality.

Mat Siddique, G. a. B. S., 2004. *Effects of Voltage Unbalance on Induction Motors.* s.l., IEEE, pp. 26-29.

Mohibullah, S. H. L., 2012. *Power Quality Issues and Need of Intelligent PQ Monitoring in the Smart Grid Environment.* London, IEEE, pp. 1-6.

Moosavian, S. R. N. S. J. S. K., 2013. Energy policy to promote photovoltaic generation. *Renewable and Sustainable Energy Reviews,* pp. 44-58.

Muhammad A. Saqib, A. Z. S., 2015. Power-quality issues and the need for reactive-power compensation in the grid integration of wind power. *Renewable and Sustainable Energy Reviews 43,* pp. 51-64.

Natgas, 2013. *Natural Gas and the Environment.* [Online] Available at: http://naturalgas.org/environment/naturalgas/

Networks, F. E., 2015. *First Energy Networks.* [Online] Available at: http://www.firstenergy.com.my/charger-locations/search-charger-locations
[Accessed 14 September 2015].

Ning, Z., Luis, F. & Daniel, S. K., 5-7 December 2011. *Investigating the impact of demand side management on residential customers.* Manchester, IEEE, pp. 1-6.

Oeng, L. & Sangwongwanich, S., 2016. *A Voltage Rise Mitigation Strategy under Voltage Unbalance for a Grid-connected Photovoltaic System.* Chiang Mai, Thailand, Elsevier, pp. 209-312.

Pillay, P. & Manyage, M., 2001. Definitions of Voltage Unbalance. *IEEE Power Engineering Review,* pp. 50-51.

Prakash K. Ray, S. R. M. a. N. K., 2013. Classification of Power Quality Disturbances Due to Environmental Characteristics in Distributed Generation System. *Sustainable Energy, IEEE Transactions on (Volume:4 , Issue: 2),* pp. 302 - 313.

Price, A., Bartley, S., Male, S. & Cooley, G., 1999. A Novel Approach to Utility Scale Energy Storage. *Power Engineering Journal,* pp. 122-129.

Qiushuo Li, S. T. X. X. J. W., 2013. *Monitoring And Analysis of Power Quality in Electric Vehicle Charging Stations.* Tainan, IEEE, pp. 277-282.

R. Romo, O. M., 2015. Power quality of actual grids with plug-in electric vehicles in presence of renewables and micro-grids. *Renewable and Sustainable Energy Reviews,* pp. 189-200.

R. Sastry Vedam, M. S. S., 2008. *Power Quality: VAR Compensation in Power Systems.* London: CRC Press .

REEEP, R. E. &. E. E. P., 2006. *Sustainable Energy Regulation and Policy making Training Manual [pdf]*. [Online] Available at: http://africa-toolkit.reeep.org/modules/Module14.pdf [Accessed 12 May 2012].

Rjakaruna, E. b. S., Shania, F. & Ghosh, A., 2015. *Plug In Electric Vehicles in Smart Grids: Integration Techniques.* Singapore: Springer.

Roberto Caldon, M. C. R. T., 2012. *Voltage Unbalance Compensation In LV Networks With Inverter Interfaced Distributed Energy Resources.* University of Padova, Italy, IEEE, pp. 527-532.

Ryan Eastman, S. G. W. C. J. H., 2014. *Climatic Atlas of Clouds Over Land and Ocean.* [Online] Available at: http://www.atmos.washington.edu/CloudMap/ [Accessed 18 September 2015].

Ryan Eastman, S. G. W. C. J. H., 2014. *Total Cloud Cover:Completely Clear Sky:Frequency of Occurance.* [Online] Available at: http://www.atmos.washington.edu/CloudMap/

S.Mekhilef, D., 2011. *Assessment of off-shore wind farms in Malaysia.* Bali, IEEE, pp. 1351-1355.

Salman Habib, M. K. U. R., 2015. Impact analysis of vehicle-to-grid technology and charging strategies of electric vehicles on distribution networks – A review. *Journal of Power Sources*, pp. 205-214.

Schoenung, S. M., 1996. Energy Storage For a Competitive Power Market. *Energy and the Environment*, pp. 347-370.

Sergio Faias, J. S. R. C., 2009. Embedded Energy Storage Systems in the Power Grid for Renewable Energy Sources Integration. In: *Renewable Energy*. Portugal: InTech, pp. 63-88.

Shahnia, F., Ghosh, A., Ledwich, G. & Zare, F., 2010. *Voltage Unbalance Reduction in Low Voltage Distribution Networks with Rooftop PVs.* Australia, IEEE, pp. 1-5.

Shamshad Ahmad, W. H. W. B. M. M. S. S., 2009. *Open Access Repository of USM Research & Publication.* [Online] Available at: http://eprints.usm.my/10959/1/Analysis_of_Wind_Speed_Variations_and_Estimation_of_Weibull_Parameters_for_Wind_Power_(PPK_Awam).pdf [Accessed 22 October 2015].

Sharad.W.Mohod, D. M. V., 2008. *Power Quality Issues & It's Mitigation Technique in Wind Energy Generation.* Wollongong, NSW, IEEE, pp. 1-6.

Singh, B. R. & Singh, O., 2010. *21st Century challenges of clean energy and global warming-can energy storage systems meet these issues?.* Cairo, IEEE, pp. 323 - 329.

Sopian, K., Haris, A., Rouss, D. & Yusof, M. A., 2005. Building Integrated Photovoltaic (BIPV) in Malaysia- Potential, Current Status Strategies For Long Term Cost Reduction. *ISESCO Journal of Science and Technology, Volume 1/Number 1,* pp. 40-44.

Suruhanjaya Tenaga (Energy Commission), 2014. *Peninsular Malaysia Electricity Supply Industry Outlook 2014,* Malaysia: Suruhanjaya Tenaga (Energy Commission), Published Number: ST(P)14/09/2014.

Suruhanjaya Tenaga (Energy Commission), 2015. *Statistics, Energy Supply.* [Online] Available at: http://meih.st.gov.my/statistics?p_auth=F1SU9reQ&p_p_id=Eng_Statistic_WAR_STOASPublicPortlet&p_p_lifecycle=1&p_p_state=maximized&p_p_mode=view&p_p_col_id=column-1&p_p_col_pos=1&p_p_col_count=2&_Eng_Statistic_WAR_STOASPublicPortlet_execution=e2s1&_Eng_Stat

Suruhanjaya Tenaga (Energy Commission), 2015. *The Malaysian Grid Code,* Malaysia: Suruhanjaya Tenaga (Energy Commission).

Suruhanjaya Tenaga, 2012. *EC- The Malaysian Distribution Code.* Malaysia: s.n.

T. Aziz, M. H. T. S. N. M., 2013. VAR Planning With Tuning of STATCOM in a DG Integrated Industrial System. *Power Delivery, IEEE Transactions, Volume 28, Issue:2,* pp. 875-885.

T. Shigematsu, T. K. H. D. T. H., 6-10 October 2002. *Applications of a vanadium redox-flow battery to maintain power quality.* Japan, IEEE. DOI: 10.1109/TDC.2002.1177625, pp. 1065-1070.

Tande, J. O. G., 2003. Grid Integration of Wind Farms, Wind Energy. *John Wiley & Sons, Ltd.*, pp. 281-295.

Teh, C., 2010. *CHRISTOPHER TEH.* [Online] Available at: http://www.christopherteh.com/blog/2010/11/wind-energy/ [Accessed 9th September 2015].

Tejas Zaveri, B. B. N. Z., 2012. Comparison of control strategies for DSTATCOM in three-phase, four-wire distribution system for power quality improvement under various source voltage and load conditions. *International Journal of Electrical Power & Energy Systems,Volume 43, Issue 1*, pp. 582-594.

TNB, D. A. H. A. S. S. D. I. Z. F. b. H. M. B. A. M. B. P. D. I. A. A. S. M. A. P. I. D. R. V. K. D. A. R., 2012. *TNB Technical Guidebook on Grid-interconnection of Photovoltaic Power Generation System to LV and MV Networks,* Malaysia: Tenaga Nasional Berhad.

Trichakis, P. et al., 2006. *An Investigation of Voltage Unbalance in Low Voltage Distribution Networks with High Levels of SSEG.* Newcastle upon Tyne, IEEE, pp. 182-186.

Trichakis, P., Taylor, P., Lyons, P. & Hair, R., 2008. Predicting the technical impacts of high levels of small-scale embedded generators on low-voltage networks. *IET Renewable Power Generation,* pp. 249-262.

Union of Concerned Scientists, 2014. *Environmental Impacts of Natural Gas.* [Online]
Available at: http://www.ucsusa.org/clean_energy/our-energy-choices/coal-and-other-fossil-fuels/environmental-impacts-of-natural-gas.html#bf-toc-3

von Appen, J. et al., 2011. *Assessment of the Economic Potential of Microgrids for Reactive Power Supply.* The Shilla Jeju, Korea, LBNL, p. 8.

Wilkins, B. L. a. A. J., 2014. Designing to Mitigate Effects of Flicker in LED Lighting: Reducing risks to health and safety. *IEEE*, pp. 18-26.

Wong, J., 2015. *Fuzzy Controlled Energy Storage System for Low-Voltage Distribution Networks with Photovoltaic Systems,* Malaysia: UTAR.

Wong, J., Lim, Y. S. & Morris, E., 2014. Novel Fuzzy Controlled Energy Storage for Low-Voltage Distribution Networks with Photovoltaic Systems under Highly Cloudy Conditions. *ASCE Journal of Energy Engineering,* p. 17.

Wong, J., Lim, Y. S., Taylor, P. & Morris, S., 2011. Optimal utilisation of small-scale embedded generators in a developing country - A case study in Malaysia. *Renewable Energy, 36,* p. 12.

Wu, H. & Liu, Y., 2011. *Novel STATCOM Control Strategy for Wind Farm Reactive Power Compensation.* Wuhan, IEEE, pp. 1-5.

Xi, Z., Parkhideh, B. & Bhattacharya, S., 2008. *Improving Distribution Syatem Performance with Integrated STATCOM and Supercapacitor Energy Storage System.* Rhodes, IEEE, pp. 1390-1395.

Yong, J. Y., Ramachandaramurthy, V. K., Tan, K. M. & Mithulanantha, N., 2015. Bi-directional electric vehicle fast charging station with novel reactive power compensation for voltage regulation. *Electrical Power and Energy Systems, Volume 64,* pp. 300-310.

Yun, J. Y., Yu, G., Kook, K. S. & Chang, B. H., 2013. A Study on the Criteria for Setting the Dynamic Control Mode of Battery Energy Storage System in Power Systems. *Transactions of the Korean Institute of Electrical Engineers,* 62(4), pp. 444-450.

Zaharim, A., Najid, S. K., Razali, A. M. & Sopian, K., 2009. Wind Speed Analysis in the East Coast of Malaysia. *European Journal of Scientific Research;Jun2009, Vol. 32 Issue 2, p208,* pp. 208-215.

Zito, R., 2010. *Energy Storage A New Approach.* Canada: Scrivener.

Zuhairuse Md Darus, N. A. H. S. N. A. M. M. A. A. R. K. N. A. M. O. A. K., 2009. The Development of Hybrid Integrated Renewable Energy System (Wind and Solar) for Sustainable Living at Perhentian Island, Malaysia. *European Journal of Social Sciences – Volume 9, Number 4 (2009),* pp. 557-563.

Appendix A: Specifications of SMA Sunny Island 5048

Output data	
Nominal AC voltage (adjustable)	230 V (202 V – 253 V)
Grid frequency adjustable	45 Hz – 55 Hz
Continuous AC output at 25 °C / 45 °C	5000 W / 4000 W
Continuous AC output at 25 °C for 30 / 5 / 1 min	6500 W / 7200 W / 8400 W
Nominal AC current	21 A
Max. current	100 A (for 100 ms)
Output voltage harmonic distortion factor	< 3 %
Power factor	–1 to +1
Input data	
Input voltage (range)	230 V (172.5 V – 250 V)
Input frequency	50 Hz (40 Hz – 70 Hz)
Max. AC input current (adjustable)	56 A (2 A – 56 A)
Max. input power	6.7 kW /12.8 kW
Battery data	
Battery voltage (range)	48 V
Max. battery charging current	120 A
Continuous charging current	100 A
Battery capacity	100 Ah to 10000 Ah
Charge control	IUoU with automatic full and equalization charge
Efficiency/power consumption	
Max. efficiency (typical)	95 %
Own consumption with no load (standby)	25 W (< 4 W)
Protection type	DIN EN 60529
Certification	CE
Device protection	short-circuit, overload, over temperature
Interfaces	2 LEDs, 4 buttons, 2-line display, 2 multifunction relays, RS485 / RS232 / CAN electrically separated (optional), MMC/SD card
Mechanical data	
Width / height / depth	18.4 / 24.1 / 9.3 inch (467 / 612 / 235 mm)
Weight	139 lbs (63 kg)
Ambient conditions	
Ambient temperature	–13°F ... 122°F (–25 °C to +50 °C)
Warranty	2 years
Accessories	
Ext. battery temperature sensor	Included
“GenMan” generator manager	Optional

Appendix B: Program written in Data Taker DT82

```
begin "UTAR"

RA100-cv 'trigger when 100cv change to zero
1MODBUS(AD10,R4:1)=1142

RB100+CV 'trigger when 100cv change from zero
'Seq for modbus40001 to start motor
'a) xxxx x1xx x111 x110 (1142d)
'b) xxxx x1xx x111 x111 (1143d)
'c) xxxx x1xx x111 1111 (1151d)

'Write to Modbus slave (AD9 is big inverter, 10 is small inverter)
1MODBUS(AD10,R4:1)=1142
1MODBUS(AD10,R4:1)=1143
1MODBUS(AD10,R4:1)=1151

RC1S
'40002 contains set frequency
1MODBUS(AD10,R4:2)=101CV  'Inverter frequency

RD10S 'Read power meter values

1MODBUS(AD2,R3:29,=1..10CV)
delay=100

1MODBUS(AD2,R3:39,=11..20CV)
delay=100

1MODBUS(AD2,R3:49,=21..26CV)
delay=100
```

1MODBUS(AD2,R3:67,=27..34CV)
delay=100

1MODBUS(AD3,R3:29,=201..210CV)
delay=100

1MODBUS(AD3,R3:39,=211..220CV)
delay=100

1MODBUS(AD3,R3:49,=221..226CV)
delay=100

1MODBUS(AD3,R3:67,=227..234CV)
delay=100

1MODBUS(AD4,R3:29,=301..310CV)
delay=100

1MODBUS(AD4,R3:39,=311..320CV)
delay=100

1MODBUS(AD4,R3:49,=321..326CV)
delay=100

1MODBUS(AD4,R3:67,=327..334CV)
delay=100

1MODBUS(AD5,R3:29,=401..410CV)
delay=100

1MODBUS(AD5,R3:39,=411..420CV)
delay=100

```
1MODBUS(AD5,R3:49,=421..426CV)
delay=100

1MODBUS(AD5,R3:67,=427..434CV)
delay=100

1MODBUS(AD6,R3:29,=501..510CV)
delay=100

1MODBUS(AD6,R3:39,=511..520CV)
delay=100

1MODBUS(AD6,R3:49,=521..526CV)
delay=100

1MODBUS(AD6,R3:67,=527..534CV)
delay=100

1MODBUS(AD10,R4:2,=102CV)

END
```